# Computational Methods for the Analysis of Nonnegative Polynomial Systems

Thesis for the degree
"Doctor of the Hungarian Academy of Sciences"

*Gábor Szederkényi*

Computer and Automation Research Institute,
Hungarian Academy of Sciences
Budapest
2011

dc_263_11

## Acknowledgements

First of all, I would like to express my sincere gratitude to Prof. Katalin M. Hangos, head of the Process Control Research Group at the Computer and Automation Research Institute (MTA SZTAKI) for the joint work on the topic of the thesis, and for her continuous encouragement and support to remain in the scientific field after obtaining my PhD. Next, let me thank Profs. Antonio A. Alonso and Julio R. Banga at the Bioprocess Engineering Group of the Marine Research Institute of CSIC (IIM-CSIC), Vigo, Spain for raising my interest in chemical reaction networks and systems biology, and for allowing me to spend the year 2011 as a guest researcher in their research group. I thank Prof. József Bokor, member of the Hungarian Academy of Sciences and head of the Systems and Control Laboratory at MTA SZTAKI for introducing me into nonlinear systems theory during the beginning of my research work, and for calling my attention to the interesting and useful classes of Hamiltonian and nonnegative systems. I'd like to thank Prof. Tamás Roska, member of the Hungarian Academy of Sciences, former head of the Cellular Sensory and Wave Computers Research Laboratory at MTA SZTAKI, and former dean of the Faculty of Information Technology at Péter Pázmány Catholic University (PPKE) for the stimulating discussions and for encouraging me to present our latest results to the students. I'm grateful to Dr. Péter Inzelt, the director of MTA SZTAKI for all his support and especially for providing us an excellent and undisturbed research environment in the institute. I wish to thank Dr. Judit Nyékyné Gaizler, dean of the Faculty of Information Technology at PPKE for kindly releasing me from teaching duties during the year 2011 that was a great help in writing this thesis. I'm grateful to Dr. György Cserey, head of the Robotics Laboratory at PPKE and to Dr. Dávid Csercsik for the joint work, and for taking over majority of my tasks at the university in 2011. Many thanks to the administrative staff of MTA SZTAKI, especially to Katalin Hargitai and Marika Farkas for all their help through the years.

I'd like to thank all my co-authors not mentioned above (in alphabetical order): Dr. Piroska Ailer, Attila Gábor, Dr. Csaba Fazekas, Prof. Péter Gáspár, Prof. Sten B. Joergensen, Matthew D. Johnston, Dr. Mihály Kovács, Dr. Niels Rode Kristensen, Dr. Attila Magyar, Dr. Irene Otero Muras, Dr. Tamás Péni, Dr. Barna Pongrácz, Szabolcs Rozgonyi, János Rudan, Prof. David Siegel, Prof. Zoltán Szabó, Zoltán Tuza, Prof. Zsolt Tuza, and Prof. Erik Weyer for sharing some interest in the topics I was working on, and for making essential contributions to the joint results.

I'm also grateful to my wife, Helga for all her patience and support, especially during thesis writing.

Finally, the financial support of the following institutions, grants and scholarships is also gratefully acknowledged. The Hungarian Scientific Research Fund (OTKA) through grants no. F046223 (Analysis Based Control of Nonlinear Dynamical Systems), T042710 (Modeling and Control of Dynamical Process Systems), K67625 (Control and Diagnosis of Nonlinear Systems Based on First Engineering Principles), Bolyai János Research Scholarship of the Hungarian Academy of Sciences: 2003-2006, and 2007-2010, Project CAFE (Computer Aided Process for Food Engineering) FP7-KBBE-2007-1 (supporting my stay in Vigo in 2011).

dc_263_11

# Contents

dc_263_11

# Notations

### Generally used notations

| | |
|---|---|
| $\mathbb{R}$ | the set of real numbers |
| $\mathbb{Z}$ | the set of integer numbers |
| $\mathbb{R}^n$ | $n$-dimensional Euclidean space |
| $\mathbb{R}^n_+$ | $n$-dimensional positive orthant |
| $\overline{\mathbb{R}}^n_+$ | $n$-dimensional nonnegative orthant |
| $v_j$ | $j$th element of a vector $v$ |
| $W_{ij}$ or $W_{i,j}$ | $(i,j)$th element of a matrix $W$ (indexing order: row, column) |
| $W_{i,\cdot}$ | $i$th column of a matrix $W$ |
| $W_{\cdot,j}$ | $j$th column of a matrix $W$ |
| $\dot{x}$ or $\frac{d}{dt}x$ | time derivative of $x$ |

### Notations for quasi-polynomial and Lotka-Volterra systems

| | |
|---|---|
| $y$ | quasi-polynomial (QP) state variable |
| $z$ | Lotka-Volterra (LV) state variable |
| $y^*$ | equilibrium point of the QP system |
| $z^*$ | equilibrium point of the LV system |
| $x$ | centered state variable of the LV system (i.e. $x = z - z^*$) |
| $A$ | $n \times m$ coefficient matrix of the QP system |
| $B$ | $m \times n$ exponent matrix of the QP system |
| $M$ | $m \times m$ coefficient matrix of the LV system ($M = BA$) |
| $V$ | entropy-like Lyapunov function: $V(z) = \sum_{i=1}^{m} c_i \left( z_i - z_i^* - z_i^* \ln \frac{z_i}{z_i^*} \right)$ |
| $C$ | $m \times m$ diagonal matrix containing the coefficients of $V$: $C = \mathrm{diag}(c_i),\ i = 1 \ldots, m$ |
| $\Omega$ | $n \times 1$ row vector containing the parameters of time-rescaling |
| $\tilde{A}$ | $n \times (m+1)$ coefficient matrix of the time-rescaled QP system |
| $\tilde{B}$ | $(m+1) \times n$ exponent matrix of the time-rescaled QP system |
| $\tilde{M}$ | $(m+1) \times (m+1)$ LV coefficient matrix of the time-rescaled system |

### Notations for kinetic systems

| | |
|---|---|
| $X$ | $n$-dimensional vector of species |
| $C$ | $m$-dimensional vector of chemical complexes |
| $[X_i]$ | concentration of specie $X_i$ |
| $x$ | $n$-dimensional vector of specie concentrations (state variable, $x = [X]$) |
| $x^*$ | equilibrium concentration vector |
| $\alpha, \beta$ | positive stoichiometric coefficients |
| $C_i \to C_j$ | reaction involving reactant (source) complex $C_i$ and product complex $C_j$ |
| $\mathcal{S}$ | the set of species |
| $\mathcal{C}$ | the set of complexes |
| $\mathcal{R}$ | the set of reactions |
| $k_j$ | reaction rate coefficient corresponding to the $j$th reaction |
| $k_{ij}$ | reaction rate coefficient corresponding to reaction $C_i \to C_j$ |
| $\rho_j$ | rate of the $j$th reaction |
| $\rho_{ij}$ | rate of the reaction corresponding to reaction $C_i \to C_j$ |
| $Y$ | $n \times m$ complex composition matrix |

| | |
|---|---|
| $A_k$ | $m \times m$ Kirchhoff (or kinetics) matrix |
| $\psi \in \mathbb{R}^n \mapsto \mathbb{R}^m$ | monomial function of the kinetic system: $\psi_j(x) = \prod_{i=1}^{n} x_i^{Y_{ij}}$ |
| $S$ | stoichiometric subspace of a reaction network |
| $\Sigma = (\mathcal{S}, \mathcal{C}, \mathcal{R})$ | kinetic system characterized by the triplet $(\mathcal{S}, \mathcal{C}, \mathcal{R})$ |
| $\Sigma = (Y, A_k)$ | kinetic system characterized by the pair $(Y, A_k)$ |
| $\mathcal{N}$ | $n \times r$ stoichiometric matrix of a reversible reaction network |
| $y$ | continuous optimization variables |
| $\delta$ | integer optimization variables |

# Chapter 1

# Introduction

Although models are "really nothing more than an imitation of reality" [75], their widespread utilization not only in research and development but also in the everyday life of developed societies is clearly indispensable. Due to the (sometimes unnecessary) complexity of system components and their possible interactions, without building, analyzing and simulating appropriate models, we could not predict the outcome of common events like a regular parlamentary election, not to mention the safe operation and maintenance of such involved systems like a modern passanger car or a power plant. When we are interested in the evolution of certain quantities usually in time and/or space, we use dynamic models. The deep understanding and the targeted manipulation of such models' behaviour are in the focus of systems and control theory that now provides us with really powerful methods for model analysis and controller synthesis in numerous classical application fields such as electrical, mechanical and process engineering. [87, 144], [B1]. The key importance of dynamics in the explanation of complex phenomena occurring in living systems is now also a commonly accepted view [137, 2]. Besides the sufficient maturity of systems and control theory, the accumulation of biological knowledge mainly in the form of reliable models and the recent fast development in computer and computing sciences converged to the birth of a new discipline called systems biology, that can hopefully address important challenges in the field of life sciences in the near future [152].

The aim of this thesis is to summarize and present analysis results for certain classes of dynamical systems that are primarily applied in the description of biochemical processes and are given in the form of nonlinear ordinary differential equations (ODEs). The purpose of the present introductory chapter is to briefly outline the state of the art in the fields related to the topic of the thesis without mathematical formulas, and to give the most important motivations of the performed work based thereon.

## 1.1 Background and motivation

### 1.1.1 Nonnegative systems

Nonnegative systems are characterized by the property that all state variables remain nonnegative if the trajectories start in the nonnegative orthant. (If strict positivity of the state elements is required then these models are often referred to as positive systems.) Thus, nonnegative systems play an important role in fields such as (bio)chemistry, economy, population dynamics or even in transportation modeling where the state variables of the models are often physically constrained to be non-

negative [44, 74]. Interesting examples of nonnegative systems from the authors' own experience are the control-oriented simplified model of the primary circuit of the Paks Nuclear Power Plant [J23, J22, J24] and its important subsystem, the pressurizer [J27].

It is important to remark that many non-positive systems can be transformed to the nonnegative (or positive) system class through appropriate coordinates-transformations. The most common way of this is the following. First, the coordinates are shifted into the positive orthant such that the state variables belonging to the studied operation domain (with the possible initial conditions) remain positive. Then there are several possibilities to ensure the nonnegativity of the system. One popular solution is the approach of Samardzija [135] where the distortion of the phase-space can be kept under control in the region of interest. Another possibility is a state-dependent time-rescaling of the model [54], [J3]. Naturally, when using such transformations, it has to be always checked that the transformed system preserves the required qualitative properties of the original one.

### 1.1.2 Quasi-polynomial systems

Quasi-polynomial (QP) systems form a wide class of smooth nonnegative systems and they clearly play an increasingly important role in the modeling of dynamical processes. The QP system class was introduced and first analyzed by Prof. Leon Brenig and his group [16, 17]. In [16] it was shown that majority of smooth ODE models can be algorithmically embedded into the QP form, and the so-called quasi-monomial (QM) transformation was defined under which the QP-model form is invariant. Furthermore, the QM transformation splits the family of QP systems into equivalence-classes, and in each class two simple canonical forms were defined in [17]. QP systems are also called Generalized Lotka-Volterra (GLV) systems, because the monomials of a QP system form a classical Lotka-Volterra (LV) system in a transformed state space which is often of higher dimension than that of the original QP system [77, 54]. Thus, numerous properties of QP models like integrability, stability, persistence or the existence of invariants can be examined using the corresponding LV system, the qualitative properties of which have been intensively studied for a long time [146]. Based on the above, we can say that LV models "have the status of canonical format" within smooth nonlinear dynamical systems [56]. Moreover, the simple matrix structure characterizing QP models allows us to perform important model analysis tasks using efficient numerical algorithms. In [80], the QP formalism was first extended to the discrete-time case demonstrating that the LV system representation plays a central role in that case, too. The conditions for transforming neural network models to QP form are considered in [117] where the most important conclusion is that generalized LV systems are universal approximators of certain dynamical systems, just as are continuous-time neural networks.

Finding constants of motion has been an important and intensively studied area of the analysis of dynamical systems for a long time. If the given dynamical system is not integrable, then its first integrals (if they exist) give us very useful information about the properties of the solutions and about possibly physically meaningful conserved quantities. Several different approaches have been proposed in the literature for the determination of invariants under various conditions (see e.g. [1, 103, 138]). Furthermore, first integrals play a great role in modern systems and control theory e.g. in the field of canonical representations, controllability and observability analysis [87] and stabilization of nonlinear systems [149, 104]. The theoretical background of

the existence of quasi-polynomial invariants is well-founded. In [52] algebraic tools are applied to find semi-invariants and invariants in quasi-polynomial systems. In [53] it is shown that any QP invariant of a QP system can be transformed into a QP invariant of a homogeneous quadratic LV model and that the existence of polynomial-type semi-invariants in the corresponding LV systems is a necessary condition for the existence of QP invariants. A general method is given in the same paper for the symbolical checking of this necessary condition with numerous valuable examples. Moreover, a computer-algebraic software package called QPSI has been implemented for the determination of quasi-polynomial invariants and the corresponding model parameter relations [55].

The stability and boundednes of the solutions of QP systems is also a widely studied subject with practically well-usable results. In [54], the authors give sufficient conditions for the existence of a logarithmic (often called 'entropy-like') Lyapunov function for QP systems. Additional important conditions are given in the same paper that the solutions remain bounded inside the strictly positive orthant. These stability conditions are formulated as purely algebraic ones in [65], and they are shown to be equivalent to the diagonal stabilizability problem that has been known for long in control theory with many applications [93]. For the determination of Lyapunov function coefficients, an effective numerical procedure is proposed in [66] that is based on a series of linear programming steps. The methods for stability analysis of QP systems were further developed in [77, 79], while a possible Hamiltonian structure in Lotka-Volterra models was studied in [78]. As it was shown in [54], by introducing additional parameters, an appropriate time-rescaling transformation can significantly extend the possibilities to find a Lyapunov function for the investigated QP system to prove its global (asymptotic) stability.

Although it was visible from the available theoretical results that the QP class is general enough to appropriatly describe the dynamics of many physical and technological systems, its utilization in the analysis or controller design for engineering models was not wide-spread in the first half of the 2000's.

### 1.1.3 Mass-action type deterministic models of chemical reaction networks

An important subset of nonnegative nonlinear dynamical systems (and also of QP systems) is the class of chemical reaction network (CRN) models obeying the mass-action law [83]. Such networks can be used to describe pure chemical reactions, but they are also widely used to model the dynamics of intracellular processes, metabolic or cell signalling pathways [73]. Thus, CRNs are able to describe key mechanisms both in industrial processes and living systems. Being able to produce all the important qualitative dynamical properties like stable and unstable equilibria, multiple equilibria, bifurcation phenomena, oscillatory and even chaotic behaviour [42], CRNs "have become a prototype of nonlinear science" [155]. Many of these phenomena have been actually observed in real chemical experiments where the practical constraints are much more severe than in the case of mathematical models [122, 112]. This 'dynamical richness' of the model class explains that CRNs have attracted significant attention not only among chemists but in numerous other fields such as physics, or even pure and applied mathematics where nonlinear dynamical systems are considered. The increasing interest towards reaction networks among mathematicians and engineers is also shown by recent tutorial and survey papers in the nonlinear control community

[143, 5, 22]. From now on, only deterministic mass-action type models are meant by CRNs in this thesis, although it is well-known that in many applications, reaction rates different from mass-action type and/or stochastic models are required.

Chemical reaction network theory (CRNT) is originated in the 1970's by the pioneering works of Horn, Jackson and Feinberg [83, 49]. Since then, many strong results have been published in the field on the relation between network structure and qualitative dynamical properties. One of the most significant results in the study of the dynamical properties of chemical reaction systems is described in [49, 50], where (among other important results) the notion of 'deficiency' is introduced. The deficiency of a CRN is a nonnegative integer number that only depends on the stoichiometry and the graph structure of a CRN but not on the reaction rate coefficients. In the same paper, the stability of CRNs with zero deficiency is proved with a given Lyapunov function that is independent of the system parameters and therefore suggests a robust stability property with respect to parameter changes. These concepts were revisited, extended and put into a control theoretic framework in [143]. Conditions for the local controllability and observability of chemical systems were given in [45] and [46], respectively. In [32] it is shown that the absence of a certain kind of autocatalysis, autoinhibition and cooperativity implies the existence of a unique, asymptotically stable, positive equilibrium point in the dynamics. Moreover, a method was given for the construction of oscillatory reactions. The relationship between the chemical network structure and the possibility of multiple equilibria is investigated in [26] from and algebraic and in [27, 29] from a graph-theoretic point of view.

Several authors studied the possibilities of dimension reduction for large chemical networks. In [47], the characterization of nonnegative linear lumping schemes is given that preserves the kinetic structure of the original system. Important conditions for the existence of nonlinear lumping functions were established in [105], and methods for the construction of such functions were proposed in [106]. The effect of lumping on the qualitative properties of the solutions of kinetic systems was studied in [148]. The method of invariant manifold (MIM) is proposed in [68] and [69] for the reduced description of kinetic equations.

Weakly reversible networks (characterized by the property that each node in their reaction graphs lies on at least one directed cycle) is a particularly important class of reaction networks because strong properties are known about their dynamics. Under a supplemental condition, which is easily derived from the reaction graph alone, it is known that there is a unique positive equilibrium concentration within each invariant manifold of the network, and that equilibrium concentration is at least locally asymptotically stable [48, 82, 83].

It is known from the so-called "fundamental dogma of chemical kinetics" that different reaction networks can produce exactly the same kinetic differential equations [101, 83]. CRNs with different parametrization (that often implies structural difference as well) will be called *dynamically equivalent* if they give rise to the same ODEs. A possible CRN (with a certain structure and parametrization) having a given dynamics will be called a *realization* of that dynamics. Naturally, the phenomenon of dynamical equivalence has an important impact on the identifiability of reaction rate constants: if a kinetic dynamics have different dynamically equivalent CRN realizations, then the model, where the parameter set to be estimated consists of all reaction rate coefficients, cannot be structurally identifiable [28]. The so-called inverse problem of reaction kinetics (i.e. the characterization of those polynomial differential equations which are

kinetic) was first addressed and solved in [86]. Here, in a constructive proof, a realization algorithm was given that produces a possible CRN realization of a given kinetic polynomial ODE system. This is certainly a fundamental result of kinetic realization theory and the numerical algorithms in chapter 5 will use it frequently.

Since many important conditions on the qualitative properties CRN dynamics are realization-dependent (see also subsection 2.5.8 in the following chapter), it is worth examining whether there exists a dynamically equivalent (or sufficiently 'similar') realization that guarantees certain properties of the corresponding dynamics that are not directly recognizable from the initial CRN or from the corresponding differential equations. Such an approach, if successful, would certainly extend the scope of many existing strong CRNT results. Moreover, the kinetic representation of even non-chemically originated models may give us additional useful information about the systems's behaviour [135]. In spite of this, beyond the examples of dynamical equivalence showed e.g in [83, 155], to the best of the author's knowledge, there was no systematic computational approach for the determination of preferred dynamically equivalent CRN realizations.

### 1.1.4 The Hamiltonian view on dynamical systems

In recent decades, motivated by mechanical systems where this kind of description arises naturally [6], much effort has been made in the field of Lagrangian and Hamiltonian modeling of electrical, fluid, thermodynamical or mixed physical systems [124]. Technically speaking, when searching for a Hamiltonian representation, after possible coordinates transformations, one typically tries to factorize the system's ODE model as a product of a state-dependent matrix (often called the structure matrix) and the (transposed) gradient of a scalar-valued function mapping from the state space, that is usually called the Hamiltonian function. Although there exist some algorithmic approaches to construct a Hamitonian structure for nonlinear systems [115, 150, 85], Hamiltonian descriptions of real models have particular value when they have clear physical meaning. In these cases, the state dependent structure matrix typically reflects the interconnection structure of the system, while the Hamiltonian function is a generalized energy function that can often serve also as a Lyapunov function if it fulfills additional geometric conditions [149].

If the nonincreasing nature (in time) of the Hamiltonian function can be proved globally through the negative definiteness of the structure matrix, the corresponding system is called a dissipative-Hamiltonian model. It is straightforward to write any stable linear time-invariant (LTI) system in dissipative-Hamiltonian form [128]. However, in the nonlinear case the dissipativity property can be local, if it applies only to a neighborhood of the equilibrium point or reference trajectory. If there are no constraints on the local or global definiteness of the structure matrix, then the description is called pseudo-Hamiltonian realization [23]. Similarly to feedback linearization [87], a nonlinear state-feedback (if applicable) is often useful in transforming an initial model to a Hamiltonian one [84].

Finding physically meaningful Hamiltonian structures in linear and nonlinear electrical circuits is a thoroughly studied area [142, 24]. First, the pure LC case was fully solved, where the Hamiltonian function is the total electrical energy of the system [114]. The RLC case is much more complex than that, and according to the latest results, an extension of the state-space is required for the Hamiltonian description [88, 41]. For thermodynamical systems, the most general Hamiltonian system factorization is given

in the so-called "Generic" structure [156]. However, the "Generic" structure cannot be applied in a straightforward way for many particular models driven by the laws of thermodynamics. The Hamiltonian description of process system models was considered in [J1, B1], where the passive mass-convection network was treated separately, and conditions were given for the allowed form of the nonlinear source terms in the system model.

The energy oriented framework of Hamiltonian description provides a particularly good ground for the so-called passivity based control techniques that have a chance to construct theoretically well-founded robust feedback loops for even complex nonlinear systems [149]. The significance and usefulness of this approach is expressed briefly in [89] as: "... energy can serve as a lingua franca to facilitate communications among scientists and engineers from different fields." In the field of chemical thermodynamics, entropy is playing a similarly important role to energy [18]. This suggests that the family of entropy-like Lyapunov functions often appearing in thermodynamical (and nonnegative) models, can be a possible choice for the integrated treatment of nonlinear dynamical systems.

### 1.1.5 Background of the applied optimization techniques and their application in chemical and process systems

As an effective decision support and design tool, optimization can give us invaluable help in selecting those solutions from a set of candidates that are the most advantageous from a certain point of view, and possibly satisfy given constraints [15, 133]. Due to the enormous recent development both in theory and in the underlying hardware/software environment, optimization is now an ubiquitous instrument in many industries (manufacturing, chemical, electrical, transportation etc.) where really large-scale problems are solved routinely.

The basic idea of linear programming (LP) is attributed to Leonid Kantorovich around 1939 for solving military resource distribution problems, then it was reinvented and first published in a significantly extended form by George B. Dantzig [33, 34, 35]. Today's best LP solvers are highly efficient and reliable, and they can cope with the solution of problems containing approximately up to a million constraints and several million variables. The two most significant approaches for the numerical solution of LP problems are the simplex-type algorithms [113] and the interior point methods [134]. If some of the variables are constrained to be integer in an LP problem, then it is called a mixed integer linear programming (MILP) problem [119, 59]. MILP problems are generally NP-hard, but there exist efficient solvers for their treatment up to a limited problem size. Mixed Integer Nonlinear Programs (MINLPs) are the most general constrained optimization problems with a single objective. These problems can contain continuous and integer decision variables without any limitations to the form and complexity of the objective function or the constraints. As it is expected, the solution of these problems is rather challenging [58].

Linear matrix inequalities (LMIs) gained increasing popularity in the systems and control community from the 1990's, since many tasks related to stability or performance analysis and (robust) controller design for linear time invariant (LTI) and linear parameter varying (LPV) systems can be expressed in LMI form [14, 8, 136]. Although the LMI structure itself was known and small LMI problems were solved by hand around 1940, the real breakthrough in this field began by the observation in the 1980's that many practically important LMIs can be formulated as convex optimiza-

tion problems. Slightly later, the development of interior-point algorithms [15] allowed of the safe numerical solution of relatively large LMI problems.

The application of different optimization techniques in (bio)chemical and process engineering is wide-spread [57, 70, 10], therefore only a short subjective list of the most relevant results related to structure design or analysis of process and reaction systems is presented here. In the chemical and biochemical fields, efficient combinatorial optimization algorithms are widely applied e.g. in permanental polynomial computation [107], metabolic pathway construction, control analysis or metabolic network reconstruction [10]. Process network synthesis (PNS) aims at designing the structure of process plants satisfying given constraints and often optimizing an objective function related to the costs, quality measure, efficiency etc. of the operation [60]. It was shown in several publications that MILP techniques can be successfully used in solving PNS problems [71, 125, 126, 127]. For the representation of process structure, a special bipartite graph called P-graph (Process graph) was introduced and analyzed in [61]. In [62], a polynomial-time algorithm was given for the generation of the maximal superstructure corresponding to a process network synthesis problem using P-graphs. From this superstructure, all possible solutions can be extracted by applying additional constraints. Building and analyzing a similar superstructure can lead to truly globally optimal solutions in separation network synthesis [100]. The P-graph methodology was successfully used for modeling and synthesizing complex reaction structures [43, 108], too.

MILP techniques were successfully used for decomposing complex reaction systems into chemically feasible steps [99]. The integration of logical expressions into mixed integer programming problems is an essential and powerful achievement in system modeling and control [153, 131, 130, 132, 12] that will be utilized heavily in chapter 5. According to these results, a propositional logic problem, where a given statement must be proved to be true given a set of compound statements containing literals, can be solved by means of a linear integer program. For this, logical variables must be introduced and associated with the literals. Then the original compound statements can be translated to linear inequalities involving the logical variables. It is also noted that the evolutionary method as an approach for global optimization can also be successful in solving complex chemically originated problems (see, e.g. [92]), but similar techniques are out of the scope of this thesis.

Probably the most important motivation for the application of optimization methods in the computation of CRN structures was that by using a properly constructed optimization framework, there is a chance of deciding feasibility and determine feasible solutions even if the underlying problem is algebraically hard to treat. Finally, it is emphasized that no new results in the theory or practice of optimization is proposed in this thesis, but certain presented results are based on the application of standard optimization methods.

## 1.2 Aims of the work

Based on the above short review of the state-of-the-art, the original aims of the performed work presented in this thesis can be summarized as:

1. **Analysis and control of QP and LV systems.** Since the QP models were first introduced and analyzed in the mathematical physics community, no connections with systems and control theory were introduced. Moreover, despite the simple

matrix structure of the models, very few computational results were available about this system class. These facts naturally raised the following questions. How this system class can be utilized in the modeling and analysis of physical systems appearing in engineering? Can we develop computational model analysis or controller design methods that make use of the structure of QP systems?

2. **Analysis of mass-action chemical reaction networks.** Although the phenomenon of dynamical equivalence was known and it was also clear that several basic model properties are realization-dependent, there were practically no constructive computation results about finding CRN realizations with prescribed properties. Therefore, it was expected that the development of such methods can be of significant interest. Moreover, it seemed to be exploitable that mass-action type deterministic CRN models form a special subset of QP systems.

3. **Hamiltonian representation of the studied systems.** Seeing the significance of Hamiltonian representation of dynamical systems, it was also challenging, how this kind of description can be applied to QP, LV and reaction kinetic systems and how it can be used for system analysis.

## 1.3 Structure and organization of the thesis

The structure of the thesis is the following. The basic notions and results previously known from literature and necessary to follow the forthcoming chapters are summarized in chapter 2. Chapters 3-7 contain the contributions of the author (with the exception of section 4.1 which introduces some further structures that are only used in that chapter). Chapter 3 presents analysis results in the fields of Hamiltonian description and the time-rescaling of QP and LV systems. Chapter 4 deals with a possible locally dissipative Hamiltonian structure in a certain CRN class. New results in the optimization-based computation of dynamically equivalent or linearly conjugate CRN structures are shown in chapters 5 and 6, while chapter 7 summarizes the most important new scientific contributions of the thesis. The operation of presented methods and algorithms will be illustrated by numerical examples, some of which can be found in the Appendix.

# Chapter 2

# Preliminaries

This chapter summarizes the basic notions and tools necessary to understand the results and methods described in chapters 3-6. For more information, the reader is referred to the cited textbooks and basic references.

## 2.1 Applied computation structures and methods

### 2.1.1 Linear and bilinear matrix inequalities

A (nonstrict) linear matrix inequality (LMI) is an inequality of the form

$$F(x) = F_0 + \sum_{i=1}^{m} x_i F_i \geq 0, \tag{2.1}$$

where $x \in \mathbb{R}^m$ is the variable and $F_i \in \mathbb{R}^{n\times n}$, $i = 0, \ldots, m$ are given symmetric matrices. The inequality symbol in (2.1) stands for the positive semidefiniteness of $F(x)$.

One of the most important properties of LMIs is the fact, that they form a convex constraint on the variables i.e. the set $\{x \mid F(x) \geq 0\}$ is convex. LMIs have been playing an increasingly important role in the field of optimization and control theory since a wide variety of different problems (linear and convex quadratic inequalities, matrix norm inequalities, convex constraints etc.) can be written as LMIs and there are computationally stable and effective (polynomial time) algorithms for their solution [14], [136].

A bilinear matrix inequality (BMI) is a diagonal block composed of $q$ matrix inequalities of the following form

$$G_0^i + \sum_{k=1}^{p} x_k G_k^i + \sum_{k=1}^{p}\sum_{j=1}^{p} x_k x_j K_{kj}^i \leq 0, \quad i = 1, \ldots, q \tag{2.2}$$

where $x \in \mathbb{R}^p$ is the decision variable to be determined and $G_k^i$, $k = 0, \ldots, p$, $i = 1, \ldots, q$ and $K_{kj}^i$, $k, j = 1, \ldots, p$, $i = 1, \ldots, q$ are symmetric, quadratic matrices.

The main properties of BMIs are that they are non-convex in $x$ (which makes their solution numerically much more complicated than that of linear matrix inequalities), and their solution is NP-hard [90]. However, there exist practically applicable and effective algorithms for BMI solution [97, 147].

### 2.1.2 Linear programming

Linear programming (LP) is an optimization technique, where a linear objective function is minimized/maximized subject to linear equality and inequality constraints [34, 35]. Beside numerous other fields, LP has been widely used in chemistry and chemical engineering in the areas of system analysis [11, 94], simulation [67] and design [96]. The standard form of linear programming problems that will be used in this thesis is the following

$$\begin{aligned} &\text{minimize} \quad c^T y && (2.3)\\ &\text{subject to:} \\ &\quad Ay = b && (2.4)\\ &\quad y \geq 0 && (2.5) \end{aligned}$$

where $y \in \mathbb{R}^n$ is the vector of decision variables, $c \in \mathbb{R}^n$ $A \in \mathbb{R}^{p \times n}$, $b \in \mathbb{R}^p$ are known vectors and matrices, and '$\geq$' in (2.5) means elementwise nonstrict inequality.

The feasibility of the simple LP problem (2.3)-(2.5) can be checked e.g. using the following necessary and sufficient condition.

**Theorem 2.1.1.** [34] Consider the auxiliary LP problem

$$\begin{aligned} &\text{minimize} \quad \sum_{i=1}^{p} z_i && (2.6)\\ &\text{subject to:} \\ &\quad Ax + z = b && (2.7)\\ &\quad y \geq 0, z \geq 0 && (2.8) \end{aligned}$$

where $z \in \mathbb{R}^p$ is a vector of auxiliary variables. There exists a feasible solution for the LP problem (2.3)-(2.5) if and only if the auxiliary LP problem (2.6)-(2.8) has optimal value 0 with $z_i = 0$ for $i = 1, \ldots, p$.

It is easy to see that $x = 0$, $z = b$ is always a feasible solution for (2.6)-(2.8). The above theorem will be useful for establishing that no feasible solution for a pure LP problem exists.

### 2.1.3 Mixed integer linear programming and propositional logic

A mixed integer linear program is the maximization or minimization of a linear function subject to linear constraints. A mixed integer linear program with $k$ variables (denoted by $y \in \mathbb{R}^k$) and $p$ constraints can be written as [119]:

$$\begin{aligned} &\text{minimize } c^T y \\ &\text{subject to:} \\ &A_1 y = b_1 \\ &A_2 y \leq b_2 && (2.9)\\ &l_i \leq y_i \leq u_i \text{ for } i = 1, \ldots, k \\ &y_j \text{ is integer for } j \in I,\ I \subseteq \{1, \ldots, k\} \end{aligned}$$

where $c \in \mathbb{R}^k$, $A_1 \in \mathbb{R}^{p_1 \times k}$, $A_2 \in \mathbb{R}^{p_2 \times k}$, and $p_1 + p_2 = p$.

If all the variables can be real, then (2.9) is a simple linear programming problem that can be solved in polynomial time. However, if any of the variables is integer, then the problem generally becomes NP-hard. In spite of this, there exist a number of free (e.g. YALMIP [110] or the GNU Linear Programming Kit [111]) and commercial (such as CPLEX or TOMLAB [81]) solvers that can efficiently handle many practical problems.

As it has been mentioned in the Introduction, statements in propositional calculus can be transformed into linear inequalities. The notations of the following summary are mostly from [12]. A statement, such as $x \leq 0$ that can have a truth value of "T" (true) or "F" false is called a *literal* and will be denoted by $S_i$. In Boolean algebra, literals can be combined into *compound statements* using the following *connectives*: "$\wedge$" (and), "$\vee$" (or), "$\sim$" (not), "$\rightarrow$" (implies), "$\leftrightarrow$" (if and only if), "$\oplus$" (exclusive or). The truth table for the previously listed connectives is given in Table 2.1.

A propositional logic problem, where a statement $S_1$ must be proved to be true given a set of compound statements containing literals $S_1, \ldots, S_n$, can be solved by means of a linear integer program. For this, logical variables denoted by $\delta_i$ ($\delta_i \in \{0, 1\}$) must be associated with the literals $S_i$. Then the original compound statements can be translated to linear inequalities involving the logical variables $\delta_i$. A list of equivalent compound statements and linear equalities or inequalities taken from [153] is shown in Table 2.2.

| $S_1$ | $S_2$ | $\sim S_1$ | $S_1 \vee S_2$ | $S_1 \wedge S_2$ | $S_1 \rightarrow S_2$ | $S_1 \leftrightarrow S_2$ | $S_1 \oplus S_2$ |
|---|---|---|---|---|---|---|---|
| T | T | F | T | T | T | T | F |
| T | F | F | T | F | F | F | T |
| F | T | T | T | F | T | F | T |
| F | F | T | F | F | T | T | F |

Table 2.1: Truth table

| compound statement | equivalent linear equality/inequality |
|---|---|
| $S_1 \vee S_2$ | $\delta_1 + \delta_2 \geq 1$ |
| $S_1 \wedge S_2$ | $\delta_1 = 1,\ \delta_2 = 1$ |
| $\sim S_1$ | $\delta_1 = 0$ |
| $S_1 \rightarrow S_2$ | $\delta_1 - \delta_2 \leq 0$ |
| $S_1 \leftrightarrow S_2$ | $\delta_1 - \delta_2 = 0$ |
| $S_1 \oplus S_2$ | $\delta_1 + \delta_2 = 1$ |

Table 2.2: Equivalent compound statements and linear equalities/inequalities

## 2.2 Positive (nonnegative) systems

The concepts and basic results in this short section are mostly taken from [22]. A function $f = [f_1 \ \ldots \ f_n]^T : [0, \infty)^n \rightarrow \mathbb{R}^n$ is called *essentially nonnegative* if, for all $i = 1, \ldots, n$, $f_i(x) \geq 0$ for all $x \in [0, \infty)^n$, whenever $x_i = 0$. In the linear case, when $f(x) = Ax$, the necessary and sufficient condition for essential nonnegativity is that the off-diagonal entries of $A$ are nonnegative (such a matrix is often called a *Metzler-matrix*).

Consider an autonomous nonlinear system

$$\dot{x} = f(x),\ x(0) = x_0 \tag{2.10}$$

where $f : \mathcal{X} \to \mathbb{R}^n$ is locally Lipschitz, $\mathcal{X}$ is an open subset of $\mathbb{R}^n$ and $x_0 \in \mathcal{X}$. Suppose that the nonnegative orthant $[0, \infty)^n = \overline{\mathbb{R}}^n_+ \subset \mathcal{X}$. Then the nonnegative orthant is invariant for the dynamics (2.10) if and only if $f$ is essentially nonnegative.

Quasi-polynomial and Lotka-Volterra models (section 2.3), and deterministic biochemical reaction networks (section 2.5) are well-known examples of essentially nonnegative systems.

## 2.3 Quasi-polynomial (QP) systems

### 2.3.1 Model form

Quasi-polynomial systems are systems of ODEs of the following form

$$\dot{y}_i = y_i \left( l_i + \sum_{j=1}^{m} A_{ij} \prod_{k=1}^{n} y_k^{B_{jk}} \right), \quad i = 1, \ldots, n, \tag{2.11}$$

where $y \in \text{int}(\mathbb{R}^n_+)$, $A \in \mathbb{R}^{n \times m}$, $B \in \mathbb{R}^{m \times n}$, $l_i \in \mathbb{R}$, $i = 1, \ldots, n$. Furthermore, $L = [l_1 \ \ldots \ l_n]^T$. Without the loss of generality we can assume that $\text{Rank}(B) = n$ and $m \geq n$ (see [79]).

Let us denote the *monomials* of (2.11) as

$$z_j = \prod_{k=1}^{n} y_k^{B_{jk}}, \quad j = 1, \ldots, m. \tag{2.12}$$

It can be easily calculated that the time derivatives of the monomials form a Lotka-Volterra system i.e.

$$\dot{z}_i = z_i(\lambda_i + \sum_{j=1}^{m} M_{ij} z_j), \quad i = 1, \ldots, m, \tag{2.13}$$

where $M = B \cdot A \in \mathbb{R}^{m \times m}$, $\lambda = (B \cdot L) \in \mathbb{R}^{m \times 1}$, and $z_i > 0$, i=1,..., m.

### 2.3.2 Transforming non-QP models into QP form

A wide class of nonlinear autonomous systems with smooth nonlinearities can be embedded into QP-form if they satisfy two requirements [76].

1. The set of nonlinear ODEs should be in the form:

$$\dot{y_s} = \sum_{i_{s1}, \ldots, i_{sn}, j_s} a_{i_{s1} \ldots i_{sn} j_s} y_1^{i_{s1}} \ldots y_n^{i_{sn}} f(\overline{y})^{j_s}, \tag{2.14}$$

$$y_s(t_0) = y_s^0, \qquad s = 1, \ldots, n$$

where $f(\overline{y})$ is some scalar valued function, which is not reducible to *quasi-monomial form* containing terms in the form of $\prod_{k=1}^{n} y_k^{\Gamma_{jk}}$, $j = 1, \ldots, m$ with $\Gamma$ being a real matrix.

2. Furthermore, we require that the partial derivatives of the model (2.14) fulfill:

$$\frac{\partial f}{\partial y_s} = \sum_{e_{s1},..,e_{sn},e_s} b_{e_{s1}..e_{sn}e_s} y_1^{e_{s1}} \dots y_n^{e_{sn}} f(\overline{y})^{e_s}.$$

The embedding is performed by introducing a *new auxiliary variable*

$$\eta = f^q \prod_{s=1}^{n} y_s^{p_s}, \qquad q \neq 0. \tag{2.15}$$

Then, instead of the non-quasi-polynomial nonlinearity $f$ we can write the original set of equations (2.14) into QP-form:

$$\dot{y_s} = \left( y_s \sum_{i_{s1},\dots,i_{sn},j_s} \left( a_{i_{s1}\dots i_{sn}j_s} \eta^{j_s/q} \prod_{k=1}^{n} y_k^{i_{sk}-\delta_{sk}-j_s p_k/q} \right) \right), \qquad s = 1,\dots,n, \tag{2.16}$$

where $\delta_{sk} = 1$ if $s = k$ and 0 otherwise. In addition, a new quasi-polynomial ODE appears for the new variable $\eta$:

$$\dot{\eta} = \eta \left[ \sum_{s=1}^{n} \left( p_s y_s^{-1} \dot{y_s} + \sum_{\substack{i_{s\alpha},j_s \\ e_{s\alpha},e_s}} a_{i_{s\alpha},j_s} b_{e_{s\alpha},e_s} q \eta^{(e_s+j_s-1)/q} \cdot \prod_{k=1}^{n} y_k^{i_{sk}+e_{sk}+(1-e_s-j_s)p_k/q} \right) \right],$$
$$\alpha = 1,\dots,n. \tag{2.17}$$

It is important to observe that the above embedding is not unique, because we can choose the parameters $p_s$ and $q$ in (2.15) in many different ways: the simplest solution is to choose ($p_s = 0,\ s = 1,...,n;\ q = 1$). Since the embedded QP system includes the original differential variables $y_i$, $i = 1,\dots,n$, it is clear that the stability of the embedded system (2.16)-(2.17) implies the stability of the original system (2.14).

### 2.3.3 Diagonal stabilizability and global stability of QP models

By the global stability of QP systems, we mean stability with respect to the positive orthant. Let us assume that the model (2.13) has at least one equilibrium point $y^*$ in the strictly positive orthant, and let us denote the corresponding equilibrium in the monomial space by

$$z^* = [z_1^* \quad z_2^* \quad \dots \quad z_m^*]^T.$$

The following Lyapunov function candidate is often used when studying the global stability properties of (2.13) and (2.11) [146].

$$V(z) = \sum_{i=1}^{m} c_i \left( z_i - z_i^* - z_i^* \ln \frac{z_i}{z_i^*} \right), \tag{2.18}$$

where $c_i > 0$, $i = 1,\dots,m$.

It can be calculated that the time derivative of $V$ satisfies

$$\dot{V}(z) = \frac{1}{2}(z - z^*)^T (M^T C + CM)(z - z^*), \tag{2.19}$$

where $C = \mathrm{diag}(c_1, \ldots, c_m)$. This means that if the linear matrix inequality

$$M^T C + CM \leq 0 \tag{2.20}$$

can be solved for a positive definite diagonal matrix $C$, then any solution of (2.11) starting in the positive orthant is bounded and componentwise bounded away from zero [54], since $V$ satisfies the requirements for being a Lyapunov function in the state-space of the original QP system (2.11), too. Naturally, in such a case $z^*$ is a globally stable equilibrium point of (2.13) with Lyapunov function (2.18), and this implies the global stability of $y^*$. In this case, we call $M$ a *diagonally stabilizable matrix*. Furthermore, if the inequality (2.20) is strict, then the stability of $z^*$ and $y^*$ is asymptotic ($M$ is *diagonally asymptotically stabilizable*). Moreover, it is shown it [54] that we can apply even milder conditions: if we assume (by appropriate ordering of the monomials) that the first $n$ rows of $B$ are linearly independent, then $c_i > 0$ for $i = 1, \ldots, n$ and $c_j \geq 0$ for $j = n+1, \ldots, m$ still guarantees the global stability of $y^*$.

Necessary and sufficient algebraic conditions of diagonal stabilizability are only available for $2 \times 2$ and $3 \times 3$ matrices [93], but it is true that a quadratic matrix $M$ is diagonally stabilizable if and only if the LMI (2.20) has a positive definite diagonal solution, i.e the LMI

$$-(M^T C + CM) \geq 0, \quad C > 0 \tag{2.21}$$

is feasible [14].

We remark that the diagonal stabilizability of a quadratic matrix is an important problem in different fields such as linear systems theory and also in other areas [95, 64, 93].

## 2.4 Generalized dissipative-Hamiltonian systems

The form of generalized dissipative Hamiltonian systems we will use is defined in [149]. In the autonomous case, this system class is given by the differential equations

$$\dot{x} = (J(x) - R(x))\mathcal{H}_x^T(x), \tag{2.22}$$

where $x \in \mathbb{R}^n$, $\mathcal{H} : \mathbb{R}^n \mapsto \mathbb{R}$ is the Hamiltonian function, $J(x)$ is an $n \times n$ skew symmetric matrix (i.e. $J^T(x) = -J(x)$), the energy conserving part of the system, and $R(x) = R^T(x)$ is the so called dissipation matrix. $\mathcal{H}_x$ denotes the gradient of $\mathcal{H}$ (row vector).

The time derivative of the Hamiltonian function is

$$\begin{aligned} \dot{\mathcal{H}} &= \mathcal{H}_x(x)(J(x) - R(x))\mathcal{H}_x^T(x) = \\ &\underbrace{\mathcal{H}_x(x)J(x)\mathcal{H}_x^T(x)}_{0} - \mathcal{H}_x(x)R(x)\mathcal{H}_x^T(x). \end{aligned} \tag{2.23}$$

In many cases, the $J$ matrix satisfies the Jacobi equations

$$\begin{aligned} &\sum_{l=1}^{n} \left[ J_{lj}(x)\frac{\partial J_{ik}}{\partial x_l}(x) + J_{li}(x)\frac{\partial J_{kj}}{\partial x_l}(x) + J_{lk}(x)\frac{\partial J_{ji}}{\partial x_l}(x) \right] = 0, \\ &i, j, k = 1, \ldots, n \end{aligned} \tag{2.24}$$

In this case, by Darboux's theorem, around any point $x_0$ where the rank of $J(x)$ is constant it's possible to find local coordinates

$$\bar{x} = \begin{bmatrix} q_1 & \ldots & q_k & p_1 & \ldots & p_k & s_1 & \ldots & s_l \end{bmatrix}^T \tag{2.25}$$

such that $J$ in the new coordinates has the form

$$J(\bar{x}) = \begin{bmatrix} 0 & I^k & 0 \\ -I^k & 0 & 0 \\ 0 & 0 & 0 \end{bmatrix} \tag{2.26}$$

where $I^k$ is a unit matrix of dimension $k \times k$, $\text{rank}(J) = 2k$, and $n = 2k + l$ (see, e.g. [151]). $J(\bar{x})$ in (2.26) is clearly symplectic if $\text{rank}(J(x)) = n$, $n$ is even, and the integrability conditions in (2.24) are satisfied. We note that even if the conditions of the local coordinates transformation (2.25) are not fulfilled, the skew symmetricity of $J$ still implies that $y^T J(x)y = 0$, $\forall x, y \in \mathbb{R}^n$, which means that $\mathcal{H}$ is a conserved quantity (first integral) of the system if $R = 0$. These facts motivate us to use the notion of *generalized Hamiltonian systems* and clearly show that this broader system class properly includes the class of classical Hamiltonian systems with symplectic structure.

It is visible from (2.23) that if $y^T R(x)y \geq 0$, $\forall x, y \in \mathbb{R}^n$ (i.e. $R$ is positive semidefinite), then the Hamiltonian function is nonincreasing. In this case, the model (2.22) is called a *(globally) dissipative-Hamiltonian* system. Of course, this property might be satisfied not globally, but only in some neighborhood of the equilibrium point (*locally dissipative-Hamiltonian* description). If there are no constraints about the local or global definiteness of $R$, the model is called a *pseudo-Hamiltonian* system [23]. It is important to note that in physical system models, the matrices $J(x)$ and $R(x)$ often reflect the physical structure or topology of the system [149].

## 2.5 Chemical reaction networks

### 2.5.1 Basic description of mass action reaction networks

The original physical picture underlying the reaction kinetic system class is a closed thermodynamic system with constant physico-chemical properties under isothermal and isobaric conditions, where chemical species $X_i,\ i = 1, ..., n$ take part in $r$ chemical reactions. The system is assumed to be perfectly stirred, i.e. concentrated parameter in the simplest case. The specie concentrations $x_i = [X_i],\ i = 1, ..., n$ form the state vector, the elements of which are non-negative by nature.

The origin of mass action law lies in the *molecular collision picture* of chemical reactions. Here the reaction occurs when either two reactant molecules collide, or a reactant molecule collides with an inactive (e.g. solvent) molecule. Clearly, the probability of having a reaction is proportional to the probability of collisions, that is proportional to the concentration of the reactant(s).

A straightforward generalization of the above molecular collision picture is when we allow to have multi-molecule collisions to obtain *elementary reaction steps* in the following form [83, 155]:

$$\sum_{i=1}^{n} \alpha_{ij} X_i \to \sum_{i=1}^{n} \beta_{ij} X_i, \quad j = 1, ..., r, \tag{2.27}$$

where the nonnegative integers $\alpha_{ij}, \beta_{ij}$ are the so-called *stoichiometric coefficient*s of component $X_i$ in the $j$th reaction. The linear combinations of the species in eq. (2.27), namely $\sum_{i=1}^{n} \alpha_{ij} X_i$ and $\sum_{i=1}^{n} \beta_{ij} X_i$ for $j = 1, \ldots, r$ are called the *complexes* and are denoted by $C_1, C_2, \ldots, C_m$. According to the extended molecular picture, the *reaction*

*rate* of the above reactions can be described as

$$\rho_j = k_j \prod_{i=1}^{n} [X_i]^{\alpha_{ij}} = k_j \prod_{i=1}^{n} x_i^{\alpha_{ij}} \quad , \quad j = 1, ..., r, \tag{2.28}$$

where $k_j > 0$ is the *reaction rate constant* (or *reaction rate coefficient*) of the $j$th reaction.

To further formalize the above description, following [49] and several other related works, we will also characterize CRNs with the following three sets.

1. $\mathcal{S} = \{X_1, \ldots, X_n\}$ is the set of *species* or chemical substances.

2. $\mathcal{C} = \{C_1, \ldots, C_m\}$ is the set of *complexes*. As it has been mentioned before, the complexes are represented as linear combinations of the species with nonnegative integer coefficients (see, eq. (2.27)).

3. $\mathcal{R} = \{(C_i, C_j) \mid C_i, C_j \in \mathcal{C},$ and $C_i$ is transformed to $C_j$ in the CRN$\}$ is the set of *reactions*. The relation $(C_i, C_j) \in \mathcal{R}$ will be denoted as $C_i \to C_j$. In this case, $C_i$ is called the *reactant* or *source complex*, and $C_j$ is the *product complex*. The nonnegative reaction rate coefficient is assigned to each reaction. When it is more convenient, we will index the reaction rate coefficients with a double index, i.e. $k_{ij}$ denotes the rate coefficient of the reaction $C_i \to C_j$.

During the numerical computations, the reaction rate coefficients of all possible reactions are often stored in matrices. In such a case, $k_{ij} = 0$ means that the reaction $C_i \to C_j$ is actually not taking place in the reaction network (i.e. $(C_i, C_j) \notin \mathcal{R}$), and the corresponding directed edge (with zero weight) is naturally not drawn in the reaction graph. If the reactions $C_i \to C_j$ and $C_j \to C_i$ are present at the same time in a reaction network for some $i, j$ then this pair of reactions is called a *reversible reaction* (but it will be treated as two separate elementary reactions in most of the forthcoming computations).

### 2.5.2 Graph representation of mass-action systems

The above description naturally gives rise to the following weighted directed graph structure [49] assigned to the CRN (2.27). The weighted directed graph $D = (V_d, E_d)$ of a reaction network (simply called the *reaction graph*) consists of a finite nonempty set $V_d$ of vertices and a finite set $E_d$ of ordered pairs of distinct vertices called directed edges. The vertices correspond to the complexes, i.e. $V_d = \{C_1, C_2, \ldots C_m\}$, while the directed edges represent the reactions, i.e. $(C_i, C_j) \in E_d$ if complex $C_i$ is transformed to $C_j$ in the reaction network. The reaction rates $k_j$ for $j = 1, \ldots, r$ in (2.28) are assigned as positive weights to the corresponding directed edges in the graph. A *walk* in the reaction graph is an alternating sequence $W = C_1 E_1 C_2 E_2 \ldots \; C_{k-1} E_{k-1} C_k E_k$ where $C_i \in V_d$, $E_i \in E_d$ for $i = 1, \ldots, k$. $W$ is a *directed path* if all the vertices in it are distinct. $P$ is called a *directed cycle* if the vertices $C_1, C_2, \ldots, C_{k-1}$ are distinct, $k \geq 3$ and $C_1 = C_k$.

A set of complexes $\{C_1, C_2, \ldots, C_k\}$ is a *linkage class* of a reaction network if the complexes of the set are linked to each other in the reaction graph but not to any other complex [50] (i.e. the individual linkage classes form the connected components of the directed graph $D$). Two different complexes are said to be *strongly linked* if there exists a directed path from one complex to the other, and a directed path from the second

complex back to the first. Moreover, each complex is defined to be strongly linked to itself. A *strong linkage class* is a set of complexes with the following properties: each pair of complexes in the set is strongly linked, and no complex in the set is strongly linked to a complex that is not in the set. A *terminal strong linkage class* is a strong linkage class that contains no complex that reacts to a complex in a different strong linkage class (i.e. there is no "exit" from a terminal strong linkage class through a directed edge).

A reaction network is called *reversible*, if whenever the reaction $C_i \to C_j$ exists, then the reverse reaction $C_j \to C_i$ is also present in the network. A reaction network is called *weakly reversible*, if each complex in the reaction graph lies on at least one directed cycle (i.e. if complex $C_j$ is reachable from complex $C_i$ on a directed path in the reaction graph, then $C_i$ is reachable from $C_j$ on a directed path). If the corresponding forward and backward reaction pairs form a cycle in the directed graph of a reversible CRN, then this cycle of reversible edge-pairs will be called a *circuit* to distinguish it from a directed cycle. E.g. the CRN in Fig. 2.3 d) contains a circuit of length 3, while the CRNs in Figs. 2.3 a), b) and c) do not contain any circuit. By the *structure of a CRN* we simply mean the unweighted directed graph of a reaction network.

### 2.5.3 Differential equations of mass-action systems

There are several possibilities to represent the dynamic equations of mass action systems (see, e.g. [49, 69, 28]. The most advantageous form for our purposes is the one that is used e.g. in Lecture 4 of [49], i.e.

$$\dot{x} = Y \cdot A_k \cdot \psi(x), \tag{2.29}$$

where $x \in \mathbb{R}^n$ is the concentration vector of the species, $Y \in \mathbb{R}^{n\times m}$ called the *complex composition matrix* stores the stoichiometric coefficients of the complexes, $A_k \in \mathbb{R}^{m\times m}$ contains the information corresponding to the weighted directed graph of the reaction network, and $\psi : \mathbb{R}^n \mapsto \mathbb{R}^m$ is a monomial-type vector mapping defined by

$$\psi_j(x) = \prod_{i=1}^{n} x_i^{Y_{ij}}, \quad j = 1, \ldots, m. \tag{2.30}$$

The exact structure of $Y$ and $A_k$ is the following. The $i$th column of $Y$ contains the composition of complex $C_i$, i.e. $Y_{ji}$ is the stoichiometric coefficient of $C_i$ corresponding to the specie $X_j$. $A_k$ is a column conservation matrix (i.e. the sum of the elements in each column is zero) defined as

$$[A_k]_{ij} = \begin{cases} -\sum_{l=1, l\neq i}^{m} k_{il}, & \text{if} \quad i = j \\ k_{ji}, & \text{if} \quad i \neq j. \end{cases} \tag{2.31}$$

Using the notions of the reaction graph, the diagonal elements $[A_k]_{ii}$ contain the negative sum of the weights of the edges starting from the node $C_i$, while the off-diagonal elements $[A_k]_{ij}$, $i \neq j$ contain the weights of the directed edges $(C_j, C_i)$ coming into $C_i$. Based on the above properties, it is appropriate to call $A_k$ the *Kirchhoff matrix* or *kinetics matrix* of a reaction network.

To handle the exchange of materials between the environment and the reaction network, the so-called "zero-complex" can be introduced and used which is a special complex with all the stoichiometric coefficients zero i.e., it is represented by a zero vector in the $Y$ matrix (for the details, see, e.g. [49] or [26]).

We can associate an $n$-dimensional vector with each reaction in the following way. For the reaction $C_i \to C_j$, the corresponding reaction vector denoted by $e_k$ is given by

$$e_k = [Y]_{\cdot,j} - [Y]_{\cdot,i}, \ k = 1, \ldots, r, \tag{2.32}$$

where $[Y]_{\cdot,i}$ denotes the $i$th column of $Y$. Any convention can be used for the numbering of the reaction vectors (e.g. the indices $i$ and $j$ in (2.32) can be treated as digits in a decimal system). The *rank* of a reaction network denoted by $s$ is defined as the rank of the vector set $H = \{e_1, e_2 \ldots, e_r\}$ where $r$ is the number of reactions. The elements of $H$ span the so-called *stoichiometric subspace*, denoted by $S$, i.e. $S = \text{span}\{e_1, \ldots, e_r\}$. The positive *stoichiometric compatibility class* containing a concentration $x_0$ is the following set [50]:

$$(x_0 + S) \cap \mathbb{R}^n_+,$$

where $\mathbb{R}^n_+$ denotes the positive orthant in $\mathbb{R}^n$. The deficiency $d$ of a reaction network is defined as [49, 50]

$$d = m - l - s, \tag{2.33}$$

where $m$ is the number of complexes in the network, $l$ is the number of linkage classes and $s$ is the rank of the reaction network. The deficiency is a very useful tool for studying the dynamical properties of reaction networks and for establishing parameter-independent global stability conditions (see subsection 2.5.6 below).

Using the notation

$$M = Y \cdot A_k, \tag{2.34}$$

equation (2.29) can be written in the form

$$\dot{x} = M \cdot \psi(x), \tag{2.35}$$

where $M$ contains the coefficients of the monomials in the polynomial ODE (2.29) describing the time-evolution of the concentrations. Using the notation $\Sigma$ for a given CRN, it is clear from the above description that the system's reaction graph and the corresponding dynamics can be characterized either by the triplet $(\mathcal{S}, \mathcal{C}, \mathcal{R})$ or equivalently by the matrix pair $(Y, A_k)$, therefore we can use the notations $\Sigma = (\mathcal{S}, \mathcal{C}, \mathcal{R})$ or $\Sigma = (Y, A_k)$. The following example illustrates the introduced basic notions on CRNs.

**Example 2.5.1.** Consider the reaction network the graph of which is shown in Fig. 2.1 with the parameters:

$$k_1 = 1, k_2 = 1.1, k_3 = 1, k_4 = 1, k_5 = 1.1, k_6 = 0.1, k_7 = 3, k_8 = 1.$$

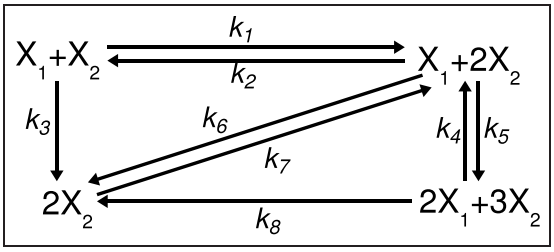


Figure 2.1: Simple reaction network of Example 2.5.1

Let us number the complexes as

$$C_1 = X_1 + X_2,\ C_2 = X_1 + 2X_2,\ C_3 = 2X_2,\ C_4 = 2X_1 + 3X_2.$$

Then the matrices of the description (2.29) are the following:

$$Y = \begin{bmatrix} 1 & 1 & 0 & 2 \\ 1 & 2 & 2 & 3 \end{bmatrix},\quad A_k = \begin{bmatrix} -2 & 1.1 & 0 & 0 \\ 1 & -2.3 & 3 & 1 \\ 1 & 0.1 & -3 & 1 \\ 0 & 1.1 & 0 & -2 \end{bmatrix} \tag{2.36}$$

$$M = YA_k = \begin{bmatrix} -1 & 1 & 3 & -3 \\ 2 & 0 & 0 & -2 \end{bmatrix}. \tag{2.37}$$

### 2.5.4 Simple algebraic condition for weak reversibility

We recall the following classical result about weakly reversible networks, which is adapted from Theorem 3.1 of [63] and Proposition 4.1 of [49]:

**Theorem 2.5.1.** Let $\ell$ be the number of linkage classes in a CRN, $A_k$ be a kinetics matrix and let $\Lambda_i$, $i = 1, \ldots, \ell$, denote the support of the $i$th linkage class (i.e. the index $j \in \Lambda_i$ if and only if the complex $C_j$ belongs to the $i$th linkage class). Then the reaction graph corresponding to $A_k$ is weakly reversible if and only if there is a basis of $\ker(A_k)$, $\left\{b^{(1)}, \ldots, b^{(\ell)}\right\}$, such that, for $i = 1, \ldots, \ell$,

$$b^{(i)} = \begin{cases} b_j^{(i)} > 0, & j \in \Lambda_i \\ b_j^{(i)} = 0, & j \notin \Lambda_i. \end{cases}$$

An immediate consequence of Theorem 2.5.1 is that there is a vector $b \in \mathbb{R}^m_{>0} \cap \ker(A_k)$ if and only if the reaction graph corresponding to $A_k$ is weakly reversible.

### 2.5.5 Kinetic realizability of nonnegative systems

An autonomous polynomial nonlinear system of the form (2.10) is called *kinetically realizable* or simply *kinetic*, if a mass action reaction mechanism given by eq. (2.29) can be associated to it that exactly realizes its dynamics, i.e. $f(x) = Y \cdot A_k \cdot \psi(x)$ where $\psi$ contains the monomials, the columns of matrix $Y$ contain the exponents of the monomials, and $A_k$ is a valid Kirchhoff matrix (see subsection 2.5.3 for its properties). In such a case, the pair $(Y, A_k)$ will be called a *realization* of the system (2.35). As it is expected from linear algebra, the same kinetic polynomial system may have many parametrically and/or structurally different realizations, and this is particularly true for kinetic systems coming from application domains other than chemistry.

The problem of kinetic realizability of polynomial vector fields was first examined and solved in [86] where the constructive proof contains a realization algorithm that produces the weighted directed graph of a possible associated mass action mechanism (called the *canonic mechanism*). According to [86], the necessary and sufficient condition for kinetic realizability of a polynomial vector field is that all coordinates functions of $f$ in (2.10) must have the form

$$f_i(x) = -x_i g_i(x) + h_i(x),\ i = 1, \ldots, n \tag{2.38}$$

where $g_i$ and $h_i$ are polynomials with nonnegative coefficients.

The very short description of the realization algorithm presented in [86] is the following. Let us write the polynomial coordinate functions of the right hand side of a kinetic system (2.10) as

$$f_i(x) = \sum_{j=1}^{r_i} m_{ij} \prod_{k=1}^{n} x^{b_{jk}}, \tag{2.39}$$

where $r_i$ is the number of monomial terms in $f_i$. Let us denote the transpose of the $i$th standard basis vector in $\mathbb{R}^n$ as $e_i$ and let $B_j = [b_{j1} \ \dots \ b_{jn}]$.

**Algorithm 1** for constructing the canonic mechanism [86]
For each $i = 1, \dots, n$ and for each $j = 1, \dots, r_i$ do:

1. $C_j = B_j + \text{sign}(m_{ij}) \cdot e_i$
2. Add the following reaction to the graph of the realization

$$\sum_{k=1}^{n} b_{jk} X_k \longrightarrow \sum_{k=1}^{n} c_{jk} X_k$$

with reaction rate coefficient $|m_{ij}|$, where $C_j = [c_{j1} \ \dots \ c_{jn}]$.

Roughly speaking, condition (2.38) means that kinetic systems cannot contain negative cross-effects. From this, it is easy to see that all nonnegative linear systems are kinetic, since a linear system characterized by a Metzler matrix where only the diagonal elements can have negative coefficients is obviously in the form of (2.38). Moreover, classical Lotka-Volterra systems with the equations (2.13) are always kinetic according to the condition (2.38). However, there are many essentially nonnegative polynomial systems that are not directly kinetic, since some of the monomials in $f_i$ that do not contain $x_i$ have negative coefficients. Such an example is shown in the following equations

$$\begin{aligned} \dot{x}_1 &= -x_1 x_2 + x_2^2 - 4x_2 + 4 \\ \dot{x}_2 &= x_2^2 + x_1^2 - 2x_1 + 2 \end{aligned} \tag{2.40}$$

To circumvent this problem, one possible way is to embed the QP system (2.40) into the LV class shown in (2.13), that can be done algorithmically (see section 2.3 and [76]). However, this solution usually results in the significant dimension increase of the state space (i.e. in the increase of species in the corresponding kinetic realization). If the equations and the possible initial conditions guarantee that all state variables remain strictly positive throughout the solutions, then a generally more advantageous method is a simple state-dependent time-rescaling (see, e.g [J3]) of the equations in the following way

$$dt = \prod_{i=1}^{n} \chi_i x_i dt' \tag{2.41}$$

where $\chi_i \in \{0,1\}$ for $i = 1,\ldots,n$ can always be chosen such that the rescaled system is kinetic. Applying (2.41) with $\chi_1 = \chi_2 = 1$, the equations of the original system (2.40) are written as

$$\begin{aligned} x_1' &= -x_1^2x_2^2 + x_1x_2^3 - 4x_1x_2^2 + 4x_1x_2 \\ x_2' &= x_1x_2^3 + x_1^3x_2 - 2x_1^2x_2 + 2x_1x_2 \end{aligned} \tag{2.42}$$

where $x_i' = \frac{dx_i}{dt'}$. It is easy to see that eq. (2.42) is kinetic. The reaction network obtained by using **Algorithm 1** can be seen in Fig. 2.2 where the reaction rate coefficients are written close to the arrows representing reactions. It is important to emphasize that as a result of the time-rescaling, the number of state variables (species) and that of the monomials (complexes) remain the same as in the original system. Moreover, such a time-rescaling preserves many important qualitative properties of the system and the solutions, since $t'$ is a strictly monotonously increasing continuous and invertible function of $t$. (But generally it does not preserve e.g. the eigenvalues of the state matrix of the linearized system as it is shown in subsection 3.2.2. This means that it depends on the particular application and problem class whether such a time-rescaling can be allowed or not.

As we can see later in certain examples of chapter 6, the canonic mechanism produced by **Algorithm 1** has usually more reactions and/or complexes than the minimal number needed for the kinetic representation of the studied polynomial system. Therefore, optimization will be applied in chapters 5 and 6 to select preferred structures from the possible reaction graphs. The main significance of **Algorithm 1** from our point of view is that it is able to generate a feasible set of complexes for the CRN representation of a kinetic polynomial system.

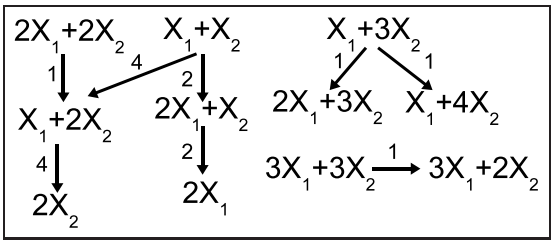


Figure 2.2: Canonic reaction network realizing eq. (2.42)

### 2.5.6 The Deficiency Zero and Deficiency One Theorems

The exact forms of the Deficiency Zero and Deficiency One Theorems are taken from [50].

**Theorem 2.5.2. Deficiency Zero Theorem**
For any reaction network of deficiency zero the following statements hold true:

1. If the network is not weakly reversible then, for arbitrary kinetics (not necessarily mass action), the differential equations for the corresponding reaction system cannot admit a positive steady state (i.e. a steady state in $\mathbb{R}_+^n$).

2. If the network is not weakly reversible then, for arbitrary kinetics (not necessarily mass action), the differential equations of the corresponding reaction system cannot admit a cyclic composition trajectory along which all species concentrations are positive.

3. If the network is weakly reversible then, for mass action kinetics (but regardless of the positive values the reaction rate coefficients take), the differential equations of the corresponding reaction system have the following properties: There exists within each positive stoichiometric compatibility class precisely one steady state; that steady state is asymptotically stable; and there is no nontrivial cyclic composition trajectory along which all species concentrations are positive.

**Theorem 2.5.3. Deficiency One Theorem**
Consider a mass action system for which the underlying reaction network has $\ell$ linkage classes, each containing just one terminal strong linkage class. Suppose that the deficiency $d$ of the network and the deficiencies of the individual linkage classes $d_i$, $i = 1, \ldots, \ell$ satisfy the following conditions:

1. $d_i \leq 1, \quad i = 1, \ldots, \ell$
2. $\sum_{i=1}^{\ell} d_i = d$

Then, no matter what (positive) values the reaction rate coefficients take, the corresponding differential equations can admit no more than one steady state within a positive stoichiometric compatibility class. If the network is weakly reversible, the differential equations admit precisely one steady state in each positive stoiciometric compatibility class.

The above theorems establish very strong results about the qualitative dynamical properties of kinetic systems that are also robust with respect to the parameters (i.e. the reaction rate coefficients) and depend on the structure and on the stoichiometry of the system.

The logarithmic Lyapunov function for the system in the case of the Deficiency Zero Theorem is the following:

$$B(x) = \sum_{i=1}^{n} x_i \left( \ln \left( \frac{x_i}{x_i^*} \right) - 1 \right) + x_i^*, \tag{2.43}$$

where $x^*$ denotes the equilibrium point in the given stoichiometric compatibility class.

We add the important fact that the stability of the system in the case of the Deficiency Zero Theorem is global if the CRN has one linkage class [4], since the deficiency zero property and weak reversibility implies complex balance (see also the following subsection).

It is also worth mentioning the following significant control related results on weakly reversible deficiency zero networks. In [21] the detectability of such systems was studied and nonlinear observers were proposed for them with proven convergence under mild conditions. It was shown in [20] that weakly reversible deficiency zero networks are input-to-state stable if the (non-vanishing) manipulable inputs are the reaction rate coefficients.

It must be stressed that by distanting ourselves from the original chemical motivations, we consider kinetic models as a general nonlinear system class, and do not require in general that such models describe a chemically strictly feasible reaction mechanism. Thus, it is allowed that certain thermodynamical constraints (such as component mass balance conservation) are not fulfilled in the examined models.

### 2.5.7 Detailed balance and complex balance

The original definition of detailed balance and complex balance came from the problem statement of the thermodynamical compatibility of kinetic system models [83, 82, 18]. However, we will be mainly interested in the stability implications of these important properties.

**Definition 2.5.1.** A CRN realization $(Y, A_k)$ is called complex balanced at $x^* \in \mathbb{R}^n_+$, if

$$A_k \psi(x^*) = 0. \tag{2.44}$$

**Definition 2.5.2.** A reversible CRN realization $(Y, A_k)$ is called detailed balanced at $x^* \in \mathbb{R}^n_+$, if

$$\rho_{ij}(x^*) = \rho_{ji}(x^*), \quad \forall i, j \text{ such that } C_i \leftrightarrows C_j \text{ exists}, \tag{2.45}$$

i.e. the forward and reverse reaction rates for each reversible reaction are equal at $x^*$.

Clearly, if a CRN is complex balanced at $x^*$, then $x^*$ is an equilibrium point, i.e. $Y A_k \psi(x^*) = 0$. Furthermore, it is easy to check that detailed balancing at $x^*$ implies complex balancing at $x^*$ for reversible networks, but the converse is generally not true.

**Definition 2.5.3.** A reversible CRN realization $(Y, A_k)$ is called complex balanced (detailed balanced), if it is complex balanced (detailed balanced) at each positive steady state.

It is important to remark that both the complex balance and detailed balance properties depend on the structure of the reaction digraph and on the numerical values of the reaction rate coefficients [25]. In [51], necessary and sufficient conditions were given for detailed balancing (see also [118] for a clear explanation of conditions) using the graph theoretical circuit and spanning forest conditions below. The *circuit conditions* require that the product of the reaction rate coefficients should be equal taken in either directions along a circuit. The *spanning forest conditions* say that

$$\prod (k_{ij})^{\gamma_{ij}} = \prod (k_{ji})^{\gamma_{ij}}, \tag{2.46}$$

where the products are taken for each reaction step in the spanning forest of the reaction digraph and $\gamma$ denotes the solutions of the equation

$$\sum_{i,j} \gamma_{ij} v_{ij} = 0, \quad \text{for all } i, j \text{ such that } C_i \longrightarrow C_j \text{ exists}, \tag{2.47}$$

and $v_{ij}$ is the reaction vector of the reaction $C_i \longrightarrow C_j$.

It is worth summarizing the following important properties and relations of detailed and complex balancing collected from [48, 82, 51, 72, 25, 36].

**P1** If there is no circuit in the reaction graph, then the spanning forest condition is alone necessary and sufficient for detailed balancing.

**P2** If the deficiency of the CRN is zero, then the circuit condition is necessary and sufficient for detailed balancing.

**P3** If the deficiency of the CRN is zero, and there is no circuit in the reaction digraph, then the reaction is detailed balanced.

**P4** If the circuit conditions are satisfied in a reversible CRN containing at least one circuit, then detailed balancing and complex balancing are equivalent.

**P5** If a CRN is complex balanced (detailed balanced) at any positive $x^*$ then it is complex balanced (detailed balanced) at all other positive equilibrium points.

**P6** If a CRN is complex balanced then it is weakly reversible.

**P7** A CRN is complex balanced for any positive values of reaction rate coefficients if and only if a) it is weakly reversible, and b) the deficiency of the system is zero.

**P8** If a CRN is complex balanced then there is precisely one equilibrium point in each stoichiometric compatibility class. Furthermore, each equilibrium point is at least locally stable with a known strict Lyapunov function.

### 2.5.8 Dynamical equivalence: possible structural non-uniqueness of CRNs

The following simple example is given to help understanding the significance of dynamical equivalence in mass action CRNs.

**Example 2.5.2.** Consider the simple reaction mechanism depicted in Fig. 2.3 a). It is easy to check that the reaction structures in Figs 2.3 b), c), d) and e) lead to the same dynamical description as the original structure a), namely

$$\begin{aligned} \dot{x}_1 &= 3k_1x_2^3 - k_2x_1^3 \\ \dot{x}_2 &= -3k_1x_2^3 + k_2x_1^3, \end{aligned} \tag{2.48}$$

for any $k_1, k_2 > 0$, $l_0 > 0$, $l_1 < \frac{3k_1}{2}$, $l_2 < k_2$ and $l_3 > 0$ (i.e. the CRNs in Fig. 2.3 are dynamically equivalent). It is worth having a look at the structural properties of the different realizations of eq. (2.48) shown in the subfigures. The realizations in Figs. 2.3.a) and b) are irreversible, the structure in Fig. 2.3.c) is weakly reversible, while the networks in Figs. 2.3.d) and e) are fully reversible. The deficiencies of the first four realizations a)–d) are 1, while the deficiency of realization e) is zero. This means that both the weaker Deficiency One Theorem and the stronger Deficiency Zero Theorem can be applied to all realizations a)–e), and this way to the dynamical system described by eq. (2.48) (see [50]). Shortly speaking, the Deficiency One Theorem for such weakly reversible networks as c) says that its differential equations admit precisely one steady state in each positive stoichiometric compatibility class. Moreover, by applying the Deficiency Zero Theorem to realization e) together with the recent important results in [4], we obtain the additional valuable fact that for any positive $k_1$ and $k_2$, each steady state of (2.48) is globally asymptotically stable within the corresponding positive stoichiometric compatibility class with the Lyapunov function (2.43), where the term "globally" refers to the positive orthant.

First of all, the above example shows very transparently that important structural properties such as deficiency, reversibility or weak reversibility are not encoded uniquely in the polynomial differential equations of a kinetic system i.e. they are realization properties. (In chapter 5, it will be illustrated that the number of linkage

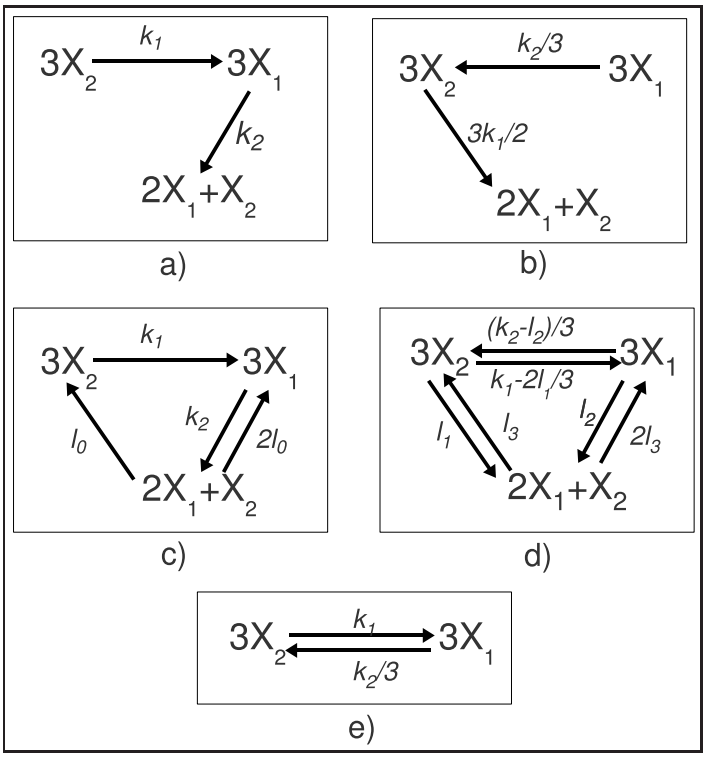


Figure 2.3: Dynamically equivalent reaction networks

classes and the detailed/complex balanced properties can also change with different realizations.) Among the concluding open questions of [86] (where the authors gave necessary and sufficient conditions for polynomial ODEs to be kinetic together with a constructive proof) we can read the following: "*We may look for a mechanism in a class of mechanisms with a given - chemically relevant - property. Such a property may be conservativity, (weak) reversibility, zero deficiency or just structural stability as well.*" Therefore, it is definitely of interest to develop computational tools to search for realizations with such properties that are useful in the dynamical analysis of given kinetic polynomial systems or CRNs.

We will call two reaction networks given by the matrix pairs $(Y^{(1)}, A_k^{(1)})$ and $(Y^{(2)}, A_k^{(2)})$ *dynamically equivalent*, if

$$Y^{(1)}A_k^{(1)}\psi^{(1)}(x) = Y^{(2)}A_k^{(2)}\psi^{(2)}(x) = f(x), \quad \forall x \in \overline{\mathbb{R}}_+^n \tag{2.49}$$

where for $i = 1, 2$, $Y^{(i)} \in \mathbb{R}^{n\times m_i}$ have nonnegative integer entries, $A_k^{(i)}$ are valid Kirchhoff matrices, and

$$\psi_j^{(i)}(x) = \prod_{k=1}^{n} x_k^{[Y^{(i)}]_{kj}}, \quad i = 1, 2, \ j = 1, \ldots, m_i. \tag{2.50}$$

In this case, $(Y^{(i)}A_k^{(i)})$ for $i = 1, 2$ are called *dynamically equivalent realizations* of the corresponding kinetic vector field $f$. It is also appropriate to call $(Y^{(1)}, A_k^{(1)})$ a *(dynamically equivalent) realization* of $(Y^{(2)}, A_k^{(2)})$ and vice versa.

### 2.5.9 Linear conjugacy of reaction networks

In [91] the authors extended the concept of dynamical equivalence to linear conjugacy. In their framework, two CRNs denoted by $\Sigma$ and $\Sigma'$ are said to be linearly conjugate

if there is a positive diagonal linear mapping which takes the flow of one network to the other. Dynamical equivalence is encompassed as a special case of linear conjugacy taking the transformation to be the identity.

Importantly, linearly conjugate networks share the same qualitative dynamics (e.g. number and stability of equilibria, persistence/extinction of species, dimensions of invariant spaces, etc.). Similarly to different realizations of the same kinetics (2.29), if a network with unknown kinetics is linearly conjugate to a network with known dynamics, then the qualitative properties of the second network are transferred to the first. The main result of [91] is the following.

**Theorem 2.5.4.** [91] Consider two mass-action systems $\Sigma = (\mathcal{S}, \mathcal{C}, \mathcal{R})$ and $\Sigma' = (\mathcal{S}, \mathcal{C}', \mathcal{R}')$ and let $Y$ be the stoichiometric matrix corresponding to the complexes in either network. Consider a kinetics matrix $A_k$ corresponding to $\Sigma$ and suppose that there is a kinetics matrix $A_b$ with the same structure as $\Sigma'$ and a vector $c \in \mathbb{R}^n_{>0}$ such that

$$Y \cdot A_k = T \cdot Y \cdot A_b \tag{2.51}$$

where $T = \text{diag}\{c\}$. Then $\Sigma$ is linearly conjugate to $\Sigma'$ with kinetics matrix

$$A'_k = A_b \cdot \text{diag}\left\{\psi(c)\right\}. \tag{2.52}$$

It is useful to summarize the proof below with notations adapted to this thesis.

*Proof.* Let $\Phi(x_0, t)$ correspond to the flow of (2.29) associated to the reaction network $\mathcal{N}$. Consider the linear mapping $\mathbf{h}(x) = T^{-1} \cdot x$ where $T = \text{diag}\{c\}$. Now define $\tilde{\Phi}(y_0, t) = T^{-1} \cdot \Phi(x_0, t)$ so that $\Phi(x_0, t) = T \cdot \tilde{\Phi}(y_0, t)$.

Since $\Phi(x_0, t)$ is a solution of (2.29) we have

$$\begin{aligned}
\frac{d}{dt}\tilde{\Phi}(y_0, t) &= T^{-1} \cdot \frac{d}{dt}\Phi(x_0, t) \\
&= T^{-1} \cdot Y \cdot A_k \cdot \psi(\Phi(x_0, t)) \\
&= T^{-1} \cdot T \cdot Y \cdot A_b \cdot \psi(T \cdot \tilde{\Phi}(y_0, t)) \\
&= Y \cdot A_b \cdot \text{diag}\left\{\psi(c)\right\} \cdot \psi(\tilde{\Phi}(y_0, t)).
\end{aligned}$$

It is clear that $\tilde{\Phi}(y_0, t)$ is the flow of (2.29) corresponding to the reaction network $\Sigma'$ with the kinetics matrix given by (2.52). We have that $\mathbf{h}(\Phi(x_0, t)) = \tilde{\Phi}(\mathbf{h}(x_0), t)$ for all $x_0 \in \mathbb{R}^n_{>0}$ and $t \geq 0$ where $y_0 = \mathbf{h}(x_0)$ since $y_0 = \tilde{\Phi}(y_0, 0) = T^{-1} \cdot \Phi(x_0, 0) = T^{-1} \cdot x_0$. It follows that the networks $\Sigma$ and $\Sigma'$ are linearly conjugate. □

It is important to remark that linear conjugacy is a special case of the general kinetic transformation (lumping) schemes analyzed e.g. in [105, 148, 47].

### 2.5.10 Three important conjectures

Chemists and chemical engineers usually accept the following three conjectures by intuition, although neither of them has been proved completely (except for special cases) until the time of writing this dissertation. Significant effort has been made in the last decades for general proofs, but it seems to be technically challenging in all three cases [25].

The *Global Attractor Conjecture* says that for any complex balanced CRN and any initial condition $x(0) \in \mathbb{R}^n_+$, the equilibrium point $x^*$ is a global attractor in the corresponding positive stoichiometric compatibility class.

A nonnegative dynamical system is called *persistent*, if no trajectory that starts in the positive orthant has an $\omega$-limit point on the boundary of $\mathbb{R}^n_+$. Chemically, persistence means that no species "die out" during the operation of the system. According to the *Persistency Conjecture*, any weakly reversible mass-action system is persistent. (Sometimes a weaker version of this conjecture is given with the additional assumption that the weakly reversible system has bounded trajectories.)

The *Boundedness Conjecture* says that any weakly reversible reaction network with mass-action kinetics has bounded trajectories. The Deficiency Zero and Deficiency One Theorems (see subsection 2.5.6) together with the Boundedness Conjecture underline the importance of weak reversibility. Seeing this, it is understandable why the following is written in [91]: "*The development of algorithms and computer software which can efficiently check for viable weakly reversible target networks ... is a primary interest*". In sections 6.3 and 6.4, two different numerical solutions for this problem will be given.

There are important relations between the notions related to the above mentioned conjectures. Firstly, it is known that complex balance implies weak reversibility [83]. Moreover, each trajectory of a complex balanced system remains bounded. Most importantly, it follows from the results in [141] that if the Persistency Conjecture were true, it would imply the Global Attractor Conjecture. Very recent results are that both the Global Attractor Conjecture and the Boundedness conjecture were successfully proved for one linkage class reaction networks by the same author [4, 3].

The above outlined results further support the motivation and significance of finding CRN realizations with required properties which is the topic of chapters 5 and 6. In particular, the finding of dynamically equivalent or "dynamically similar" complex balanced or weakly reversible structures is of significant interest.

# Chapter 3

# Analysis results for quasi-polynomial systems

This chapter presents new results in the field of the dynamic analysis of QP systems. Section 3.1 describes an interesting connection between the global stability and the existence of a Hamiltonian structure in QP systems. In section 3.2, a frequently used time-rescaling transformation is studied from a computational point of view. Section 3.3 shortly summarizes additional related results that could not be fit into the thesis in full detail due to length constraints. The main motivating factors of the work are described in chapter 1, while the basic notions corresponding to QP systems can be found in section 2.3.

## 3.1 Global stability and quadratic Hamiltonian structure in Lotka-Volterra sytems

For the dissipative-Hamiltonian description of LV systems, the definitions and notations of sections 2.3 and 2.4 will be used.

### 3.1.1 Dissipative Hamiltonian description of LV systems with a quadratic Hamiltonian function

Similarly to subsection 2.3.3, let us assume again that the LV model (2.13) has an equilibrium point in the strictly positive orthant and denote the equilibrium point of interest with $z^*$. For the forthcoming calculations, it is comfortable to apply a coordinates shift to place the equilibrium into the origin in the new coordinates, i.e. let us define the vector of new variables as

$$x = z - z^*. \tag{3.1}$$

With this transformation, the model (2.13) in the new coordinates reads

$$\begin{aligned}\dot{x}_i &= (x_i + z_i^*)\left(\lambda_i + \sum_{j=1}^{m} M_{ij}(x_j + z_j^*)\right) = \\ &(x_i + z_i^*)\left(\underbrace{\lambda_i + \sum_{j=1}^{m} M_{ij} z_j^*}_{0} + \sum_{j=1}^{m} M_{ij} x_j\right) = \\ &(x_i + z_i^*)\sum_{j=1}^{m} M_{ij} x_j, \quad i = 1, \ldots, m.\end{aligned} \tag{3.2}$$

Consider a quadratic Hamiltonian function candidate

$$\mathcal{H}(x) = \frac{1}{2}(h_1 x_1^2 + h_2 x_2^2 + \cdots + h_m x_m^2), \tag{3.3}$$

where $h_i \in \mathbb{R},\ i = 1, \ldots, m$. The gradient of $\mathcal{H}$ is then

$$\mathcal{H}_x(x) = [h_1 x_1 \quad h_2 x_2 \quad \ldots \quad h_m x_m]. \tag{3.4}$$

Then the system model (3.2) can be written as

$$\dot{x} = \Gamma(x) M H^{-1} \mathcal{H}_x^T(x), \tag{3.5}$$

where

$$M = \begin{bmatrix} M_{11} & M_{12} & \ldots & M_{1m} \\ M_{21} & M_{22} & \ldots & M_{2m} \\ \vdots & & & \vdots \\ M_{m1} & M_{m2} & \ldots & M_{mm} \end{bmatrix}, \tag{3.6}$$

$$\Gamma(x) = \operatorname{diag}(x_i + z_i^*) = \begin{bmatrix} (x_1 + z_1^*) & 0 & \ldots & 0 \\ 0 & (x_1 + z_2^*) & \ldots & 0 \\ \vdots & \vdots & \vdots & \vdots \\ 0 & \ldots & 0 & (x_m + z_m^*) \end{bmatrix} \tag{3.7}$$

and

$$H = \operatorname{diag}(h_1, \ldots, h_m). \tag{3.8}$$

Let us use the notation $S(x) = \Gamma(x) M H^{-1}$. Now we decompose $S(x)$ to a skew symmetric and a symmetric part in the following way

$$S(x) = \frac{1}{2}\left(\underbrace{S(x) - S^T(x)}_{\text{skew symm.}} + \underbrace{S(x) + S^T(x)}_{\text{symm.}}\right). \tag{3.9}$$

Therefore $R(x) = -\frac{1}{2}(S(x) + S^T(x))$ in our model. This means that the dissipative Hamiltonian structure can be investigated through studying the definiteness of $S(x) + S^T(x)$.

We note that also in this special case, the Jacobi equations (2.24) are not necessarily fulfilled for $J(x) = (S(x) - S^T(x))/2$, but the skew symmetric property of $J$ is enough for the derivation of the forthcoming results.

It is useful to further decompose $\Gamma(x)$ as

$$\Gamma(x) = X + Z^*, \tag{3.10}$$

where $X = \mathrm{diag}(x_i)$, $Z^* = \mathrm{diag}(z_i^*)$, $i = 1, \ldots, m$. Then we can write

$$S(x) + S^T(x) = \Gamma(x)MH^{-1} + H^{-1}M^T\Gamma^T(x) = \tag{3.11}$$
$$XMH^{-1} + H^{-1}M^TX + Z^*MH^{-1} + H^{-1}M^TZ^*. \tag{3.12}$$

Since $X$ and $Z^*$ are diagonal (and therefore symmetric), the positive semidefiniteness of $R(x)$ in (2.22) leads to the following matrix inequality

$$XMH^{-1} + H^{-1}M^TX \leq -(Z^*MH^{-1} + H^{-1}M^TZ^*). \tag{3.13}$$

There are in principle two sets of unknowns in the above matrix inequality: the coefficients of the Hamiltonian function in $H^{-1}$ and the state variables in the matrix $X$. In these two sets, (3.13) is clearly a bilinear matrix inequality.

Since we are interested in the local dissipative-Hamiltonian description of the system around the equilibrium point, first we solve (3.13) for a positive definite diagonal $H^{-1}$ with $X = 0$. Having determined the reciprocals of the coefficients in the Hamiltonian function (i.e. $H^{-1}$), the dissipativity region can be approximated by searching for a convex set in the state-space which satisfies (3.13).

The question might arise why a uniform weighting of $\mathcal{H}$ in (3.3) (i.e. $h_i = 1$, $i = 1, \ldots, m$) is not necessarily enough for our purpose. From (3.13) it can be seen that the parametrization of the Hamiltonian function in the form of eq. (3.3) is needed, because if $M^TZ^* + Z^*M$ is itself indefinite, but $M^TZ^*$ is diagonally stabilizable, then there is a convex neighborhood of the origin where $\Gamma(x)MH^{-1} + H^{-1}M^T\Gamma^T(x)$ is positive (semi)definite, but there is no such neighborhood where $\Gamma(x)M + M^T\Gamma^T(x)$ is positive (semi)definite.

The **method of searching for a locally dissipative generalized Hamiltonian description of (2.13)** can be summarized as follows:

1. Determine the equilibrium point of interest ($Z^*$) and center the coordinates according to (3.1).

2. Try to solve the LMI
$$Z^*MH^{-1} + H^{-1}M^TZ^* \leq 0 \tag{3.14}$$
for a positive definite diagonal $H^{-1}$. If the LMI is feasible, then

3. Define the Hamiltonian function with the reciprocals of the diagonal elements in $H^{-1}$ as coefficients, i.e.
$$\mathcal{H}(x) = \sum_{i=1}^{n} h_i x_i^2. \tag{3.15}$$

4. Find an appropriate convex set around $x = 0$, for which (3.13) is valid.

### 3.1.2 Equivalence to global stability with the logarithmic Lyapunov function

Now we show that the diagonal stabilizability of $M$ is equivalent to the solvability of (3.14) i.e. to the local dissipativity of $R(x)$. For this, we use the following well-known fact from matrix algebra.

**Lemma 3.1.1.** [13] An $n \times n$ symmetric matrix $W$ is positive semidefinite if and only if $Q \cdot W \cdot Q^T$ is positive semidefinite for an arbitrary nonsingular quadratic matrix $Q$ of dimension $n \times n$.

Using the above lemma, we can state the following theorem.

**Theorem 3.1.1.** For given $Z^* > 0$ and $M$, the LMI

$$Z^* M H^{-1} + H^{-1} M^T Z^* \leq 0 \tag{3.16}$$

is solvable for a diagonal $H^{-1}$ if and only if $M$ is diagonally stabilizable i.e. there exists a diagonal $C > 0$ such that

$$M^T C + C M \leq 0. \tag{3.17}$$

**Proof**

1. Assume that (3.16) holds for a diagonal $H^{-1} > 0$. Then by Lemma 3.1.1

$$H(Z^* M H^{-1} + H^{-1} M^T Z^*) H = H Z^* M + M^T Z^* H \leq 0, \tag{3.18}$$

   and therefore the positive definite diagonal $C$ in (3.17) can be chosen as $HZ^* = Z^* H$, so $M$ is diagonally stabilizable.

2. Assume that $M$ is diagonally stabilizable i.e. (3.17) holds for a diagonal $C > 0$. Then we can write $C$ as a product of $Z^*$ and another positive definite diagonal matrix $H$ i.e. $C = HZ^* = Z^* H$. Now (3.17) can be written as $HZ^* M + M^T Z^* H \leq 0$, and again by Lemma 3.1.1

$$H^{-1}(H Z^* M + M^T Z^* H) H^{-1} = Z^* M H^{-1} + H^{-1} M^T Z^* \leq 0. \tag{3.19}$$

### 3.1.3 Examples

**Example 3.1.1.** Let the parameters of the LV system (2.13) be given as

$$M = \begin{bmatrix} -1 & 0.3 \\ 7 & -5 \end{bmatrix}, \ \lambda = \begin{bmatrix} 3.5 & -10 \end{bmatrix}^T. \tag{3.20}$$

Using the above parameters it can be checked that an equilibrium point is at $z^* = [5 \ \ 5]^T$. Solving the LMI (2.21) we get that $M$ is diagonally stabilizable e.g. with the positive definite diagonal matrix

$$C = \begin{bmatrix} 10 & 0 \\ 0 & 1 \end{bmatrix}. \tag{3.21}$$

One can check that the eigenvalues of $M^T C + CM$ are $\lambda_1 = -26.1803$ and $\lambda_2 = -3.8197$. This means that the LV system with the parameters above admits a local

dissipative Hamiltonian description with a quadratic Hamiltonian function in a neighborhood of $z^*$. Based on Theorem 3.1.1, the Hamiltonian function in the centered coordinates can be computed as

$$\mathcal{H}(x) = 2x_1^2 + 0.2x_2^2. \tag{3.22}$$

A very rough estimate of the neighborhood of the equilibirum point where $R$ is positive definite can be obtained by using a simple interval-halving algorithm for finding four corner points along the axes of the coordinates system. With a tolerance level of $10^{-6}$, the four corner points in $z$-coordinates are the following

$$z_{c1} = [1.5790 \;\; 5]^T, \quad z_{c2} = [86.1987 \;\; 5]^T \tag{3.23}$$

$$z_{c3} = [5 \;\; 0.2900]^T, \quad z_{c4} = [5 \;\; 15.8324]^T \tag{3.24}$$

Naturally, the corresponding estimate of the quadratic stability region is the largest level set (ellipsoid) of (3.22) that is inside the polygon defined by the above corner points.

It can be checked that the Jacobi-identites (2.24) are satisfied for $J(x)$, $\forall x \in \mathbb{R}^2$ in this example.

**Example 3.1.2.** As another illustrative example, consider a 3 dimensional LV-system with the following parameters

$$M = \begin{bmatrix} -0.15 & 0.004 & 0.01 \\ 0.06 & -0.5 & 0.2 \\ 0.9 & 0.3 & -1 \end{bmatrix}, \quad \lambda = \begin{bmatrix} 0.132 \\ 0.74 \\ -0.5 \end{bmatrix} \tag{3.25}$$

The equilibrium point of the system is then at $z^* = [1 \;\; 2 \;\; 1]^T$. Solving the LMI (3.14) gives that the Hamiltonian function

$$\mathcal{H}(x) = 10x_1^2 + 0.5x_2^2 + 0.3x_3^2 \tag{3.26}$$

is decreasing in a neighborhood of the origin (the corner points of the dissipativity region of $R$ can be computed exactly the same way as in the previous case). However, one can check that the Jacobi identities (2.24) are not satisfied for $J$ in the cases of e.g. $i = 1$, $j = 2$, $k = 3$ or $i = 2$, $j = 3$, $k = 1$.

We note that often the best geometry of the level sets of the Hamiltonian function (which are ellipsoids) can be achieved by finding $H$ with minimal condition number, and this problem is also easily solvable numerically [14].

It is remarked that QP description and the above described method was successfully applied to get an estimate of the stability region of the zero dynamics of a nonlinear gas turbine model that had been identified from real measurement data [C2, J16].

## 3.2 Computing a state dependent time-rescaling transformation for QP systems

### 3.2.1 Definition of the time-rescaling transformation

**The generic case**

Let $\Omega = [\Omega_1 \;\; \dots \;\; \Omega_n]^T \in \mathbb{R}^n$. It is shown e.g. in [54] that the following reparametrization of time

$$dt = \prod_{k=1}^{n} y_k^{\Omega_k} dt' \tag{3.27}$$

transforms the original QP system (2.11) into the following (also QP) form

$$\frac{dy_i}{dt'} = y_i \sum_{j=1}^{m+1} [\tilde{A}]_{i,j} \prod_{k=1}^{n} y_k^{[\tilde{B}]_{j,k}}, \ i = 1, \ldots, n, \tag{3.28}$$

where $\tilde{A} \in \mathbb{R}^{n \times (m+1)}$, $\tilde{B} \in \mathbb{R}^{(m+1) \times n}$ and

$$[\tilde{A}]_{i,j} = [A]_{i,j}, \quad i = 1, \ldots, n; \ j = 1, \ldots, m \tag{3.29}$$
$$[\tilde{A}]_{i,m+1} = L_i, \quad i = 1, \ldots, n \tag{3.30}$$

and

$$[\tilde{B}]_{i,j} = [B]_{i,j} + \Omega_j, \quad i = 1, \ldots, m; \ j = 1, \ldots, n \tag{3.31}$$
$$[\tilde{B}]_{m+1,j} = \Omega_j, \quad j = 1, \ldots, n. \tag{3.32}$$

It can be seen that the number of monomials is increased by one and vector $\tilde{L}$ is zero in the transformed system.

**A special (non-generic) case**

A special case of the time-reparametrization or new time transformation occurs when the following relation holds:

$$\Omega^T = -b_j, \quad 1 \leq j \leq m, \tag{3.33}$$

where $b_j$ is an arbitrary row of the $B$ matrix of the original system (2.11). From eqs. (3.31)-(3.32) we can see that in this case the $j$-th row of $\tilde{B}$ is a zero vector. This means that the number of monomials in the transformed system (3.28) remains the same as in the original QP system (2.11) and a nonzero $\tilde{L}$ vector that is equal to the $j$-th column of $A$ appears in the transformed system (for an example, see [54]).

In this case, the $\Omega$ vector can take only $m$ possible different values (see eq. (3.33)), therefore the stability analysis of the transformed system reduces to the feasibility check of $m$ different LMIs of the form (2.20). However, our approach treats the $\Omega$ vector as part of the unknowns to be determined, therefore from now on we will only consider the generic case defined in eq. (3.27).

### 3.2.2 Properties of the time-reparametrization transformation

The most important properties of the time-reparametrization transformation that are used for analyzing local and global stability are as follows.

**Monomials**

The set of monomials $p_1, \ldots, p_{m+1}$ for the reparametrized system can be written up in terms of the original monomials:

$$p_j = \prod_{k=1}^{n} y_k^{\Omega_k} \cdot \prod_{k=1}^{n} y_k^{[B]_{j,k}} = \prod_{k=1}^{n} y_k^{[B]_{j,k}+\Omega_k}, \quad j = 1, \ldots, m$$

and

$$p_{m+1} = \prod_{k=1}^{n} y_k^{\Omega_k},$$

or using a shorter notation:

$$p_j = r \cdot z_j, \quad j = 1, \ldots, m$$

$$p_{m+1} = r$$

where $z_j$ is given in (2.12) and

$$r = \prod_{k=1}^{n} y_k^{\Omega_k}.$$

**Equilibrium points**

Since the equations of the reparametrized system (3.28) can be written as

$$\frac{dy_i}{dt'} = y_i(L_i + \sum_{j=1}^{m}[A]_{i,j} \prod_{k=1}^{n} y_k^{[B]_{j,k}}) \prod_{k=1}^{n} y_k^{\Omega_k}, \quad i = 1, \ldots, n \tag{3.34}$$

and we assume that $y_i > 0$, $i = 1, \ldots, n$, it is clear that the equilibrium point $y^*$ of the original QP system (2.11) is also an equilibrium point of the reparametrized system (3.34).

**Local stability**

Let us denote the Jacobian matrix of the original QP system (2.1) at the equilibrium point by $J_{QP}(y^*)$. Then the Jacobian matrix of the time reparametrized QP system at the equilibrium point can be computed by using the formula described in [40]:

$$\tilde{J}_{QP}(y^*) = Y^* \cdot \tilde{A} \cdot \tilde{Z}^* \cdot \tilde{B} \cdot (Y^*)^{-1} = r^* \cdot J_{QP}(y^*) = \prod_{k=1}^{n} {y_k^*}^{\Omega_k} \cdot J_{QP}(y^*), \tag{3.35}$$

where

$$\tilde{Z}^* = diag(p_1^*, \ldots, p_m^*, p_{m+1}^*) \quad , \quad Y^* = diag(y_1^*, \ldots, y_n^*)$$

are the quasi-monomials of the time-reparametrized system and the state variables at the equilibrium point, respectively. From eq. (3.35) one can see that (as we naturally expect) local stability is not affected by the time-reparametrization, because this transformation just multiplies the eigenvalues of the Jacobian by a positive constant $r^*$.

**Global stability**

Rewriting (3.27) gives

$$\frac{dt}{dt'} = \prod_{k=1}^{n} (y_k(t'))^{\Omega_k} \tag{3.36}$$

from which we can see that $t$ is a strictly monotonously increasing continuous and invertible function of $t'$ if the state variables are strictly positive. This means that global stability of any strictly positive equilibrium point in the original time scale in this case is equivalent to the global stability of the same equilibrium in rescaled time.

dc_263_11

### 3.2.3 The time-reparametrization problem as a bilinear matrix inequality

We denote an $n \times m$ matrix containing zero elements by $0^{n\times m}$. Let us define two auxiliary matrices by extending $A$ with a zero column and $B$ with a zero row, i.e.

$$\bar{A} = \left[\begin{array}{c|c} A & 0^{n\times 1} \end{array}\right] \in \mathbb{R}^{n\times(m+1)}, \tag{3.37}$$

and

$$\bar{B} = \left[\begin{array}{c} B \\ \hline 0^{1\times n} \end{array}\right] \in \mathbb{R}^{(m+1)\times n}. \tag{3.38}$$

Then $\tilde{A}$ and $\tilde{B}$ can be written as

$$\tilde{A} = [A|L] = \bar{A} + [0^{n\times m}|L], \tag{3.39}$$

and

$$\tilde{B} = \begin{bmatrix} b_1 + \Omega^T \\ b_2 + \Omega^T \\ \vdots \\ b_m + \Omega^T \\ \Omega^T \end{bmatrix} = \bar{B} + S \cdot \Omega^*, \tag{3.40}$$

where

$$\Omega^* = \mathrm{diag}(\Omega) \in \mathbb{R}^{n\times n}, \tag{3.41}$$

and

$$S = \begin{bmatrix} 1 & 1 & \dots & 1 \\ 1 & 1 & \dots & 1 \\ \vdots & & & \\ 1 & 1 & \dots & 1 \end{bmatrix} \in \mathbb{R}^{(m+1)\times n}. \tag{3.42}$$

It can be seen from eqs. (3.39) and (3.40) that the invariant matrix of the reparametrized system is

$$\tilde{M} = \tilde{B} \cdot \tilde{A} = (\bar{B} + S \cdot \Omega^*) \cdot \tilde{A}. \tag{3.43}$$

Therefore the matrix inequality for examining the global stability of the reparametrized system is the following

$$-C < 0 \tag{3.44}$$

$$\tilde{M}^T \cdot C + C \cdot \tilde{M} \leq 0 \tag{3.45}$$

i.e.

$$-C < 0 \tag{3.46}$$

$$\tilde{A}^T(\bar{B}^T + \Omega^* S^T)C + C(\bar{B} + S\Omega^*)\tilde{A} \leq 0 \tag{3.47}$$

which clearly has the same form as (2.2) with the following set of unknowns:

$$x = \begin{bmatrix} x_1 \\ x_2 \\ \vdots \\ x_{m+1} \\ x_{m+2} \\ \vdots \\ x_{m+n+1} \end{bmatrix} = \begin{bmatrix} c_1 \\ c_2 \\ \vdots \\ c_{m+1} \\ \Omega_1 \\ \vdots \\ \Omega_n \end{bmatrix} \tag{3.48}$$

Now we are ready to construct the matrices in the BMI (2.2) starting with

$$G_0^1 = G_0^2 = 0^{(m+1)\times(m+1)}, \tag{3.49}$$

$$\begin{aligned} &[G_k^1]_{i,j} = \begin{cases} -1, & i = j = k \\ 0, & \text{otherwise} \end{cases} \\ &i, j, k = 1, \ldots, m+1, \end{aligned} \tag{3.50}$$

$$G_k^1 = 0^{(m+1)\times(m+1)}, \quad k = m+2, \ldots, m+n+1 \tag{3.51}$$

and

$$K_{kl}^1 = 0^{(m+1)\times(m+1)}, \quad k, l = 1, \ldots, m+n+1. \tag{3.52}$$

Furthermore, let us introduce the following notations

$$\begin{aligned} &P_k \in \mathbb{R}^{(m+1)\times(m+1)}, \\ &[P_k]_{i,j} = \begin{cases} [\bar{B} \cdot \tilde{A}]_{i,j}, & i = k \\ 0, & i \neq k \end{cases}, \\ &i, j, k = 1, \ldots, m+1 \end{aligned} \tag{3.53}$$

and

$$\begin{aligned} &Q_{kl} \in \mathbb{R}^{(m+1)\times(m+1)}, \\ &[Q_{kl}]_{i,j} = \begin{cases} [\tilde{A}]_{l-m-1,j}, & i = k \\ 0, & i \neq k \end{cases}, \\ &i, j, k = 1, \ldots, m+1, \ l = m+2, \ldots, m+n+1. \end{aligned} \tag{3.54}$$

Then

$$G_k^2 = \begin{cases} P_k + P_k^T, & k = 1, \ldots, m+1 \\ 0^{(m+1)\times(m+1)}, & k = m+2, \ldots, m+n+1, \end{cases}, \tag{3.55}$$

and

$$\begin{aligned} &K_{kl} = \begin{cases} Q_{kl} + Q_{kl}^T, & k = 1, \ldots, m+1, \ l = m+2, \ldots, m+n+1 \\ 0^{(m+1)\times(m+1)}, & \text{otherwise} \end{cases} \\ &k, l = 1, \ldots, m+n+1. \end{aligned} \tag{3.56}$$

We note that in certain cases the feasibility of a BMI can be traced back to the feasibility of equivalent LMIs (see [14] or [136]), but in our case it is not possible because of the structural (diagonality) constraint on both of the unknown matrices $\Omega^*$ and $C$ in (3.47).

### 3.2.4 Example

In order to illustrate the above proposed method of finding time-reparametrization transformations for global stability analysis, a simple example is presented.

**Example 3.2.1. Example with a full rank $M$ matrix.** Consider a QP system with the following matrices

$$A = \begin{bmatrix} \frac{2}{3} & -\frac{8}{3} \\ \frac{2}{3} & -\frac{7}{3} \end{bmatrix} \approx \begin{bmatrix} 0.6667 & -2.6667 \\ 0.6667 & -2.3333 \end{bmatrix}, \tag{3.57}$$

$$B = \begin{bmatrix} \frac{2}{3} & -\frac{1}{3} \\ -\frac{8}{3} & \frac{16}{3} \end{bmatrix} \approx \begin{bmatrix} 0.6667 & -0.3333 \\ -2.6667 & 5.3333 \end{bmatrix}, \tag{3.58}$$

$$L = \begin{bmatrix} 2 \\ \frac{5}{3} \end{bmatrix} \approx \begin{bmatrix} 2 \\ 1.6667 \end{bmatrix}. \tag{3.59}$$

Its equilibrium point of interest is:

$$y^* = [1 \quad 1]^T. \tag{3.60}$$

The Jacobian matrix of the locally linearized system in $y^*$ has the following eigenvalues: -0.1187, -4.9924. This shows that the investigated equilibrium point is at least locally asymptotically stable.

Using an appropriate LMI solver (e.g. Matlab's LMI Control Toolbox) it can be checked that the LMI (2.20) cannot be solved for a diagonal $C$ if $M = B \cdot A$. However, using the algorithm [97] for solving the corresponding BMI we find that a feasible solution of (3.47) is e.g.

$$C = \begin{bmatrix} 1 & 0 & 0 \\ 0 & 1 & 0 \\ 0 & 0 & 1 \end{bmatrix}, \quad \Omega = \begin{bmatrix} \frac{2}{3} & -\frac{5}{3} \end{bmatrix}^T. \tag{3.61}$$

The eigenvalues of $\tilde{M}^T \cdot C + C \cdot \tilde{M}$ are

$$\lambda_1 = 0, \quad \lambda_2 \approx -0.2374, \quad \lambda_3 \approx -9.9848, \tag{3.62}$$

which shows that the examined equilibrium point of the system is globally stable.

Example A.1.1 in the Appendix demonstrates the use of time-rescaling in designing a simple globally stabilizing static nonlinear feedback for an open generalized mass action kinetic system.

## 3.3 Short summary of further related results

As it turned out from the previous results, the simple algebraic structure of QP systems makes them especially suitable to apply matrix-based computation methods. The following two related methods (that are only briefly summarized due to the page constraints) are also based on this property.

### 3.3.1 An algorithm for finding invariants in QP systems

In this subsection, we use slightly different notations for QP systems from the ones defined in section 2.3 because of practical reasons. These notations are introduced below. We will represent an $(n+1)$ dimensional QP system in the following general form:

$$\dot{y}_i = y_i \left( \lambda_i + \sum_{j=1}^{m-1} \bar{A}_{i,j} U_j \right), \quad U_j = \prod_{k=1}^{n+1} y_k^{\bar{B}_{j,k}}, \qquad i = 1, \ldots, n+1 \tag{3.63}$$

where $\bar{A} \in \mathbb{R}^{(n+1)\times(m-1)}$, $\bar{B} \in \mathbb{R}^{(m-1)\times(n+1)}$, $\lambda_i \in \mathbb{R}$, $i = 1, \ldots, n+1$. Furthermore, $\lambda = [\lambda_1 \ \ldots \ \lambda_{n+1}]^T$. Without the loss of generality we can assume that $m - 1 \geq n + 1$, and that the matrices $\bar{A}$ and $\bar{B}$ are of full rank i.e. $\mathrm{Rank}(\bar{A}) = \mathrm{Rank}(\bar{B}) = n + 1$ [79].

If $\lambda_i \neq 0$ for some $i$, then it is useful to introduce a so-called unit monomial $U_m = \prod_{k=1}^{n+1} y_k^0 = 1$. This way, the general equations (3.63) can be written in a *homogeneous* form (see e.g. [17]) as

$$\dot{y}_i = y_i \left( \sum_{j=1}^{m} A_{i,j} U_j \right) , \quad U_j = \prod_{k=1}^{n+1} y_k^{B_{j,k}}, \qquad i = 1, \ldots, n+1 \tag{3.64}$$

where the matrices $A \in \mathbb{R}^{(n+1)\times m}$ and $B \in \mathbb{R}^{m\times(n+1)}$ are the following:

$$\begin{aligned} &A_{i,j} = \bar{A}_{i,j}, \quad i = 1, \ldots, n+1; \; j = 1, \ldots, m-1 \\ &A_{i,m} = \lambda_i, \quad i = 1, \ldots, n+1 \end{aligned}$$

and

$$\begin{aligned} &B_{i,j} = \bar{B}_{i,j}, \quad i = 1, \ldots, m-1; \; j = 1, \ldots, n+1 \\ &B_{m,j} = 0, \quad j = 1, \ldots, n+1 \end{aligned}$$

i.e. $\lambda$ is inserted as a column vector after the last column of $\bar{A}$, and a zero row vector is inserted after the last row of $\bar{B}$. The facts that $\bar{A}$ and $\bar{B}$ contain $n+1$ linearly independent rows and columns, respectively, and the row and column ranks of a matrix are equal, imply that the rank of both $A$ and $B$ remains $n+1$. Then, it follows from the relation $n+1 < m$ that $A$ and $B$ are also of full rank, which is a necessary condition for the applicability of the described algorithm.

**The examined class of invariants**

A function $I : \mathbb{R}^{n+1} \mapsto \mathbb{R}$ is called an invariant of (3.64) if

$$\frac{d}{dt} I = \frac{\partial I}{\partial y} \cdot \dot{y} = 0. \tag{3.65}$$

We consider quasi-polynomial invariants in (3.64) that can be written in the following special form:

$$I = F(y) - y_i^{\frac{1}{\beta}}, \quad \beta \in \mathbb{R} \tag{3.66}$$

where

$$F(y) = \sum_{k=1}^{p} c_k \prod_{j=1, j\neq i}^{n+1} y_j^{\alpha_{kj}}, \quad c_k, \alpha_{kj} \in \mathbb{R} \tag{3.67}$$

It's clear that (3.66) can be rewritten as

$$y_i^{\frac{1}{\beta}} = F(y) + c_0, \quad c_0 \in \mathbb{R} \tag{3.68}$$

This is a narrower class of invariants than the one examined in [52] since it contains those first integrals from where at least one of the variables can be expressed explicitly. However, many types of first integrals (e.g. conserved mechanical, thermodynamical or electrical energy) in physical system models belong to this class.

**The underlying principle of the algorithm**

Consider a set of $(n+1)$ QP differential equations in the *homogeneous* form of (3.64). Let us assume without loss of generality that $i = n+1$ in (3.68) (because the QP form of the equations is obviously preserved under permutation of the differential variables) i.e. the following algebraic dependence is present in (3.64)

$$y_{n+1}^{\frac{1}{\beta}} = c_0 + \sum_{\ell=1}^{L} c_\ell V_\ell \tag{3.69}$$

where $\beta, c_\ell \in \mathbb{R},\ \ell = 0, \ldots, L,\ \beta \neq 0$, and

$$V_\ell = \prod_{k=1}^{n} y_k^{\alpha_{\ell k}}, \quad \alpha_{\ell k} \in \mathbb{R},\ \ell = 1, \ldots, L,\ k = 1, \ldots, n \tag{3.70}$$

It is clear that (3.69) is equivalent to the existence of a first integral of the form (3.66)-(3.67).

Taking the time derivative of (3.69) we obtain

$$\dot{y}_{n+1} = \beta \left( c_0 + \sum_{\ell=1}^{L} c_\ell V_\ell \right)^{\beta-1} \cdot \sum_{\ell=1}^{L} c_\ell \dot{V}_\ell \tag{3.71}$$

Using (3.69) and the fact that the monomials $V_\ell$, $\ell = 1, \ldots, L$ do not depend on $y_{n+1}$ we can further write

$$\dot{y}_{n+1} = \beta y_{n+1}^{\frac{\beta-1}{\beta}} \sum_{\ell=1}^{L} c_\ell \cdot \sum_{i=1}^{n} \frac{\partial V_\ell}{\partial y_i} \dot{y}_i \tag{3.72}$$

Finally, we can rewrite (3.72) to the standard QP form as

$$\dot{y}_{n+1} = y_{n+1} \left( \sum_{\ell=1}^{L} \sum_{i=1}^{n} \beta \cdot c_\ell \cdot \alpha_{\ell i} \cdot V_\ell \cdot y_{n+1}^{-\frac{1}{\beta}} \sum_{j=1}^{m} A_{i,j} U_j \right) \tag{3.73}$$

It is easy to see that the monomials in (3.73) (denoted by $R_{\ell j}$) are the following

$$R_{\ell j} = V_\ell \cdot U_j \cdot y_{n+1}^{-\frac{1}{\beta}} = y_1^{\alpha_{\ell 1} + B_{j1}} \cdot y_2^{\alpha_{\ell 2} + B_{j2}} \cdot \cdots \cdot y_n^{\alpha_{\ell n} + B_{jn}} \cdot y_{n+1}^{-\frac{1}{\beta}} \tag{3.74}$$

$$j = 1, \ldots, m, \quad \ell = 1, \ldots, L \tag{3.75}$$

while the coefficients of the monomials are

$$\gamma_{\ell j} = \sum_{i=1}^{n} \beta c_\ell \alpha_{\ell i} A_{i,j} \tag{3.76}$$

$$i = 1, \ldots, n, \quad j = 1, \ldots, m, \quad \ell = 1, \ldots, L \tag{3.77}$$

where the subscript $i$ refers to that the partial differentiation in (3.72) has been performed by $x_i$.

Now, the aim of our algorithm is to determine $\beta$, the coefficients $c_\ell$ and the exponents $\alpha_{\ell i}$, $\ell = 1, \ldots, L$, $i = 1, \ldots n$ in (3.69)–(3.70) using the special form of the equation (3.73) and that of the monomials in (3.74).

The *input required by the algorithm* consists of the matrices $A$ and $B$ of the QP model in its *homogeneous form* defined in (3.64).

The *operational condition of the algorithm* is that, consistently to our preliminary assumptions, matrices $A$ and $B$ are of full rank.

Without the loss of generality we can assume that the explicit variable of the possible first integral is the last differential variable $y_{n+1}$. By a simple permutation of variables, each variable can be checked whether it is the explicit variable of a first integral.

The main steps of the algorithm can be summarized as (the details can be found in [J14])

1. *Determination of the monomial candidates*
   To find a first integral in the form (3.69), one has to use the relationship (3.74) defined between the monomials $U_j, j = 1, \ldots, m$ of the original differential equations and the monomials $R_{\ell j}, \ell = 1, \ldots, L, j = 1, \ldots, m$ of the ODE for the algebraically dependent variable $y_{n+1}$.

2. *Determination of $\beta$*
   To have a QP-type first integral from which $y_{n+1}$ can be given explicitly, *the exponents of $y_{n+1}$ in all of its monomials have to be identical.* This step classifies the exponent row vectors of the monomial candidates of the first integral by their last element.

3. *Determination of the coefficients*
   The last step to be performed is to search for a first integral with the collected monomial candidates. Since the exponents of the monomial candidates are already given, only their coefficients have to be determined. If these coefficients exist, the first integral exists for the current $\beta$, and it is completely determined by the algorithm.

This algorithm is capable of finding QP type first integrals which are explicit in (at least) one of their variables, moreover it operates without any heuristic steps. It can be shown that the time-complexity of the algorithm is polynomial [J14]. It is also remarked that coordinates transformations like the quasi-monomial transformation have an important effect on whether a first integral in some coordinates is explicit in one of its variables or not.

**Example 3.3.1. A fed-batch fermentation process.** In this example we use the model of an isotherm fed-batch fermentation process [J12]. The continuous version of the model is treated in [J13].

The model equations are given by

$$\dot{y}_1 = K_r y_1 y_2 - \frac{y_1}{y_3} F \tag{3.78}$$

$$\dot{y}_2 = -\frac{1}{Y} K_r y_1 y_2 + \frac{S_F - y_2}{y_3} F \tag{3.79}$$

$$\dot{y}_3 = F \tag{3.80}$$

The variables of the model and their units in square brackets are

| | | |
|---|---|---|
| $y_1$ | biomass concentration | [g/l] |
| $y_2$ | substrate concentration | [g/l] |
| $y_3$ | volume | [l] |
| $F$ | feed flow rate | [l/h]. |

The constant parameters and their typical values are the following

| | | |
|---|---|---|
| $Y = 0.5$ | yield coefficient | |
| $K_r = 1$ | kinetic parameter | [g/l] |
| $S_F = 10$ | influent substrate concentration | [g/l] |

The feed flow-rate $F$ is the physical control input variable and will be treated as a constant parameter during the retrieval process. The model (3.78-3.80) can be given as a QP-ODE in its homogeneous form (3.64):

$$\dot{y}_1 = y_1\big(K_r y_2 - F y_3^{-1}\big) \tag{3.81}$$

$$\dot{y}_2 = y_2\big(-\frac{1}{Y}K_r y_1 + S_F F y_2^{-1} y_3^{-1} - F y_3^{-1}\big) \tag{3.82}$$

$$\dot{y}_3 = y_3\big(F x_3^{-1}\big) \tag{3.83}$$

The $A$ and $B$ matrices of the QP model are:

$$A = \begin{bmatrix} K_r & -F & 0 & 0 \\ 0 & -F & -\frac{K_r}{Y} & S_F F \\ 0 & F & 0 & 0 \end{bmatrix},\ B = \begin{bmatrix} 0 & 1 & 0 \\ 0 & 0 & -1 \\ 1 & 0 & 0 \\ 0 & -1 & -1 \end{bmatrix}$$

Applying the retrieval algorithm, we obtain a first integral in the following form:

$$x_3\big(\frac{1}{Y}x_1 - x_2 + S_F\big) = \frac{S_F}{c_0} \tag{3.84}$$

where $c_0$ comes from the initial conditions of the model.

It is remarked that this first integral was computed in [J12] by the total integration of the reachability distribution thus proving that the modeled fermentation process is not reachable locally in the nonlinear sense [87] around any point in the state-space. However, the integration involved the manual solution of partial differential equations, while in the present case, the proposed first integral retreiving algorithm gave the same result after the straightforward transformation of the system model into QP form.

### 3.3.2 Globally stabilizing feedback design for a class of QP systems

#### Input-affine QP system models

An input-affine nonlinear system model [87] with state vector $y$, input vector $u$ and output vector $\eta$

$$\begin{aligned} \dot{y} &= f(y) + \sum_{i=1}^{p} g_i(y) u_i \\ \eta &= h(y) \end{aligned} \tag{3.85}$$

is in QP-form if all of the functions $f$, $g$ and $h$ are in QP-form. Then the general form of the state equation of an input-affine QP system model with $p$-inputs can be written

as:

$$\dot{y}_i = y_i \left( L_{0_i} + \sum_{j=1}^{m} A_{0_{ij}} \prod_{k=1}^{n} y_k^{B_{jk}} \right) + \sum_{l=1}^{p} y_i \left( L_{l_i} + \sum_{j=1}^{m} A_{l_{ij}} \prod_{k=1}^{n} y_k^{B_{jk}} \right) u_l \quad (3.86)$$

where

$$i = 1, \ldots, n, \quad A_0, A_l \in \mathbb{R}^{n \times m}, \quad B \in \mathbb{R}^{m \times n},$$

$$L_0, L_l \in \mathbb{R}^n, \quad l = 1, \ldots, p.$$

The corresponding input-affine Lotka-Volterra model is in the form

$$\dot{z}_j = z_j \left( N_{0_j} + \sum_{k=1}^{m} M_{0_{jk}} z_k \right) + \sum_{l=1}^{p} z_j \left( N_{l_j} + \sum_{k=1}^{m} M_{l_{jk}} z_k \right) u_l \quad (3.87)$$

where

$$j = 1, \ldots, m, \quad M_0, M_l \in \mathbb{R}^{m \times m}, \quad N_0, N_l \in \mathbb{R}^m, \quad l = 1, \ldots, p,$$

and the parameters can be obtained from the input-affine QP system's ones in the following way

$$\begin{array}{rcl} M_0 & = & B \cdot A_0 \\ N_0 & = & B \cdot L_0 \\ M_l & = & B \cdot A_l \\ N_l & = & B \cdot L_l \end{array} \qquad l = 1, \ldots, p. \quad (3.88)$$

**The controller design problem**

*Globally stabilizing QP state feedback* design problem for QP systems can be formulated as follows. Consider arbitrary quasi-polynomial inputs in the form:

$$u_l = \sum_{i=1}^{r} k_{il} \hat{q}_i, \quad l = 1 \ldots, p, \quad (3.89)$$

where $\hat{q}_i = \hat{q}_i(y_1, \ldots, y_n),\ i = 1, ..., r$ are arbitrary quasi-monomial functions of the state variables of (3.86) and $k_{il}$ is the constant gain of the quasi-monomial function $\hat{q}_i$ in the $l$-th input $u_l$. The closed loop system will also be a QP system with matrices

$$\hat{A} = A_0 + \sum_{l=1}^{p} \sum_{i=1}^{r} k_{il} A_{il}, \quad \hat{B}, \quad (3.90)$$

$$\hat{L} = L_0 + \sum_{l=1}^{p} \sum_{i=1}^{r} k_{il} L_{il}. \quad (3.91)$$

Note that the number of quasi-monomials in the closed-loop system (i.e. the dimension of the matrices) together with the matrix $\hat{B}$ may significantly change depending on the choice of the feedback structure, i.e. on the quasi-monomial functions $\hat{q}_i$.

Furthermore, the closed loop LV coefficient matrix $\hat{M}$ can also be expressed in the form:

$$\hat{M} = \hat{B} \cdot \hat{A} = M_0 + \sum_{l=1}^{p} \sum_{i=1}^{r} k_{il} M_{il}.$$

Then the global stability analysis of the closed loop system with unknown feedback gains $k_{il}$ leads to the following *bilinear matrix inequality*

$$\hat{M}^T C + C\hat{M} = M_0^T C + CM_0 + \sum_{l=1}^{p}\sum_{i=1}^{r} k_{il}\left(M_{il}^T C + CM_{il}\right) \leq 0. \tag{3.92}$$

The variables of the BMI are the $p \times r$ $k_{il}$ feedback gain parameters and the $c_j,\ j = 1,..,m$ parameters of the Lyapunov function. If the BMI above is feasible then there exists a globally stabilizing feedback with the selected structure.

**Approaches for numerical solution**

**Direct solution of BMIs** There are just few software tools available for solving general bilinear matrix inequalities that is a computationally hard problem. In some rare cases with a suitable change of variables quadratic matrix inequalities can be rewritten as linear matrix inequalities (see e.g. [14]), but generally the structure of the matrix variable of (3.92) does not fall into this fortunate problem class.

In Matlab environment the TomLab/PENBMI solver [98] can be used effectively to solve bilinear matrix inequalities. Rewriting the above matrix inequality (3.92) in the form (2.2) one gets the following expression which can be directly solved by [98] as a BMI feasibility problem:

$$\begin{aligned} \sum_{j=1}^{m} c_j \bar{M}_{0,j} + \sum_{j=1}^{m}\sum_{l=1}^{p}\sum_{i=1}^{r} c_j k_{il} \bar{M}_{il,j} &\leq 0 \\ -C &< 0. \end{aligned} \tag{3.93}$$

The two disjoint sets of BMI variables are the $c_j$ parameters of the Lyapunov function and the $k_{il}$ feedback parameters. The parameters of the problem $\bar{M}_{0,j}$ ($\bar{M}_{il,j}$, respectively) are the symmetric matrices obtained from $M_0$ ($M_{il}$, respectively) by adding the $m \times m$ matrix that contains only the $j$-th column of $M_0$ ($M_{il}$, respectively) to its transpose, i.e.

$$[\bar{M}]_{s,j} = \begin{bmatrix} 0 & \cdots & M_{1j} & \cdots & 0 \\ \vdots & & \vdots & & \vdots \\ M_{1j} & \cdots & 2M_{jj} & \cdots & M_{mj} \\ \vdots & & \vdots & & \vdots \\ 0 & \cdots & M_{mj} & \cdots & 0 \end{bmatrix}, \tag{3.94}$$

where $M_{ij} = [M_s]_{ij}$ for $s \in \{0, il\}$.

Note that for low dimensions (i.e. for $m < 3$) there exist algebraic conditions for diagonal stablity to avoid BMI solutions [93], but presently these cannot be extended to the practically important higher dimensional case.

**Applying iterative LMI solution** Because of the NP-hard nature of the general BMI solution problem, it is worthwhile to search for an approximate but numerically efficient alternative way of solution. As shown below, the special structure of the QP stabilizing feedback design BMI feasibility problem allows us to apply a computationally feasible method for its solution that solves an LMI in each of its iterative approximation step. The iterative LMI (ILMI) algorithm used for static output feedback stabilization published in [19] is used for this purpose.

In order to be able to use the ILMI algorithm, it is necessary to write the QP stabilizing feedback design problem as a static output feedback stabilization problem for LTI systems. In what follows the globally stabilizing feedback design BMI (3.92) is used in the form

$$(M_0 + \Theta K)^T C + C(M_0 + \Theta K) < 0. \tag{3.95}$$

where

$$\Theta = \left[ \overbrace{M_1, \ldots, M_p}^{1\text{st}}, \ldots, \overbrace{M_1, \ldots, M_p}^{r\text{th}} \right], \quad K = \begin{bmatrix} k_{11} \cdot I_{m\times m} \\ \vdots \\ k_{1p} \cdot I_{m\times m} \\ \vdots \\ k_{r1} \cdot I_{m\times m} \\ \vdots \\ k_{rp} \cdot I_{m\times m} \end{bmatrix}.$$

The above problem is structurally equivalent to a standard LTI output feedback stabilization problem

$$(A + BFC)^T P + P(A + BFC) < 0,$$

with $M_0$ corresponding to the state matrix $A$, $\Theta$ playing the role of the input matrix $B$, and $K$ serving as $FC$ and $P$ is the unknown matrix variable of the problem. Now, the iterative LMI solution method described in [19] can be directly applied for our problem. A more detailed description of the proposed method with illustrative examples can be found in [J15].

## 3.4 Summary

The relation between the global stability and the dissipative Hamiltonian structure of LV and QP systems was investigated in section 3.1. It was shown that the monomials of a QP system form a locally dissipative generalized Hamiltonian system with a diagonal quadratic Hamiltonian function if and only if the LV (and QP) system is globally stable with the Lyapunov function (2.18). Furthermore, a systematic method was presented for finding the quadratic Hamiltonian function through the solution of linear matrix inequalities. The local dissipativity region in the monomial space can also be estimated by using LMIs. The generalized Hamiltonian description and the estimation of the dissipativity neighborhood was illustrated by two numerical examples.

In section 3.2 it was shown that the solvability of a class of time-reparametrization problem used in global stability analysis of QP systems is equivalent to the feasibility of a bilinear matrix inequality, where the unknowns to be determined are the coefficients of the Lyapunov function candidate and the parameters of the time-reparametrization transformation. Using the proposed method, it is possible to decide whether an appropriate time-reparametrization exists and to determine the time-reparametrizing transformation and the Lyapunov function together, using the same algorithm. Although the solution of BMIs is known to be an NP-hard problem, there exist effective numerical algorithms for handling them. A simple example was given, where global stability could not be proven in the original time-scale but after solving the corresponding BMI and finding the right time-reparametrization parameters, it turned out that the system is globally stable.

Finally, in section 3.3 an algorithm for finding invariants in QP systems, and a globally stabilizing feedback design method were briefly presented.

# Chapter 4

# Hamiltonian structure in reversible reaction networks with mass action kinetics

In this section, a possible locally dissipative-Hamiltonian structure for a class of reversible deficiency zero CRNs will be presented.

## 4.1 Some further notions: the structure of reversible reaction networks

In describing the underlying dynamic structure of reaction networks, we adopt the notation employed in [69] for the dissipative reaction network kinetics.

Let us consider the isolated and homogeneous isotherm systems where $n$ chemical species participate on a $r$-step reaction network, represented by the following reversible stoichiometric mechanism obeying the mass action law:

$$\sum_{i=1}^{n} \alpha_{ij} X_i \rightleftarrows \sum_{i=1}^{n} \beta_{ij} X_i \quad \text{for } j = 1, \ldots, r \tag{4.1}$$

with $\alpha_{ij}$, $\beta_{ij}$ being the constant stoichiometric coefficients for specie $X_i$ in the reaction step $j$. The linear combinations of the species in eq. (4.1), namely $\sum_{i=1}^{n} \alpha_{ij} X_i$ and $\sum_{i=1}^{n} \beta_{ij} X_i$ for $j = 1, \ldots, r$ are the complexes. The overall reaction rates are given by [49]:

$$W_j(x) = k_j^+ \prod_{i=1}^{n} x_i^{\alpha_{ij}} - k_j^- \prod_{i=1}^{n} x_i^{\beta_{ij}}, \quad j = 1, \ldots, r \tag{4.2}$$

where $k_j^+$ and $k_j^-$ are the constants of the forward and reverse rates of the $j$-th reaction step, respectively, and $x_i \geq 0$ represents the concentration of the specie $X_i$. Each concentration evolves in time according to the ordinary differential equation:

$$\dot{x}_i = \sum_{j=1}^{r} \nu_{ij} W_j(x), \quad i = 1, \ldots, n, \tag{4.3}$$

where $\nu_{ij} = \alpha_{ij} - \beta_{ij}$ is positive or negative depending on whether the specie $i$ is a product or a reactant in the reaction $j$. The dynamic evolution of the network can then be represented by a set of ordinary differential equations which in compact matrix form is written as:

$$\dot{x} = \mathcal{N} \cdot W(x), \tag{4.4}$$

where $\mathcal{N} = [\nu_{ij}]$ is the $n \times r$ coefficient matrix the columns of which are the so-called stoichiometric vectors $\nu_{.j} = \beta_{.j} - \alpha_{.j}$, and $W(x) \in \mathbb{R}^r$ denotes the vector of reaction rates. The following simple example illustrates the above notions.

**Example 4.1.1.** Let the set of species be given by $X_1$,$X_2$,$X_3$, and $X_4$, while the set of complexes is $X_1$, $X_2 + X_3$, and $X_4$. The reactions are

$$X_1 \underset{k_1^-}{\overset{k_1^+}{\rightleftarrows}} X_2 + X_3 \underset{k_2^-}{\overset{k_2^+}{\rightleftarrows}} X_4. \tag{4.5}$$

The $\alpha$ and $\beta$ matrices are given by

$$\alpha = \begin{bmatrix} 1 & 0 \\ 0 & 1 \\ 0 & 1 \\ 0 & 0 \end{bmatrix}, \quad \beta = \begin{bmatrix} 0 & 0 \\ 1 & 0 \\ 1 & 0 \\ 0 & 1 \end{bmatrix}, \tag{4.6}$$

from which $\mathcal{N}$ can be calculated as

$$\mathcal{N} = \beta - \alpha = \begin{bmatrix} -1 & 0 \\ 1 & -1 \\ 1 & -1 \\ 0 & 1 \end{bmatrix}. \tag{4.7}$$

The reaction rates are given by

$$W_1(x) = k_1^+ x_1 - k_1^- x_2 x_3 \tag{4.8}$$
$$W_2(x) = k_2^+ x_2 x_3 - k_2^- x_4 \tag{4.9}$$

Now, let us modify the structure of (4.5) in such a way that there is a further reaction step between $X_1$ and $X_4$:

$$X_1 \underset{k_1^-}{\overset{k_1^+}{\rightleftarrows}} X_2 + X_3 \underset{k_2^-}{\overset{k_2^+}{\rightleftarrows}} X_4 \underset{k_3^-}{\overset{k_3^+}{\rightleftarrows}} X_1 \tag{4.10}$$

Now, the modified stoichiometric matrix is

$$\mathcal{N}' = \begin{bmatrix} -1 & 0 & 1 \\ 1 & -1 & 0 \\ 1 & -1 & 0 \\ 0 & 1 & -1 \end{bmatrix} \tag{4.11}$$

and the third reaction rate (in addition to (4.8) and (4.9)) reads

$$W_3(x) = k_3^+ x_4 - k_3^- x_1 \tag{4.12}$$

Observe that the columns of the original $\mathcal{N}$ are linearly independent which means that $\mathcal{N}$ is of maximal rank. In this case, we say that the elementary reaction-pairs (or the corresponding stoichiometric vectors) are independent. It is also visible, that the rank of the modified $\mathcal{N}'$ is only two, because the structure of the modified reaction is such that the third column of $\mathcal{N}'$ is a linear combination of the columns of $\mathcal{N}$.

From now, we assume that $r \leq n$ and the the columns of $\mathcal{N}$ are linearly independent i.e., the rank of $\mathcal{N}$ is exactly $r$. With this assumption, we only deal with a proper subclass of closed reversible reaction networks, since many reaction networks occurring in natural or technological systems contain linearly dependent column vectors in $\mathcal{N}$.

*The reaction polyhedron.* It is easy to see from (4.4) that any vector $c_k \in \mathbb{R}^n$, $k = 1, \ldots, n-r$ belonging to the kernel of $\mathcal{N}^T$ defines a linear first integral:

$$c_k^T x(t) = c_k^T x(0) =: \mathcal{C}_k^0, \quad \forall t \geq 0, \quad k = 1, \ldots, n-r, \tag{4.13}$$

since $c_k^T \dot{x} = 0$. For a given initial condition $x(0)$, equation (4.13) defines a simple invariant manifold denoted by $\mathcal{M}_{x_0}$. The intersection of the positive orthant with $\mathcal{M}_{x_0}$ is called the *reaction polyhedron* denoted by $\Omega(x_0)$:

$$\Omega(x_0) = \left\{ x \in \mathbb{R}_n^+ \mid c_k^T (x - x_0) = 0, \quad k = 1, ..., n-r \right\}, \tag{4.14}$$

that is also invariant for the system dynamics.

*The equilibrium manifold.* From the assumption $r \leq n$ and from the rank condition on $\mathcal{N}$ it follows that $\dot{x} = 0$ if and only if $W(x) = 0$, which determines the set of equilibrium points of the closed system. It is easy to check that the assumptions described above imply the deficiency zero property of the studied network class: the rank of the network is exactly $r$, and it is known from graph theory that the number of edges in a forest with no isolated vertices is the difference between the number of vertices and the number of connected components in a graph [9]. Then it follows from the Deficiency Zero Theorem that within each reaction polyhedron, there is exactly one equlibrium point which is stable in the space of positive concentrations (i.e., $\mathbb{R}_+^n$). Therefore, assuming that the value of $x(0)$ is known, it is common to study the dynamics of (4.4) restricted to $\Omega(x_0)$ using the linear equations (4.13) [143]. The equilibrium point of interest will be denoted by $x^*$ throughout the chapter.

## 4.2 Local Hamiltonian structure of reaction networks

In this section, a possible Hamiltonian structure for the studied class of reaction networks will be given using the generalized dissipative-Hamiltonian framework described in section 2.4.

### 4.2.1 Coordinates change and the resulting Hamiltonian structure

Let us denote the forward and backward parts of the reaction rates in the following way

$$p_j(x) = k_j^+ \prod_{i=1}^{n} x_i^{\alpha_{ij}}, \quad q_j(x) = k_j^- \prod_{i=1}^{n} x_i^{\beta_{ij}}, \quad j = 1, \ldots, r \tag{4.15}$$

We define the *reaction space* as follows (the $x$ arguments are suppressed in $p$ and $q$):

$$z_j = \ln p_j - \ln q_j, \quad j = 1, \ldots, r \tag{4.16}$$

Note that the product $RTz_j$ (with R being the gas constant and T the temperature) is the chemical affinity corresponding to the reaction step $j$ [37].

In order to construct an invertible mapping between $x$ and $z$, let us extend (4.16) with the conserved quantities as additional coordinate functions in the following way

$$\bar{z} = \Psi(x), \tag{4.17}$$

where

$$\bar{z}_j = z_j = \ln\left(\frac{k_j^+}{k_j^-}\prod_{i=1}^{n} x_i^{\nu_{ij}}\right), \quad j = 1, \ldots, r \tag{4.18}$$

$$\bar{z}_k = c_{k-r}^T \cdot x, \quad k = r+1, \ldots, n \tag{4.19}$$

We assume that we know the value of $x$ at any time instant, therefore $\bar{z}_k$ in (4.19) are known and constant. Furthermore, it is assumed that the inverse $x = \Psi^{-1}(z)$ exists in the whole positive orthant.

The time-derivative of $z_j$ is given by

$$\begin{aligned}\dot{z}_j &= \frac{1}{p_j}\dot{p}_j - \frac{1}{q_j}\dot{q}_j = \frac{1}{p_j}\frac{\partial p_j}{\partial x}\dot{x} - \frac{1}{q_j}\frac{\partial q_j}{\partial x}\dot{x} = \\ &= \left[\frac{1}{x_1}(\alpha_{1j} - \beta_{1j}) \;\; \frac{1}{x_2}(\alpha_{2j} - \beta_{2j}) \;\; \ldots \;\; \frac{1}{x_n}(\alpha_{nj} - \beta_{nj})\right]\dot{x}.\end{aligned} \tag{4.20}$$

Using (4.4) and (4.20), the time derivative of the vector $z$ can be written as

$$\dot{z} = -\mathcal{N}^T\Gamma(x)\cdot\dot{x} = -\mathcal{N}^T\Gamma(x)\mathcal{N}\cdot W(x), \tag{4.21}$$

where

$$\Gamma(x) = \operatorname{diag}\left(\frac{1}{x_1}, \frac{1}{x_2}, \ldots, \frac{1}{x_n}\right). \tag{4.22}$$

The rank of $\mathcal{N}$ is always $r$ and $x_i > 0$ for $i = 1, \ldots, n$, therefore the matrix $\mathcal{N}^T\Gamma(x)\mathcal{N}$ is nonsingular and positive definite at any fixed $x$, since it can be written as $P^TP$, where

$$P = (\Gamma(x))^{1/2}\mathcal{N}. \tag{4.23}$$

This means, that the system (4.21) is at equilibrium if and only if $W(x) = 0$ i.e. the unique equilibrium point in the $z$-coordinates is at $z_i = 0$, $i = 1, \ldots, r$.

Furthermore, from eqs. (4.2), (4.15) and (4.16) the reaction rates can be expressed as

$$W_j = p_j - q_j = \exp(z_j)q_j - q_j = q_j\left[\exp(z_j) - 1\right]. \tag{4.24}$$

Let us use the following notation:

$$F(x) = \operatorname{diag}(q_1(x), \ldots, q_r(x)). \tag{4.25}$$

Let the Hamiltonian function $\mathcal{H}$ be defined as

$$\mathcal{H}(z) = \sum_{j=1}^{r} q_j^*\left[\exp(z_j) - z_j - 1\right], \tag{4.26}$$

where $q_i^*$ denotes the value of $q_i$ at the equilibrium point $x^*$. It is easy to show that $\mathcal{H}$ is globally convex and bounded from below, therefore it can be used as a Lyapunov function candidate.

Using Eqs. (4.21), (4.24) and (4.26) we can write

$$\dot{z} = -\mathcal{N}^T \Gamma(x) \mathcal{N} \cdot F(q) \cdot (F(q^*))^{-1} \cdot \mathcal{H}_z^T(z), \tag{4.27}$$

or shortly

$$\dot{z} = -G(x) \cdot \mathcal{H}_z^T(z), \tag{4.28}$$

where

$$G(x) = \mathcal{N}^T \Gamma(x) \mathcal{N} \cdot F(q) \cdot (F(q^*))^{-1}, \tag{4.29}$$

and $\mathcal{H}_z^T$ denotes the gradient transpose of $\mathcal{H}$. Using the assumption that $\Psi$ is invertible, (4.28) can be written as

$$\dot{z} = -G(\Psi^{-1}(\bar{z})) \cdot \mathcal{H}_z^T(z) \tag{4.30}$$

It is easy to see, that $G + G^T$ is positive definite in a neighborhood of the equilibrium point, since it is smooth with respect to $x$ in the positive orthant and

$$G(x^*) = \mathcal{N}^T \Gamma(x^*) \mathcal{N} \cdot F(q^*) \cdot (F(q^*))^{-1} = \mathcal{N}^T \Gamma(x^*) \mathcal{N}. \tag{4.31}$$

However, it cannot be guaranteed for an arbitrary reaction network that $G + G^T$ is positive definite in the whole concentration space. Therefore we can state the following proposition

**Proposition 4.2.1.** For any closed reaction kinetic system of the form (4.4) with independent elementary reaction-pairs, there exists a neighborhood $U$ around the equilibrium point $z^* = 0$, where the system admits a dissipative-Hamiltonian description with Hamiltonian function (4.26).

### 4.2.2 Physical interpretation

The G matrix in the Hamiltonian description reflects the connectivity properties of the reaction network (since $\mathcal{N}$ together with the chemical composition of the complexes defines the graph structure of the system). It is also visible that $G(x^*)$ is symmetric and $G$ generally loses its symmetry outside the equilibrium point. The Hamiltonian function $\mathcal{H}$ contains the scaled chemical affinities, but it is rather an abstract construction and not the total energy of the system as in the case of many mechanical and electrical systems.

In a thermodynamic sense, the local definiteness of $G + G^T$ is related to the so-called entropy production function given by the product of thermodynamic fluxes and forces:

$$\dot{B} = -z^T \cdot W = -\sum_{j=1}^{r} \ln \frac{p_j}{q_j} (p_j - q_j) \tag{4.32}$$

where the transformed entropy function $B$ in the space of the chemical concentrations is defined as

$$B(x) = \sum_{i=1}^{n} x_i \left( \ln \left( \frac{x_i}{x_i^*} \right) - 1 \right) + x_i^*. \tag{4.33}$$

It is known that $B$ (which is a measure of the inner dissipation of the system) is globally convex in the positive orthant and it is nonincreasing in time (see, e.g. [69]). Therefore $\dot{B}$ is globally negative semidefinite but it is only locally concave (as a function of the concentrations) in a neighborhood of the equilibrium point determined by the topology of the reaction network and the kinetic constants. $\dot{B}$ loses its concavity

in the so called far from equilibrium region of the concentration space [121]. This property can be a source of complex nonlinear behavior (e.g. multiple steady states or nonlinear oscillations) when the system is opened and the exchange of material with its environment is permitted that can be modeled as external manipulable (or disturbance) inputs [J4].

### 4.2.3 Comparison to the GENERIC structure

In this subsection, the general dissipative Hamiltonian structure described in section 2.4 and the so-called GENERIC structure proposed in [156] will be compared.

The general equation for the time-evolution of beyond-equilibrium systems is formalized in the GENERIC structure that accounts for the reversible and irreversible contributions of the total energy $E(x)$ and the entropy $P(x)$:

$$\dot{x} = L(x) \cdot E_x^T(x) + M(x) \cdot P_x^T(x), \tag{4.34}$$

where $x$ is a set of independent variables required for a complete description of the system (e.g. energies, velocities, etc.) and $E_x$ and $P_x$ denote the gradients of $E$ and $P$, respectively. In addition, the skew-symmetric matrix $L(x)$ and the positive semi-definite $M(x)$ satisfy the so called degeneracy properties:

$$L \cdot P_x^T(x) = 0 \tag{4.35}$$

$$M \cdot E_x^T(x) = 0, \tag{4.36}$$

and the impositions of the First and Second Laws of Thermodynamics:

$$\frac{dE}{dt} = 0 \tag{4.37}$$

$$\frac{dP}{dt} \geq 0. \tag{4.38}$$

It is visible that taking into consideration eqs. (4.35)-(4.36), the algebraic structure of (2.22) matches the GENERIC structure (4.34) with $L = J$, $M = R$, $E = \mathcal{H}$, and $P = -\mathcal{H}$. However, the restrictive relations (4.35)-(4.36) and (4.37)-(4.38) are clearly generally not fulfilled for the local dissipative-Hamiltonian description.

## 4.3 Examples

**Example 4.3.1. Global dissipative Hamiltonian description.** Let the reaction system with six species $X_1, \ldots, X_6$ (together with the corresponding concentrations $x_1, \ldots, x_6$, respectively) and four complexes $X_1 + X_2$, $X_3$, $X_4 + X_5$ and $X_6$ be given in the following form.

$$X_1 + X_2 \quad \underset{k_1^-}{\overset{k_1^+}{\rightleftarrows}} \quad X_3 \tag{4.39}$$

$$X_4 + X_5 \quad \underset{k_2^-}{\overset{k_2^+}{\rightleftarrows}} \quad X_6. \tag{4.40}$$

The matrices characterizing the reaction network are given by

$$\mathcal{N}^T = \begin{bmatrix} -1 & -1 & 1 & 0 & 0 & 0 \\ 0 & 0 & 0 & -1 & -1 & 1 \end{bmatrix} \tag{4.41}$$

$$\Gamma(x) = \operatorname{diag}\left(\frac{1}{x_1}, \ldots, \frac{1}{x_6}\right), \quad F(x) = \operatorname{diag}(q_1(x), q_2(x)), \tag{4.42}$$

and

$$G(x) = \begin{bmatrix} \frac{(x_1^{-1}+x_2^{-1}+x_3^{-1})x_3}{x_3^*} & 0 \\ 0 & \frac{(x_4^{-1}+x_5^{-1}+x_6^{-1})x_6}{x_6^*} \end{bmatrix}. \tag{4.43}$$

We can see that $G$ is globally positive definite in the whole positive orthant, which means that the reaction system admits a global dissipative Hamiltonian structure. Based on the above calculations, it is easy to see that any set of independent reactions of the type

$$\sum_{j=1}^{\alpha_i} c_{ij} X_{ij} \underset{k_i^-}{\overset{k_i^+}{\rightleftarrows}} \sum_{l=\alpha_i+1}^{n_i} c_{il} X_{il}, \quad \alpha_i < n_i, \quad i = 1, \ldots, r \tag{4.44}$$

defines a global dissipative Hamiltonian structure.

**Example 4.3.2. Local dissipative Hamiltonian description.**

**Model of the reaction network** Consider the following simple reaction network with three species ($X_1$, $X_2$, $X_3$) and four complexes $X_1 + X_2$, $X_3$, $X_2 + X_3$ and $2X_3$:

$$X_1 + X_2 \underset{k_1^-}{\overset{k_1^+}{\rightleftarrows}} X_3 \tag{4.45}$$

$$X_2 + X_3 \underset{k_2^-}{\overset{k_2^+}{\rightleftarrows}} 2X_3. \tag{4.46}$$

The matrix $\mathcal{N}$ of the system is written as

$$\mathcal{N} = \begin{bmatrix} -1 & 0 \\ -1 & -1 \\ 1 & 1 \end{bmatrix}. \tag{4.47}$$

The forward and backward reaction rates are

$$p_1 = k_1^+ x_1 x_2, \; q_1 = k_1^- x_3 \tag{4.48}$$

$$p_2 = k_2^+ x_2 x_3, \; q_2 = k_2^- x_3^2. \tag{4.49}$$

From the above equations, the components of the vector $W$ are calculated as

$$W_1 = p_1 - q_1 = k_1^+ x_1 x_2 - k_1^- x_3 \tag{4.50}$$

$$W_2 = p_2 - q_2 = k_2^+ x_2 x_3 - k_2^- x_3^2. \tag{4.51}$$

Using $N$ and $W$, the equations of the reaction system are the following

$$\dot{x}_1 = k_1^- x_3 - k_1^+ x_1 x_2 \tag{4.52}$$

$$\dot{x}_2 = k_1^- x_3 - k_1^+ x_1 x_2 + k_2^- x_3^2 - k_2^+ x_2 x_3 \tag{4.53}$$

$$\dot{x}_3 = k_1^+ x_1 x_2 - k_1^- x_3 + k_2^+ x_2 x_3 - k_2^- x_3^2 \tag{4.54}$$

**Dissipative Hamiltonian structure of the closed system.** The coordinates-transformation $\Psi$ is given by

$$\bar{z}_1 = \ln\left(\frac{p_1}{q_1}\right) = \ln\left(\frac{k_1^+}{k_1^-}x_1x_2x_3^{-1}\right) \tag{4.55}$$

$$\bar{z}_2 = \ln\left(\frac{p_2}{q_2}\right) = \ln\left(\frac{k_2^+}{k_2^-}x_2x_3^{-1}\right) \tag{4.56}$$

$$\bar{z}_3 = x_2 + x_3. \tag{4.57}$$

Then the inverse transformation $\Psi^{-1}$ can be calculated as

$$x_1 = \frac{k_2^+k_1^-}{k_2^-k_1^+}\exp(\bar{z}_1 - \bar{z}_2) \tag{4.58}$$

$$x_2 = \frac{k_2^-z_3\exp(\bar{z}_2)}{k_2^-\exp(\bar{z}_2) + k_2^+} \tag{4.59}$$

$$x_3 = \frac{k_2^+\bar{z}_3}{k_2^-\exp(\bar{z}_2) + k_2^+}. \tag{4.60}$$

We can see from eqs. (4.55)-(4.60) that $\Psi$ and $\Psi^{-1}$ are globally defined in the positive orthant of the space of concentrations.

The dissipative Hamiltonian structure (4.28) for the model (4.52)-(4.54) is computed as

$$\begin{bmatrix} \dot{z}_1 \\ \dot{z}_2 \end{bmatrix} = -\begin{bmatrix} \frac{1}{x_1}+\frac{1}{x_2}+\frac{1}{x_3} & \frac{1}{x_2}+\frac{1}{x_3} \\ \frac{1}{x_2}+\frac{1}{x_3} & \frac{1}{x_2}+\frac{1}{x_3} \end{bmatrix} \cdot \begin{bmatrix} \frac{x_3}{x_3^*} & 0 \\ 0 & \frac{x_3^2}{(x_3^*)^2} \end{bmatrix} \cdot \mathcal{H}_z^T(z), \tag{4.61}$$

where

$$\mathcal{H}_z = \begin{bmatrix} k_1^-x_3^*(\exp(z_1)-1) & k_2^-(x_3^*)^2(\exp(z_2)-1) \end{bmatrix}. \tag{4.62}$$

For the forthcoming calculations, the values of the reaction rate constants $k_1^+$, $k_1^-$, $k_2^+$, $k_2^-$ were chosen to be uniformly 1. The dissipativity region (i.e. the region inside which the matrix $G+G^T$ is positive definite) and the level sets of $\mathcal{H}$ for $x^* = [1\ \ 5\ \ 5]^T$ in the $(x_1, x_2)$ and $(z_1, z_2)$ planes can be seen in Figs 4.1 and 4.2, respectively. It is visible that the dissipative Hamiltonian description is valid in a wide neighborhood of the equilibrium point for the selected reaction polyhedron.

## 4.4 Summary

It has been shown in this chapter that closed reversible reaction networks with independent elementary reaction-pairs admit a global pseudo Hamiltonian and a local dissipative Hamiltonian structure around any positive equilibrium point. The Hamiltonian structure has been described in a transformed coordinates system called the reaction space which is generally of lower dimension than the concentration space. The structure matrix which is a smooth function of the concentrations depends on the topology of the reaction network and the coefficients of the Hamiltonian function depend on the reaction polyhedron on which the system dynamics evolve. The theoretical results have been illustrated by two examples.

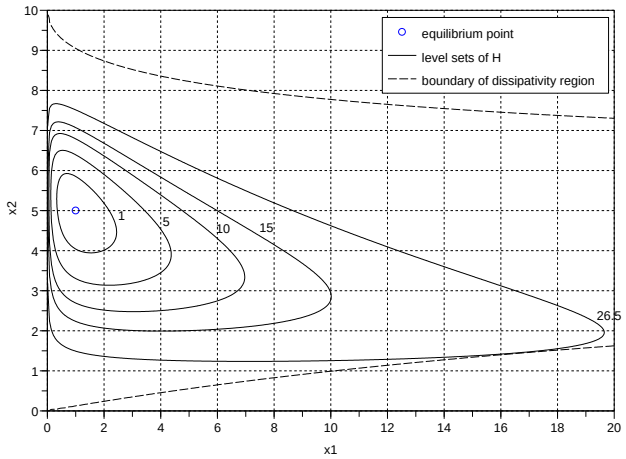


Figure 4.1: Dissipativity region and level sets of the Hamiltonian function in the $(x_1,\ x_2)$ plane

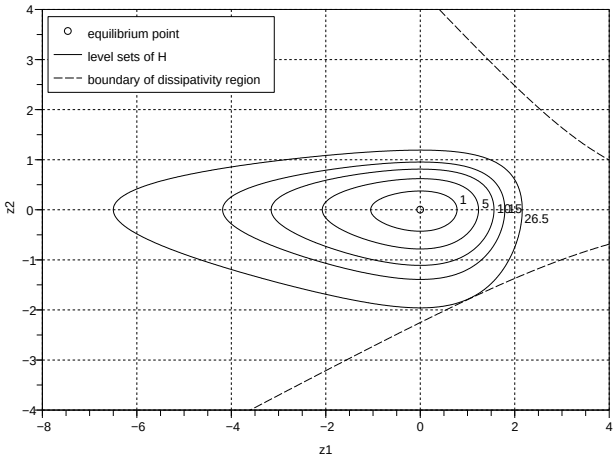


Figure 4.2: Dissipativity region and level sets of the Hamiltonian function in the $(z_1,\ z_2)$ plane

# Chapter 5

# Dense and sparse realizations of kinetic systems

The second part of the thesis deals with the optimization-based computation of dynamically equivalent and linearly conjugate reaction network topologies. In this chapter, the emphasis will be put on the so-called dense and sparse realizations containing the maximal or minimal number of nonzero reaction rate coefficients, respectively.

## 5.1 Additional motivations of the work

As it has been mentioned in the Introduction, one of the very few rigorous works before 2009 studying dynamical equivalence of reaction networks is [28], where the authors examine the distinguishability of chemical reaction networks with mass action kinetics. In [28], two reaction networks are called *confoundable* "if they produce the same mass-action differential equations for some choice of the rate constants". Valuable results are presented in the paper, in particular, a necessary and sufficient condition is given for the unique identifiability of rate constants in reaction networks that is very easy to check. However, the authors did not take into consideration a special case in **Theorem 4.4**, when the monomials corresponding to certain source complexes are cancelled out in the differential equations of the reaction network. In [28], **Theorem 4.4** says:

*"Under the mass-action kinetics assumption, two chemical reaction networks ($\mathcal{S}$, $\mathcal{C}'$, $\mathcal{R}'$) and ($\mathcal{S}$, $\mathcal{C}''$, $\mathcal{R}''$) are confoundable if and only if they have the same source complexes and $Cone_{\mathcal{R}'}(y) \cap Cone_{\mathcal{R}''}(y)$ is nonempty for every source complex $y$."*

The possibility of the above mentioned monomial cancellation is illustrated in the following example published originally in [J6].

**Example 5.1.1.** Consider the reaction network denoted by $R$ shown in Fig. 5.1(a) with the following parameters:

$$k_i = 1, \quad i = 1, 2, 3, 4.$$

The differential equations of $R$ can be computed as

$$\begin{aligned} \begin{bmatrix} \dot{x}_1 \\ \dot{x}_2 \end{bmatrix} &= k_1 x_1^2 \begin{bmatrix} -2 \\ 1 \end{bmatrix} + k_2 x_1^2 \begin{bmatrix} -1 \\ 1 \end{bmatrix} + k_3 x_1^2 \begin{bmatrix} 1 \\ 0 \end{bmatrix} + k_4 x_1^2 \begin{bmatrix} 0 \\ 1 \end{bmatrix} \\ &= \begin{bmatrix} -2x_1^2 \\ 3x_1^2 \end{bmatrix}. \end{aligned} \tag{5.1}$$

Now, take the reaction system $R'$ depicted in Fig 5.1(b) with the parameters:

$$k_1' = 1,\ k_2' = k_3' = k_5' = k_6' = 0.1,\ k_4' = 1.9.$$

The equations of $R'$ are

$$\begin{bmatrix} \dot{x}_1 \\ \dot{x}_2 \end{bmatrix} = 1 \cdot x_1^2 \begin{bmatrix} -2 \\ 1 \end{bmatrix} + 0.1x_1^2 \begin{bmatrix} -1 \\ 1 \end{bmatrix} + 0.1x_1^2 \begin{bmatrix} 1 \\ 0 \end{bmatrix} + 1.9x_1^2 \begin{bmatrix} 0 \\ 1 \end{bmatrix} + 0.1x_1x_2 \begin{bmatrix} -1 \\ 0 \end{bmatrix} + 0.1x_1x_2 \begin{bmatrix} 1 \\ 0 \end{bmatrix} = \begin{bmatrix} -2x_1^2 \\ 3x_1^2 \end{bmatrix}. \tag{5.2}$$

It is clear from Eqs. (5.1)-(5.2) that $R$ and $R'$ are confoundable in the sense of the original definition given in [28]. However, the source complexes in the two networks are not identical, since $X_1 + X_2$ is a source complex in $R'$ but not in $R$.

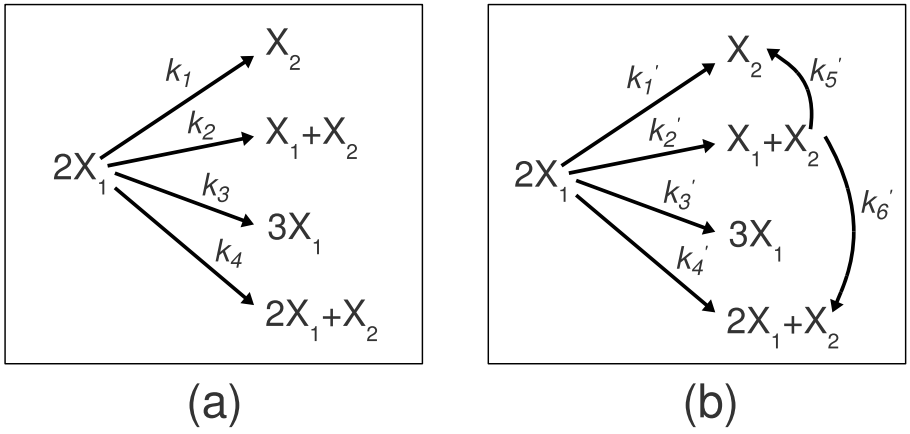


Figure 5.1: (a) Reaction network $R$, (b) Reaction network $R'$

The consequences of the defect in Theorem 4.4 in [28] are even more transparent from Example 2.5.2 in subsection 2.5.8 that is also a counterexample. If we accepted Theorem 4.4, then we could deduce that the CRN in Fig. 2.3(a) has no weakly reversible dynamically equivalent realization with complexes $3X_2$, $3X_1$ and $2X_1 + X_2$, since $2X_1 + X_2$ is not a source complex. However, it is clearly shown (see Figs. 2.3(c) and (d)) that for *any* positive values of $k_1$ and $k_2$ there are more than one possible dynamically equivalent weakly reversible structures involving all three complexes, that also gives essential qualitative information about the dynamics, since the Deficiency One Theorem is immediately applicable to the system. Moreover, the example also shows that by adding appropriately selected new complexes to a given CRN (in this case, $2X_1 + X_2$ to the network in Fig. 2.3(e)), there might be chance to obtain additional information about the dynamics. However, we will not elaborate on new complex selection and it will be assumed throughout the presented computation methods that the set of complexes (i.e. the stoichiometric matrix $Y$) is fixed and known before the computations. Of course, this does not mean that all the complexes in $Y$ have to take part in a reaction if an initial network is given, so $Y$ can be considered to contain a "maximal allowable" set of complexes. In this case, the condition (2.49) for dynamical equivalence can be written as

$$Y \cdot A_k^{(1)} = Y \cdot A_k^{(2)} =: M, \tag{5.3}$$

where $A_k^{(1)}$ and $A_k^{(2)}$ are valid Kirchhoff matrices and $M$ is the invariant matrix containing the coefficients of the monomials on the right hand side of the polynomial ODEs. It is clear that if for a given set of complexes $Y$ a CRN has two different dynamically equivalent realizations characterized by $A_k^{(1)}$ and $A_k^{(2)}$, then it has infinitely many, since e.g. $A_k^{(3)} = \frac{A_k^{(1)}+A_k^{(2)}}{2}$ also defines a valid realization with $Y$. Therefore, after examining the so-called dense and sparse realizations in this chapter, chapter 6 will focus on computing CRN realizations with additional given properties.

## 5.2 The notion of dense and sparse realizations

Among the dynamically equivalent CRN realizations, we will define the following characteristic ones. Assuming that the set of complexes (i.e. the stoichiometric matrix $Y$) is given, a *sparse realization* contains the minimal number of reactions that is needed for the exact description of the corresponding dynamics (2.29). A *dense realization* contains the maximal number of reactions among dynamically equivalent realizations with a fixed complex set.

The starting point for the forthcoming calculations is that a reaction network is given with its reaction graph or equivalently with any of its realizations $(Y, A_k)$, and we want to compute its sparse or dense realization denoted by $(Y^s, A_k^s)$ and $(Y^d, A_k^d)$, respectively. In agreement with our initial assumptions, $Y$ in the initial realization contains the maximal possible set of complexes that we want to work with. This means that $A_k$ may contain zero rows and columns if we allow such complexes in $Y$ that do not react in the initial CRN realization and are therefore isolated nodes in its reaction graph. We remark that obviously, the sparse or dense realizations may not be unique parametrically for a given dynamics, but here our intital goal is to find one possible solution.

## 5.3 Representation of mass action kinetics as linear equality constraints

For the computations, let us represent the Kirchhoff matrix of a reaction network containing $m$ complexes as

$$A_k = \begin{bmatrix} -a_{11} & a_{12} & \dots & a_{1m} \\ a_{21} & -a_{22} & \dots & a_{2m} \\ \vdots & & & \vdots \\ a_{m1} & a_{m2} & \dots & -a_{mm} \end{bmatrix}. \tag{5.4}$$

Keeping in mind the properties of $A_k$, the negative sign in (5.4) for the diagonal elements $a_{ii}$ for $i = 1, \dots, m$ will allow us to set a uniform nonnegativity (or identically tractable lower and upper bound) constraint for all $a_{ij}$ in the later computations.

Let us denote the $i$th row and $i$th column of a matrix $W$ by $[W]_{i,\cdot}$ and $[W]_{\cdot,i}$, respectively. Using (5.4), the individual linear equations of the matrix equation (2.34)

can be written as

$$-y_{11}a_{11} + y_{12}a_{21} + \cdots + y_{1m}a_{m1} = [M]_{11} \tag{5.5}$$
$$\vdots$$
$$-y_{n1}a_{11} + y_{n2}a_{21} + \cdots + y_{nm}a_{m1} = [M]_{n1} \tag{5.6}$$
$$y_{11}a_{12} - y_{12}a_{22} + \cdots + y_{1m}a_{m2} = [M]_{12} \tag{5.7}$$
$$\vdots$$
$$y_{n1}a_{12} - y_{n2}a_{22} + \cdots + y_{nm}a_{m2} = [M]_{n2} \tag{5.8}$$
$$\vdots$$
$$y_{11}a_{1m} + y_{12}a_{2m} + \cdots - y_{1m}a_{mm} = [M]_{1m} \tag{5.9}$$
$$\vdots$$
$$y_{n1}a_{1m} + y_{n2}a_{2m} + \cdots - y_{nm}a_{mm} = [M]_{nm}\,. \tag{5.10}$$

The property that $A_k$ is a column conservation matrix can also be expressed in the form of linear equations:

$$-a_{11} + a_{21} + a_{31} + a_{41} = 0 \tag{5.11}$$
$$a_{12} - a_{22} + a_{32} + a_{42} = 0 \tag{5.12}$$
$$\vdots$$
$$a_{1m} + a_{2m} + \cdots - a_{mm} = 0. \tag{5.13}$$

Equations (5.5)-(5.13) can be written in the following more compact form:

$$\begin{bmatrix} \bar{Y}^1 & 0 & 0 & \dots & 0 \\ 0 & \bar{Y}^2 & 0 & \dots & 0 \\ \vdots & & & & \\ 0 & 0 & 0 & \dots & \bar{Y}^m \end{bmatrix} \begin{bmatrix} [A_k]_{\cdot,1} \\ [A_k]_{\cdot,2} \\ \vdots \\ [A_k]_{\cdot,m} \end{bmatrix} = \begin{bmatrix} \left[\bar{M}\right]_{\cdot,1} \\ \left[\bar{M}\right]_{\cdot,2} \\ \vdots \\ \left[\bar{M}\right]_{\cdot,m} \end{bmatrix}, \tag{5.14}$$

where the zeros denote zero matrix blocks of size $(n+1) \times m$ and

$$\bar{Y}^i = \begin{bmatrix} [Y]_{\cdot,1} & [Y]_{\cdot,2} & \dots & [Y]_{\cdot,i-1} & -[Y]_{\cdot,i} & [Y]_{\cdot,i+1} & \dots & [Y]_{\cdot,m} \\ 1 & 1 & \dots & 1 & -1 & 1 & \dots & 1 \end{bmatrix} \in \mathbb{R}^{(n+1)\times m}, \tag{5.15}$$

$$\bar{M} = \begin{bmatrix} & M & \\ 0 & \dots & 0 \end{bmatrix} \in \mathbb{R}^{(n+1)\times m} \tag{5.16}$$

## 5.4 Constructing the optimization problem

It is visible from (5.14) that the optimization variable will contain the reaction rate coefficients, i.e. the elements of $A_k$ as the matrix $Y$ is known and fixed by the problem statement. For the sake of simplicity, let us use the notation

$$z = \begin{bmatrix} z^{(1)} \\ z^{(2)} \\ \vdots \\ z^{(m)} \end{bmatrix} = \begin{bmatrix} [A_k]_{\cdot,1} \\ [A_k]_{\cdot,2} \\ \vdots \\ [A_k]_{\cdot,m} \end{bmatrix}, \tag{5.17}$$

where obviously, $z^{(i)} \in \mathbb{R}^m$, $i = 1, \ldots, m$.

When we seek the sparse realization of the original reaction network $(A_k, Y)$ then we are searching for the sparsest solution of (5.14), i.e. the one containing the maximal number of zeros (or the minimal number of zeros, if the dense realization is to be computed). For this, let us associate logical variables $\delta_j^{(i)}$ with the continuous variables $z_j^{(i)}$ for $i, j = 1, \ldots, m$. Then the optimization variable previously denoted by $y$ is

$$y = \begin{bmatrix} z \\ \delta \end{bmatrix}. \tag{5.18}$$

Following from the problem statement and construction, the lower bound for the continuous variables is zero. For the solvability of the MILP problem, also an upper bound is introduced for the elements of $z$, i.e.

$$0 \leq \ z_i \leq u_i, \ u_i > 0, \ i = 1, \ldots, m^2. \tag{5.19}$$

To minimize (or maximize) the number of nonzeros in the continuous solution part $z$, the following compound statement has to be translated to linear inequalities

$$\delta_i = 1 \leftrightarrow z_i > 0, \ i = 1, \ldots, m^2. \tag{5.20}$$

To be able to numerically distinguish between practically zero and nonzero solutions, (5.20) is modified to

$$\delta_i = 1 \leftrightarrow z_i > \epsilon, \ i = 1, \ldots, m^2, \tag{5.21}$$

where $\epsilon$ is a sufficiently small positive value (i.e. solutions below $\epsilon$ are treated as zero). Taking into consideration (5.19), the linear inequalities corresponding to (5.21) are

$$0 \leq z_i - \epsilon\delta_i, \ i = 1, \ldots, m^2 \tag{5.22}$$

$$0 \leq -z_i + u_i\delta_i, \ i = 1, \ldots, m^2. \tag{5.23}$$

Now, the MILP problem for finding a possible sparse realization can be constructed as

$$\text{minimize} \sum_{m^2+1}^{2m^2} y_i \tag{5.24}$$

subject to:

$$\begin{bmatrix} \bar{Y}^1 & 0 & 0 & \ldots & 0 \\ 0 & \bar{Y}^2 & 0 & \ldots & 0 \\ \vdots & & & & \\ 0 & 0 & 0 & \ldots & \bar{Y}^m \end{bmatrix} \begin{bmatrix} y_1 \\ y_2 \\ \vdots \\ y_{m^2} \end{bmatrix} = \begin{bmatrix} [\bar{M}]_{\cdot,1} \\ [\bar{M}]_{\cdot,2} \\ \vdots \\ [\bar{M}]_{\cdot,m} \end{bmatrix} \tag{5.25}$$

$$0 \leq y_i \leq u_i \text{ for } i = 1, \ldots, m^2 \tag{5.26}$$

$$0 \leq y_i - \epsilon y_{i+m^2}, \ i = 1, \ldots, m^2 \tag{5.27}$$

$$0 \leq -y_i + u_i y_{i+m^2}, \ i = 1, \ldots, m^2 \tag{5.28}$$

$$y_j \text{ is integer for } j = m^2 + 1, \ldots, 2m^2. \tag{5.29}$$

In the case when a dense realization is searched for, the optimization task (5.24) is simply changed to

$$\text{minimize} \left( - \sum_{m^2+1}^{2m^2} y_i \right). \tag{5.30}$$

The following remarks contain important additional information about the solved problem.

**Remark 1**. By setting the lower and upper bounds for $y_i$ differently from what is given in (5.26), the presence or omission of certain reactions can be forced during the optimization.

**Remark 2**. The block-diagonal structure of the coefficient matrix in (5.25) and the independence of the inequalities (5.26)-(5.28) allow us to partition the optimization variable $y$ to $m$ partitions and thus to solve the $m$ resulting MILP subproblems parallely (i.e. columnwise) which is a significant advantage from a computational point of view [7].

**Remark 3**. The block-diagonal structure mentioned in the previous remark makes it possible to combine different objective functions for different source complexes (since column $i$ of $A_k$ contains the rate coefficients corresponding to the reactions starting from complex $C_i$). E.g., the number of reactions starting from certain complexes can be minimized while it can be maximized for other complexes.

**Remark 4**. We note that the sparsest solution of certain sets of underdetermined linear equations can be obtained in polynomial time using linear programming (LP) [39, 38]. However, the applicability conditions of this LP solution are not fulfilled for most reaction networks.

**Remark 5**. Using the dense realization, an upper bound for the rank of the possible dynamically equivalent realizations (see subsection 2.5.3) and a lower bound for the number of linkage classes can be obtained immediately.

## 5.5 Properties of dense realizations and their consequences

The main result of this section is that the dense realization of a CRN is structurally unique if the set of possible complexes is fixed. Firstly, we state the following result.

**Theorem 5.5.1.** Let $\Sigma = (Y, A_k)$ be a kinetic system and $M = YA_k$. Furthermore, let $\Sigma^d = (Y, A_k^d)$ and $\Sigma^s = (Y, A_k^s)$ denote a dynamically equivalent dense and sparse realization of $\Sigma$, respectively. Then for any dynamically equivalent realization of $\Sigma$ of the form $\Sigma' = (Y, A_k')$ the following hold.

**P1** The unweighted reaction graph of $\Sigma'$ is the subgraph of the unweighted reaction graph of $\Sigma^d$.

**P2** The unweighted reaction graph of $\Sigma^d$ is unique.

**P3** The unweighted reaction graph of a kinetic system with a given set of complexes is unique if and only if the graph structures of its sparse and dense realizations are identical.

*Proof.* **P1**, **P2**. (indirect) Assume that the Kirchhoff matrix $A_k$ is a dense solution of $YA_k = M$, i.e. it contains the maximal number of nonzero off-diagonal elements. Furthermore, assume for a Kirchhoff matrix $A'_k$ that $YA'_k = M$ and $\exists\, i, j,\ i \neq j$ such that $[A_k]_{ij} = 0$ but $[A'_k]_{ij} > 0$. Then $A''_k = \frac{1}{2}(A_k + A'_k)$ is a Kirchhoff matrix of another dynamically equivalent realization to $\Sigma$ but $A''_k$ contains more nonzero off-diagonal elements than $A_k$ which is a contradiction.
**P3**. This fact is easy to see: If the structures (i.e. the unweighted reaction graphs) of the dense and sparse realizations are identical, then it directly follows that the graph structures of all dynamically equivalent CRNs are the same, since the only possible unique structure is determined by the dense realization (that is the sparse realization at the same time). In other words, any realization of the CRN can contain neither more nor less reactions than the dense realization does, the structure of which is unique. If the graph structure of the CRN is unique, then it trivially implies that the structures of the dense and sparse realizations are identical. □

The following remarks contain some important immediate consequences and additions to Theorem 5.5.1.

**R1** According to Theorem 5.5.1, dense realizations give a unique "superstructure" for a CRN in the sense that the reactions of any realization of a CRN must form a subset of the reactions of the dense realization if the set of possible complexes is given. In other words, reactions that are not present in the dense realization cannot appear in any other realization.

**R2** Obviously, dense realizations are parametrically not unique. There may exist several dense realizations for a CRN with different reaction rate constants (weights) but always with the same graph structure.

**R3** The dense realization of a CRN is not only a theoretical construction but it can be practically determined using well-formulated numerical procedures that are treatable even in the case of several hundred complexes and species (see, e.g. [59, 132]).

**R4** Sparse realizations of CRNs are structurally not unique, there may exist several sparse realizations for a given CRN with different graph structures (see Example A.2.1).

## 5.6 Examples

The following examples were computed using the MILP solver of the YALMIP toolbox [110] under the MATLAB® computational environment.

**Example 5.6.1.** Consider again the simple reaction network of Example 2.5.1. The computed dense and sparse realizations are shown in Figs 5.2 and 5.3, respectively. The Kirchhoff-matrix of the computed sparse realization is

$$A_k^s = \begin{bmatrix} -2 & 1 & 0 & 0 \\ 1 & -2 & 3 & 1 \\ 1 & 0 & -3 & 1 \\ 0 & 1 & 0 & -2 \end{bmatrix}, \tag{5.31}$$

while the dense realization is characterized by

$$A_k^d = \begin{bmatrix} -1.7 & 1.1 & 0.966 & 0.3 \\ 0.1 & -2.3 & 0.1 & 0.1 \\ 1.3 & 0.1 & -2.033 & 1.3 \\ 0.3 & 1.1 & 0.966 & -1.7 \end{bmatrix}, \tag{5.32}$$

Furthermore, $Y^s = Y^d = Y$. It is easy to check that $Y^s \cdot A_k^s = Y^d \cdot A_k^d = M$. The deficiency of all three networks is 1, since $m = 4$, $l = 1$ and $s = 2$ in all cases. Furthermore, both the sparse and dense realizations have the weak reversibility property.

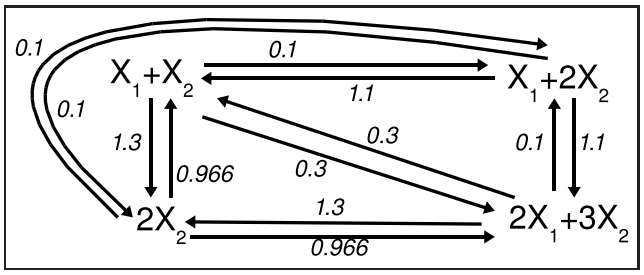


Figure 5.2: Dense realization of the reaction network of Example 2.5.1

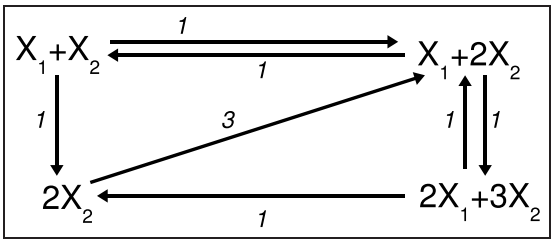


Figure 5.3: Sparse realization of the reaction network of Example 2.5.1

**Example 5.6.2.** This example shows that the number of linkage classes can also be different in dynamically equivalent CRN realizations. Fig. 5.4(a) shows a simple reaction network with two linkage classes. Let the reaction rate coefficients be 1 for each reaction again. The deficiency of the network is 4 ($m = 8$, $l = 2$, $s = 2$). The $Y$ and $A_k$ matrices of the network are

$$Y = \begin{bmatrix} 1 & 0 & 1 & 3 & 2 & 1 & 0 & 1 \\ 0 & 1 & 1 & 1 & 1 & 2 & 3 & 3 \end{bmatrix} \tag{5.33}$$

$$A_k = \begin{bmatrix} -1 & 0 & 0 & 0 & 0 & 0 & 0 & 0 \\ 1 & -2 & 0 & 0 & 0 & 0 & 0 & 0 \\ 0 & 1 & 0 & 0 & 0 & 0 & 0 & 0 \\ 0 & 1 & 0 & 0 & 0 & 0 & 0 & 0 \\ 0 & 0 & 0 & 0 & -3 & 0 & 0 & 0 \\ 0 & 0 & 0 & 0 & 1 & 0 & 0 & 0 \\ 0 & 0 & 0 & 0 & 1 & 0 & 0 & 0 \\ 0 & 0 & 0 & 0 & 1 & 0 & 0 & 0 \end{bmatrix} \tag{5.34}$$

dc_263_11

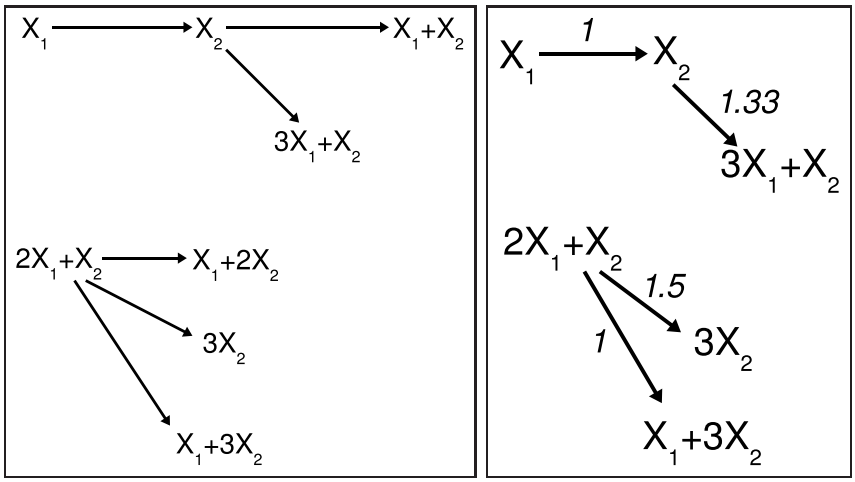


Figure 5.4: (a) Reaction network of Example 5.6.2. All the rate coefficients are chosen to be 1. (b) Sparse realization of the reaction network of Example 5.6.2

Both sparse and dense realizations have been computed for this network. Fig. 5.4(b) shows a sparse realization containing only 6 complexes and 4 reactions with the Kirchhoff matrix

$$A_k^s = \begin{bmatrix} -1 & 0 & 0 & 0 & 0 & 0 & 0 & 0 \\ 1 & -1.33 & 0 & 0 & 0 & 0 & 0 & 0 \\ 0 & 0 & 0 & 0 & 0 & 0 & 0 & 0 \\ 0 & 1.33 & 0 & 0 & 0 & 0 & 0 & 0 \\ 0 & 0 & 0 & 0 & -2.5 & 0 & 0 & 0 \\ 0 & 0 & 0 & 0 & 0 & 0 & 0 & 0 \\ 0 & 0 & 0 & 0 & 1.5 & 0 & 0 & 0 \\ 0 & 0 & 0 & 0 & 1 & 0 & 0 & 0 \end{bmatrix}. \tag{5.35}$$

The deficiency of the sparse realization is 2 ($m = 6$, $l = 2$, $s = 2$).

The computed dense realization is depicted in Fig. 5.5. It is visible that in contrast to the previous two cases, the dense realization consists of only one linkage class. In this case, the number of complexes is 8, the number of reactions is 29 and the Kirchhoff matrix is given by

$$A_k^d = \begin{bmatrix} -1 & 0.5 & 0.5 & 0 & 0.1 & 0.1 & 0 & 0 \\ 1 & -2 & 0.2 & 0 & 0.1 & 0.1 & 0 & 0 \\ 0 & 0.1 & -1.2 & 0 & 0.1 & 0.1 & 0 & 0 \\ 0 & 1 & 0.1 & 0 & 0.1 & 0.1 & 0 & 0 \\ 0 & 0.1 & 0.1 & 0 & -3 & 0.1 & 0 & 0 \\ 0 & 0.1 & 0.1 & 0 & 0.1 & -1.1 & 0 & 0 \\ 0 & 0.1 & 0.1 & 0 & 1.1 & 0.2 & 0 & 0 \\ 0 & 0.1 & 0.1 & 0 & 1.4 & 0.4 & 0 & 0 \end{bmatrix} \tag{5.36}$$

The deficiency of the dense realization is 5 ($m = 8$, $l = 1$, $s = 2$). It is straightforward to check that

$$M = YA_k = YA_k^s = YA_k^d = \begin{bmatrix} -1 & 4 & 0 & 0 & -4 & 0 & 0 & 0 \\ 1 & 0 & 0 & 0 & 5 & 0 & 0 & 0 \end{bmatrix}. \tag{5.37}$$

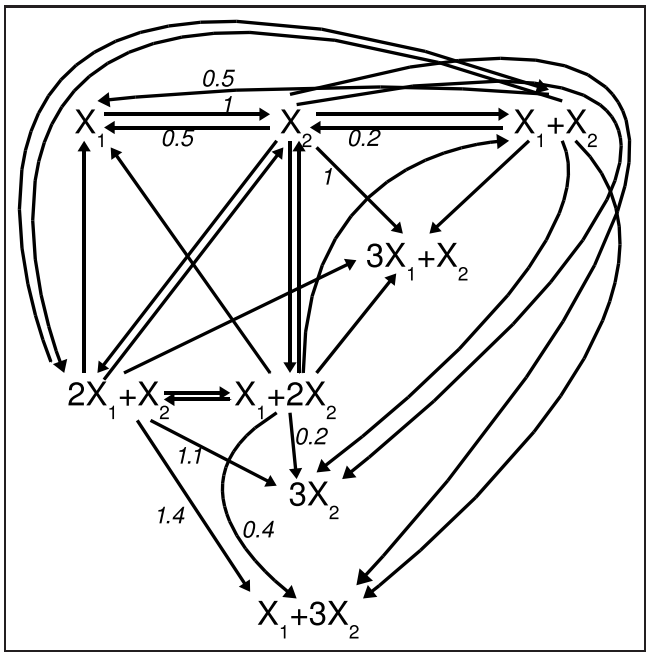


Figure 5.5: Dense realization of the reaction network of Example 5.6.2. Only those reaction rate coefficients are indicated that are different from 0.1.

The structural non-uniqueness of sparse realizations is illustrated by Example A.2.1 in the Appendix.

## 5.7 Summary

An optimization-based method has been proposed in this chapter for the computation of sparse and dense realizations of reaction networks obeying the mass-action law. Starting from an appropriate form (2.29) of the kinetic equations, the mass-action kinetics can be expressed as linear constraints with a block-diagonal structure. The computation of the dense and sparse realizations is traced back to a MILP problem where the optimization variables are the reaction rate coefficients and the corresponding integer auxiliary variables. The proposed method can be used e.g. for finding the "most identifiable" parametrization of a complex reaction network (i.e. the one that has the minimal number of rate coefficients as parameters to be estimated). It has been shown that the structure of a so-called dense realization of a given CRN is unique, and that the structure of any other realization is the subgraph of the dense realization if the set of complexes is given. By computing a possible sparse realization, it is also possible to test numerically, whether the structure of a CRN is unique or not.

The theoretical findings have been illustrated on examples. The results clearly show the power of linear programming combined with propositional logic. In the author's opinion, the presented examples raise interesting problems worth further studying, especially about which important properties of reaction networks can be determined directly from their kinetic differential equations.

# Chapter 6

# Computing dynamically equivalent realizations of kinetic systems with preferred properties

Using a similar optimization approach that was described in the previous chapter, additional problems of interest will be solved here for the computation of dynamically equivalent CRN structures with given properties. Moreover, the notion of dynamical equivalence will be slightly extended using the concept of linear conjugacy.

## 6.1 Additional structural constraints represented in the form of linear inequalities

This section presents some further answers to the open problems originally set in [86] from a numerical aspect. To state the results, we give the constraint set characterizing mass action dynamics described in a shorter and more convenient form. Without reversing the sign of the diagonal elements in $A_k$, (5.14) can be written as

$$Y \cdot A_k = M \tag{6.1}$$

$$\sum_{i=1}^{m} [A_k]_{ij} = 0, \quad j = 1, \ldots, m \tag{6.2}$$

$$[A_k]_{ij} \geq 0, \quad i, j = 1, \ldots, m, \quad i \neq j \tag{6.3}$$

$$[A_k]_{ii} \leq 0, \quad i = 1, \ldots, m, \tag{6.4}$$

where the decision variables are the off-diagonal elements of $A_k$. The additional bounds for these elements (originally described in (5.19)) are given as

$$[A_k]_{ij} \leq l_{ij}, \quad i, j = 1, \ldots, m, \quad i \neq j \tag{6.5}$$

$$l_{ii} \leq [A_k]_{ii}, \quad i = 1, \ldots, m. \tag{6.6}$$

Then, the compound statements given in eq. (5.21) corresponding to the nonzero property of the individual reaction rate coefficients can now be written as

$$\delta_{ij} = 1 \leftrightarrow [A_k]_{ij} > \epsilon, \quad i, j = 1, \ldots, m, \quad i \neq j. \tag{6.7}$$

The linear inequalities corresponding to (6.7) can be translated to the following linear inequalities (see, eqs. (5.22)-(5.23))

$$0 \leq [A_k]_{ij} - \epsilon\delta_{ij}, \quad i,j = 1,\ldots,m,\ i \neq j \tag{6.8}$$
$$0 \leq -[A_k]_{ij} + l_{ij}\delta_{ij}, \quad i,j = 1,\ldots,m,\ i \neq j. \tag{6.9}$$

Finally, the objective function to be minimized/maximized to compute sparse and dense realizations is given by

$$C_1(\delta) = \sum_{\substack{i,j=1 \\ i \neq j}}^{m} \delta_{ij} \tag{6.10}$$

### 6.1.1 Computing realizations with the minimal/maximal number of complexes

In this section, the detailed MILP formalism will be presented for computing CRN realizations that contain the minimal/maximal number of complexes from a predefined complex set.

The constraints written in eqs. (6.1)-(6.6) corresponding to the characteristics of mass-action dynamics are used here again without change. Then, the minimization or maximization of the number of non-isolated complexes in the reaction graph is based on the following simple observation. A complex can be omitted from the reaction network's graph, if both the corresponding column and row in $A_k$ contain only zeros. This means that no directed edges start from or point to this complex in the graph and therefore it becomes an isolated vertex.

For the optimization, $m$ boolean variables denoted by $\delta_i$, $i = 1,\ldots,m$ are introduced. Using these boolean variables, the following compound statements are introduced:

$$\delta_i = 1 \leftrightarrow \sum_{\substack{j_1=1 \\ j_1 \neq i}}^{m} [A_k]_{i,j_1} + \sum_{\substack{j_2=1 \\ j_2 \neq i}}^{m} [A_k]_{j_2,i} > 0, \quad i = 1\ldots,m. \tag{6.11}$$

Eq. (6.11) means that the value of $\delta_i$ is 1 if and only if there is at least one incoming or outgoing directed edge in the reaction graph to/from the $i$th complex. For practical computations, the statement (6.11) is modified as follows:

$$\delta_i = 1 \leftrightarrow \sum_{\substack{j_1=1 \\ j_1 \neq i}}^{m} [A_k]_{i,j_1} + \sum_{\substack{j_2=1 \\ j_2 \neq i}}^{m} [A_k]_{j_2,i} > \epsilon, \quad i = 1\ldots,m \tag{6.12}$$

where again $\epsilon$ is a sufficiently small positive number. Using the bound constraints

(6.5)-(6.6), the linear inequalities corresponding to (6.12) are the following

$$0 \leq \sum_{\substack{j_1=1 \\ j_1 \neq i}}^{m} [A_k]_{i,j_1} + \sum_{\substack{j_2=1 \\ j_2 \neq i}}^{m} [A_k]_{j_2,i} - \epsilon\delta_i, \quad i = 1, \ldots, m \tag{6.13}$$

$$0 \leq -\sum_{\substack{j_1=1 \\ j_1 \neq i}}^{m} [A_k]_{i,j_1} - \sum_{\substack{j_2=1 \\ j_2 \neq i}}^{m} [A_k]_{j_2,i} + \epsilon + \left( \sum_{\substack{j_1=1 \\ j_1 \neq i}}^{m} l_{ij_1} + \sum_{\substack{j_2=1 \\ j_2 \neq i}}^{m} l_{j_2 i} - \epsilon \right) \cdot \delta_i, \quad i = 1, \ldots, m \tag{6.14}$$

Now, the objective function to be minimized or maximized can be written as

$$C_2(\delta) = \sum_{i=1}^{m} \delta_i \tag{6.15}$$

In contrast to the algorithm for computing dense and sparse realization, minimizing/maximizing the number of non-isolated complexes is not straightforward to parallelize (see also [J7]). However, the number of integer variables in this case is only $m$, compared to $m^2 - m$ when minimizing/maximizing the number of reactions.

### 6.1.2 Computing reversible realizations

Here, the basic constraints (6.1)-(6.6) expressing the properties of mass action dynamics and lower and upper bounds for the reaction rate coefficients will be used again for the optimization. To distinguish between zero and nonzero reaction rate coefficients, a small positive scalar $\epsilon$ is applied again, similarly to the previous cases.

The additional constraint for the full reversibility of the CRN structure is not difficult to formulate as

$$[A_k]_{i,j} > \epsilon_2 \leftrightarrow [A_k]_{j,i} > \epsilon_2, \quad \forall i > j. \tag{6.16}$$

where $\epsilon_2$ is a small positive threshold value such that $\epsilon < \epsilon_2$. The linear inequalities equivalent to (6.16) can be written as

$$0 \leq (\epsilon_2 - \epsilon) - [A_k]_{ij} + (l_{ij} - \epsilon_2) \cdot \delta_{ij}^{(1)}, \quad \forall i > j \tag{6.17}$$

$$0 \leq (\epsilon_2 - \epsilon) - [A_k]_{ji} + (l_{ji} - \epsilon_2) \cdot \delta_{ij}^{(1)}, \quad \forall i > j \tag{6.18}$$

$$0 \leq [A_k]_{ij} - \epsilon_2 \cdot \delta_{ij}^{(1)}, \quad \forall i > j \tag{6.19}$$

$$0 \leq [A_k]_{ji} - \epsilon_2 \cdot \delta_{ij}^{(1)}, \quad \forall i > j, \tag{6.20}$$

where $l_{ij}$ is the upper bound for $[A_k]_{ij}$ as it is introduced in eq. (6.5). Furthermore, $\frac{m(m-1)}{2}$ integer variables are introduced for the representation of the reversibility constraint that are denoted by $\delta_{ij}^{(1)}$, $\forall i > j$.

In order to obtain a numerically stable solution via the exclusion of reaction rate coefficients between $\epsilon$ and $\epsilon_2$, the following additional constraints in the form of a compound statement are introduced

$$[A_k]_{ij} < \epsilon \ \text{ OR } \ [A_k]_{ij} > \epsilon_2 + \gamma, \tag{6.21}$$

where $\gamma$ is a small positive threshold value that is in the same order of magnitude as $\epsilon_2$. The set of inequalities equivalent to (6.21) is given by

$$0 \leq \delta_{ij}^{(2)}, \quad i \neq j \tag{6.22}$$
$$0 \leq l_{ij} - [A_k]_{ij} - (l_{ij} - \epsilon) \cdot \delta_{ij}^{(3)}, \quad i \neq j \tag{6.23}$$
$$0 \leq [A_k]_{ij} - (\epsilon_2 + \gamma) \cdot \delta_{ij}^{(4)}, \quad i \neq j \tag{6.24}$$
$$0 \leq -\delta_{ij}^{(2)} + \delta_{ij}^{(3)} + \delta_{ij}^{(4)}, \quad i \neq j \tag{6.25}$$
$$0 \leq \delta_{ij}^{(2)} - \delta_{ij}^{(3)}, \quad i \neq j \tag{6.26}$$
$$0 \leq \delta_{ij}^{(2)} - \delta_{ij}^{(4)}, \quad i \neq j \tag{6.27}$$

where $\delta^{(2)}$, $\delta^{(3)}$ and $\delta^{(4)}$ represent altogether $3(m^2 - m)$ integer variables.

It is remarked that the inequalities (6.17) – (6.20) and (6.22) – (6.27) express only constraints and no objective function is associated to reversibility in itself. However, the reversibility constraints can be easily combined with the minimization/maximization of either the number of reactions or that of the non-isolated complexes, still in the framework of mixed integer linear programming. Moreover, the strict reversibility constraint can be modified to the minimization/maximization of reversible reaction pairs in a straightforward way. It is emphasized finally, that the constraints presented in this subsection together with an appropriate MILP solver are suitable for practically deciding whether a reversible realization exists for a given CRN or not (of course for such problem sizes that can be safely handled by the applied solver).

### 6.1.3 Examples

**Example 6.1.1. Motivating example continued**. Consider again the reaction network shown in Fig. 2.3(a) with parameters $k_1 = 1$, $k_2 = 2$. The matrices characterizing the CRN realization are the following.

$$Y = \begin{bmatrix} 0 & 3 & 2 \\ 3 & 0 & 1 \end{bmatrix}, \quad A_k = \begin{bmatrix} -1 & 0 & 0 \\ 1 & -2 & 0 \\ 0 & 2 & 0 \end{bmatrix} \tag{6.28}$$

$$M = Y \cdot A_k = \begin{bmatrix} 3 & -2 & 0 \\ -3 & 2 & 0 \end{bmatrix}. \tag{6.29}$$

**Computing a realization with the minimal number of complexes** Finding a realization with the minimal number of complexes with parameters $l_{ij} = 100 \ \forall i, j$ and $\epsilon = 10^{-8}$ gives the following result:

$$A_k^{(2)} = \begin{bmatrix} -1 & 0.6667 & 0 \\ 1 & -0.6667 & 0 \\ 0 & 0 & 0 \end{bmatrix}. \tag{6.30}$$

It's straightforward to check that $M = Y \cdot A_k^{(2)}$. Here, $A_k^{(2)}$ gives a deficiency 0 structure that is shown in Fig. 2.3(e).

**Computing a dense reversible realization** If we search for a reversible realization given by eq. 6.29 that contains the maximal number of nonzero reaction rate coefficients (i.e. a dense reversible realization), we have to combine constraints (6.1)-(6.6), (6.17)-(6.20), (6.22)-(6.27) and (6.8)-(6.9), and maximize the objective function (6.10). Using the parameters $\epsilon = 10^{-8}$, $\epsilon_2 = 0.05$, $\gamma = 0.01$ we obtain a fully reversible structure given by the following Kirchhoff matrix

$$A_k^{(3)} = \begin{bmatrix} -1.0200 & 0.6467 & 33.3333 \\ 0.9600 & -0.7067 & 66.6667 \\ 0.0600 & 0.0600 & -100.0000 \end{bmatrix}, \tag{6.31}$$

which gives a deficiency 1 structure shown in Fig. 2.3(d). Again, it's clear that $Y \cdot A_k = Y \cdot A_k^{(3)}$.

**Example 6.1.2. Computing a reversible realization for an oscillating kinetic system.** Consider the reversible variant of the well-known Brusselator model [120] shown in Fig. 6.1. The equations describing the dynamics of the closed system can be

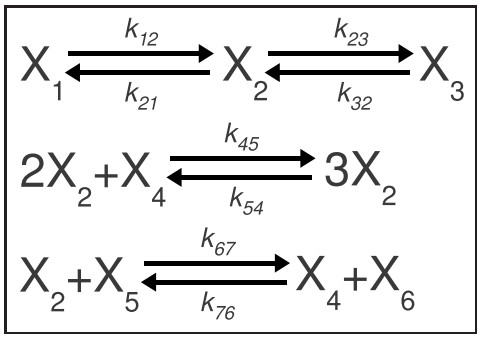


Figure 6.1: Reversible Brusselator reaction scheme

written as

$$\dot{x}_1 = -k_{12}x_1 + k_{21}x_2 \tag{6.32}$$
$$\dot{x}_2 = k_{12}x_1 - (k_{21} + k_{23})x_2 + k_{32}x_3 + k_{45}x_2^2x_4 - k_{54}x_2^3 - k_{67}x_2x_5 + k_{76}x_4x_6 \tag{6.33}$$
$$\dot{x}_3 = k_{23}x_2 - k_{32}x_3 \tag{6.34}$$
$$\dot{x}_4 = -k_{45}x_2^2x_4 + k_{54}x_2^3 + k_{67}x_2x_5 - k_{76}x_4x_6 \tag{6.35}$$
$$\dot{x}_5 = -k_{67}x_2x_5 + k_{76}x_4x_6 \tag{6.36}$$
$$\dot{x}_6 = k_{67}x_2x_5 - k_{76}x_4x_6. \tag{6.37}$$

It can be easily computed that the deficiency is zero for the above model. It follows from the Deficiency Zero Theorem, that it can produce no complex dynamical phenomena like oscillations for any positive values of the rate coefficients in its original closed form. For the forthcoming computations, the following parameter values were used: $k_{ij} = 1,\ \forall i, j$. To obtain oscillatory behaviour, the following steady state assumptions have to be made:

$$x_i = x_i^*, \quad \text{for } i = 1, 3, 5, 6. \tag{6.38}$$

We note that these assumptions require some kind of control of concentrations in an experimental setup and thus the opening of the originally closed system towards the

environment. The following steady states were used: $x_1^* = 1$, $x_3^* = 1$, $x_5^* = 16$, $x_6^* = 0.5$, that are known to cause oscillatory behaviour [120]. The remaining dynamics of the system is then given by

$$\dot{x}_2 = (k_{12}x_1^* + k_{32}x_3^*) + (-k_{21} - k_{23} - k_{67}x_5^*)x_2 - k_{54}x_2^3 + k_{45}x_2^2x_4 + (k_{76}x_6^*)x_4 \quad (6.39)$$

$$\dot{x}_4 = -k_{45}x_2^2x_4 + k_{54}x_2^3 + k_{67}x_5^*x_2 - k_{76}x_6^*x_4. \quad (6.40)$$

It is immediately visible that equations (6.39) - (6.39) are kinetic, therefore we can run **Algorithm 1** (see subsection 2.5.5) to compute a canonic CRN realization which is shown in figure 6.2. It can be seen from the figure that this realization of deficiency 4 contains 8 reactions and none of the two linkage classes is (at least weakly) reversible.

However, an attempt to compute a fully reversible realization is successful in this case and gives the CRN that is depicted in figure 6.3. We remark that this CRN is also a sparse realization of the dynamics (6.39) - (6.40), since the corresponding MILP optimization method tells us that the minimal number of reactions needed to realize that dynamics is 6. The deficiency of the obtained reversible network is 1. The stable limit cycle produced by the CRN started from the initial state $x(0) = [2\ 2.5]^T$ can be seen in figure 6.4. We mention that the existence of reversible oscillating CRNs was listed as an open problem in [140] in 2008. Although it is very hard to precisely check this claim, the above system might be one of the first such examples. In e.g. [31], three simple network structures with proven limit cycle behaviour are proposed one of which is weakly reversible, but none of them is fully reversible.

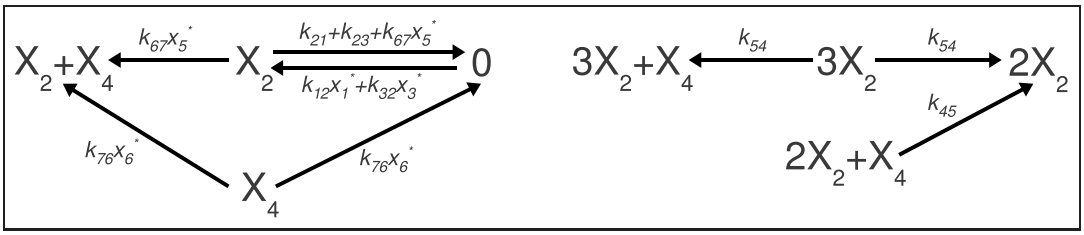


Figure 6.2: Canonic reaction network produced by **Algorithm 1** corresponding to the kinetic system (6.39) - (6.40)

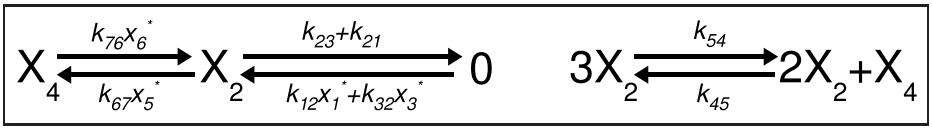


Figure 6.3: Sparse reversible realization corresponding to the kinetic system (6.39) - (6.40)

Another example for the dynamically equivalent reversible realization of an originally irreversible network is given in Example A.2.2 in the Appendix.

## 6.2 Finding detailed balanced and complex balanced CRN realizations using linear programming

In this section, we assume again that an initial CRN realization $(Y^{(1)}, A_k^{(1)})$ or a kinetic polynomial system is given together with an arbitrary positive steady state $x^*$ that

dc_263_11

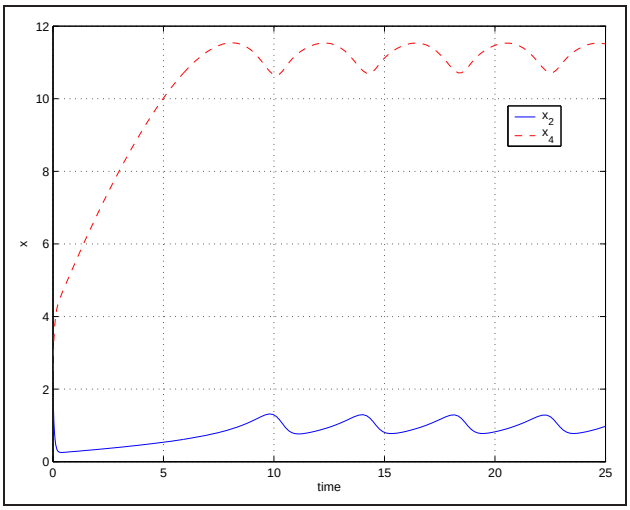


Figure 6.4: Time-domain behaviour of the kinetic system (6.39) - (6.40)

has been determined analytically or simply through simulations. Our purpose is to decide whether the system has a detailed balanced or complex balanced dynamically equivalent realization and to give some solution (possibly with additional properties) if the feasibility is fulfilled. The notions of detailed and complex balance were defined in subsection 2.5.7. If we start from a kinetic polynomial system, we use **Algorithm 1** described in subsection 2.5.5 for generating an initial (canonic) realization $(Y^{(1)}, A_k^{(1)})$. In any case, $M^{(1)} = Y^{(1)} \cdot A_k^{(1)}$. Let us denote $\psi(x^*)$ simply by $\psi^*$.

The decision variables denoted by $y$ will be the elements of the Kirchhoff matrix and we use the linear constraint set (5.14) again for characterizing dynamical equivalence and the properties of the Kirchhoff matrix. Note that in this case no integer variables are needed for solving the problems, therefore all the elements of $y$ will be continuous variables.

### 6.2.1 Additional constraints for complex balancing

Using the definition of a complex balanced steady state, the equality constraints for complex balancing are

$$-a_{11}\psi_1^* + a_{12}\psi_2^* + \cdots + a_{1m}\psi_m^* = 0 \tag{6.41}$$

$$a_{21}\psi_1^* - a_{22}\psi_2^* + \cdots + a_{2m}\psi_m^* = 0 \tag{6.42}$$

$$\vdots$$

$$a_{m1}\psi_1^* + \cdots + a_{m(m-1)}\psi_{m-1}^* - a_{mm}\psi_m^* = 0. \tag{6.43}$$

Clearly, these constraints can be written as

$$A_{e2} \cdot y = B_{e2}, \tag{6.44}$$

where

$$A_{e2} = \begin{bmatrix} -\psi_1^* & 0^{m-1} & \psi_2^* & 0^{m-1} & \dots & \psi_m^* & 0^{m-1} \\ 0 & \psi_1^* & 0^{m-1} & -\psi_2^* & \dots & \psi_m^* & 0^{m-2} \\ \vdots & & & & & & \\ 0^{m-1} & \psi_1^* & 0^{m-1} & \psi_2^* & \dots & 0^{m-1} & -\psi_m^* \end{bmatrix}, \quad B_{e2} = 0 \in \mathbb{R}^m, \tag{6.45}$$

and $0^k$ denotes a $1 \times k$ row vector of zeros.

### 6.2.2 Further constraints for detailed balancing

The most suitable form of detailed balancing constraints is taken from [154]. According to this, a given steady state $x^*$ is detailed balancing if and only if

$$G \cdot A_k^T = A_k \cdot G \tag{6.46}$$

where $G = \mathrm{diag}(\psi^*)$. It is easy to see that (6.46), if satisfied, implies reversibility of the obtained reaction network. Eq. (6.46) encodes a maximum of $\frac{m(m-1)}{2}$ independent equations that can be written into the linear programming problem as

$$\psi_i^* y_{(i-1)m+j} - \psi_j^* y_{(j-1)m+i} = 0, \quad \forall i > j, \tag{6.47}$$

since $[A_k]_{ij} = y_{(j-1)m+i}$ for $i \neq j$ according to eq. (5.17).

### 6.2.3 The choice of the objective function

In principle, the objective function of the form (2.3) can be any linear function of $y$. In section 6.2.4, we will minimize or maximize the sum of reaction rate coefficients. The minimization of the sum corresponds to the choice of $c = \frac{1}{2}[1 \ \ldots \ 1]^T$ in the standard LP-problem (2.3)-(2.5), while the maximization is obtained by selecting $c = -\frac{1}{2}[1 \ \ldots \ 1]^T$. Note that the minimum of the sum of reaction rate coefficients is bounded if the LP constraints are feasible, but the maximum is not necessarily, and this must be kept in mind.

### 6.2.4 Examples

**Example 6.2.1. Multiple detailed balanced realizations of a simple irreversible network**.

Consider again the simple reaction network shown in Fig. 2.3(a) with parameters $k_1 = 1$, $k_2 = 1.5$. The $M$ matrix characterizing the polynomial ODEs of the system is

$$M = Y \cdot A_k = \begin{bmatrix} 3 & -1.5 & 0 \\ -3 & 1.5 & 0 \end{bmatrix}. \tag{6.48}$$

Thus, the ODE model is given by

$$\dot{x}_1 = 3x_2^3 - 1.5x_1^3 \tag{6.49}$$
$$\dot{x}_2 = -3x_2^3 + 1.5x_1^3. \tag{6.50}$$

It's easy to compute that e.g. $x^* = [1.6725 \ \ 1.3275]^T$ is a steady state for the system (6.49)-(6.50). The corresponding values of the monomials are $\psi^* = \psi(x^*) = [2.3393 \ \ 4.6786 \ \ 3.7134]^T$. Clearly, the realization shown in Fig. 2.3(a) cannot be complex balanced or detailed balanced, since it is not weakly reversible.

In the first step, let us define the objective function as

$$h(y) = \frac{1}{2}\sum_{i=1}^{9} y_i \tag{6.51}$$

which is the $L1$-norm of the reaction rate coefficient vector (note that the diagonal elements of $A_k$ with a negative sign contain the sum of the reaction rate coefficients

in the corresponding column). Minimizing the objective function $h$ in (6.51) subject to the conditions (5.14) and (6.47) gives the detailed balance solution

$$y_{opt} = \begin{bmatrix} 1 & 1 & 0 & 0.5 & 0.5 & 0 & 0 & 0 & 0 \end{bmatrix}^T, \tag{6.52}$$

that corresponds to the following realization

$$Y' = Y, \quad A'_k = \begin{bmatrix} -1 & 0.5 & 0 \\ 1 & -0.5 & 0 \\ 0 & 0 & 0 \end{bmatrix}. \tag{6.53}$$

The detailed balance condition at the steady state can be checked as

$$1 \cdot (x_2^*)^3 = 0.5 \cdot (x_1^*)^3 = 2.3393. \tag{6.54}$$

Since the obtained realization is a weakly reversible deficiency zero one, we can apply the Deficiency Zero Theorem and the latest developments about the stability of complex balanced systems [4] and deduce that the positive equilibrium points of the dynamics of the initial irreversible network are also globally stable with a known Lyapunov function of the form (2.43).

In the second step, let us maximize $h$ in (6.51). The obtained realization is now given by

$$Y'' = Y, \quad A''_k = \begin{bmatrix} -1.5 & 0 & 0.9449 \\ 0 & -1.5 & 1.8899 \\ 1.5 & 1.5 & -2.8348 \end{bmatrix}. \tag{6.55}$$

The deficiency of the network in this case is 1. The detailed balance property is fulfilled in this case as

$$1.5 \cdot (x_2^*)^3 = 0.9449 \cdot (x_1^*)^2 x_2^* = 3.5088, \tag{6.56}$$

$$1.5 \cdot (x_1^*)^3 = 1.8899 \cdot (x_1^*)^2 x_2^* = 7.0179. \tag{6.57}$$

The reaction digraphs of the above computed detailed balanced realizations can be seen in Figs. 6.5 a) and b), respectively.

The motivation for trying to minimize and maximize the $L1$ norm of the reaction rate coefficients to get potentially different detailed balanced realizations came from [39] and [38]. We remark that the exact conditions under which the sparsest solution of an underdetermined set of linear equations is the minimal $L1$ norm solution are not fulfilled in our case, but the two obtained solutions are structurally different, and our purpose here was only to illustrate that different detailed balanced realizations of the same (very simple) kinetic system may exist.

It's worth mentioning that the detailed balancing constraints described in section 6.2.2 can easily be combined with the computation of dense and sparse realizations (see chapter 5). However, the problem in this case becomes NP-hard. A dense detailed balanced realization can be seen in Fig. 6.5 c) that is determined by the following matrices:

$$Y''' = Y, \quad A'''_k = \begin{bmatrix} -1.0333 & 0.4667 & 0.0630 \\ 0.9333 & -0.5667 & 0.1260 \\ 0.1000 & 0.1000 & -0.1890 \end{bmatrix} \tag{6.58}$$

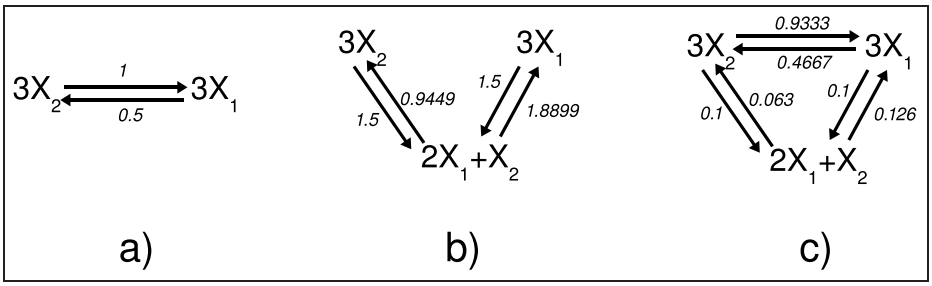


Figure 6.5: Dynamically equivalent detailed balanced realizations of the CRN in example 6.2.1. a) deficiency zero realization; b), c) deficiency one realizations

The detailed balancing condition is met in this case, too, since

$$0.9333 \cdot (x_2^*)^3 = 0.4667 \cdot (x_1^*)^3 = 2.1833 \tag{6.59}$$

$$0.1 \cdot (x_2^*)^3 = 0.063 \cdot (x_1^*)^2 x_2^* = 0.2339 \tag{6.60}$$

$$0.1 \cdot (x_1^*)^3 = 0.126 \cdot (x_1^*)^2 x_2^* = 0.4679 \tag{6.61}$$

The average running time of the LP based methods (using the `linprog` command) was 0.06 second, while the MILP based algorithm (using the freely available GLPK solver) found the dense realization in 1.04 second in the MATLAB computation environment on a notebook computer with an 1.66 GHz Intel Atom N280 Processor.

**Example 6.2.2. Finding complex balanced realization of a kinetic polynomial system**. The following polynomial system is given:

$$\begin{aligned}
\dot{x}_1 &= x_3^2 - x_1 x_2 + x_3 x_4 - 2x_1 x_2^2 x_3 \\
\dot{x}_2 &= x_3^2 - x_1 x_2 + 2x_3 x_4 - 4x_1 x_2^2 x_3 \\
\dot{x}_3 &= -2x_3^2 + x_1 x_2 - x_1 x_2^2 x_3 + 2x_4^3 \\
\dot{x}_4 &= x_1 x_2 - x_3 x_4 + 4x_1 x_2^2 x_3 - 3x_4^3
\end{aligned} \tag{6.62}$$

It can be seen that (6.62) is essentially nonnegative and kinetic. After running **Algorithm 1**, we obtain an initial canonic structure with 19 complexes and 16 reactions that is visible in Fig. 6.6, where the numbering of complexes (in rectangles) is the following:

$$\begin{aligned}
&1 : 2X_3,\ 2 : X_3 + X_4,\ 3 : X_1 + 2X_3,\ 4 : X_2 + 2X_3, \\
&5 : X_3,\ 6 : X_1 + X_3 + X_4,\ 7 : X_2 + X_3 + X_4, \\
&8 : X_1 + X_2,\ 9 : X_1 + 2X_2 + X_3,\ 10 : X_1,\ 11 : X_2, \\
&12 : X_1 + X_2 + X_4,\ 13 : X_1 + X_2 + X_3,\ 14 : 2X_2 + X_3, \\
&15 : X_1 + 2X_2,\ 16 : X_1 + 2X_2 + X_3 + X_4, \\
&17 : 3X_4,\ 18 : X_3 + 3X_4,\ 19 : 2X_4
\end{aligned} \tag{6.63}$$

In this case, we were searching for a complex balanced realization as it was described in subsection 6.2.1. The objective function that was minimized was also the sum of reaction rate coefficients, i.e.

$$h(y) = \frac{1}{2} \sum_{i=1}^{361} y_i \tag{6.64}$$

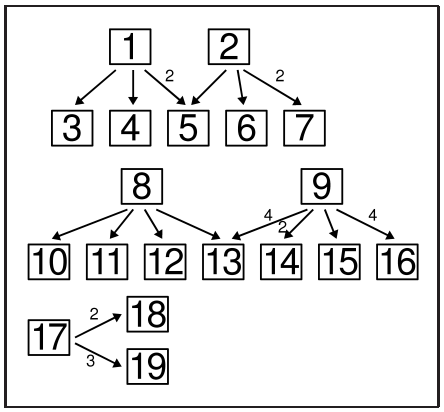


Figure 6.6: Reaction network realizing eq. (6.62) obtained using **Algorithm 1**. Only those reaction rate coefficients are indicated that are different from 1.

The joint running time of **Algorithm 1** and the solution of the LP problem with 361 variables was 0.45 second on the same hardware/software environment as in the previous example. The obtained complex balanced and thus weakly reversible realization of the initial CRN is visible in Fig. 6.7. The isolated complexes (i.e. the ones with no incoming and no outgoing directed edges) are naturally omitted from the realization and not drawn in the figure. It can be checked that the deficiency of the complex balanced realization is 0 (in sharp contrast with the deficiency of 12 of the initial network in Fig. 6.6). Therefore, the autonomous system (6.62) has well-characterizable equilibrium points in the positive orthant that are globally stable with a known Lyapunov function.

An attempt to find a detailed balanced realization using the constraints described in subsection 6.2.2 is unsuccessful in this case. After checking the feasibility condition given in Theorem 2.1.1, we can deduce that such detailed balanced realization does not exist with the complex set listed in eq. (6.63).

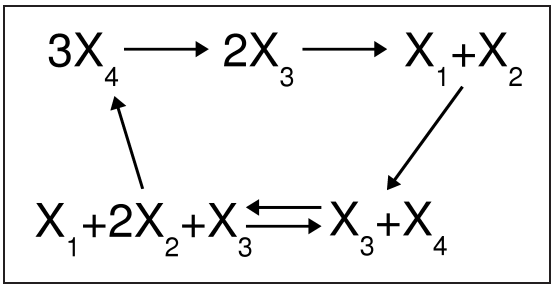


Figure 6.7: Complex balanced realization of the CRN shown in Fig. 6.6. All reaction rate coefficients are 1.

## 6.3 Computing weakly reversible dynamically equivalent CRN realizations

Although complex balance implies weak reversibility, the opposite is generally not true. Therefore, it is worth examining the possibility of finding dynamically equivalent weakly reversible networks with a completely different strategy from the one that was followed in the previous subsection. Based on the fact that with a given $Y$, all possible reactions are contained in the structurally unique dense realization, a straightforward

idea is to try to find a dynamically equivalent weakly reversible mechanism starting from this superstructure. For this, some additional notions will be introduced.

### 6.3.1 Constrained dense and sparse realizations

The simple constraint set denoted by $\mathcal{K}$ will be used for the exclusion of selected reactions from the CRN, i.e. it is of the form:

$$\mathcal{K} = \{[A_k]_{i_1,j_1} = 0,\ \ldots,\ [A_k]_{i_s,j_s} = 0\}, \tag{6.65}$$

where $s$ is the number of individual constraints, and $i_k \neq j_k$ for $k = 1, \ldots, s$. Now we can introduce the following definitions. A dynamically equivalent $\mathcal{K}$-*constrained realization* of a CRN $(Y, A_k)$ is a reaction network $(Y, A'_k)$ such that $Y \cdot A_k = Y \cdot A'_k$ and the prescribed constraints $\mathcal{K}$ in the form of eq. (6.65) are fulfilled for $A'_k$. A dynamically equivalent $\mathcal{K}$-*constrained dense realization* of a chemical reaction network $(Y, A_k)$ is a $\mathcal{K}$-constrained realization that contains the maximal number of nonzero elements in $A'_k$. Similarly, a $\mathcal{K}$-*constrained sparse realization* is a $\mathcal{K}$-constrained realization with the minimal number of nonzeros in $A'_k$. To characterize constrained dense/sparse realizations, the results of subsection 5.5 can be extended in a straightforward way as follows.

**Theorem 6.3.1.** Consider a CRN $\Sigma = (Y, A_k)$ and let $\mathcal{K}$ be a constraint set of the form (6.65) such that there exists a $\mathcal{K}$-constrained CRN realization that is dynamically equivalent to $\Sigma$. Let $\Sigma^d_{\mathcal{K}} = (Y, A^d_k)$ be a dynamically equivalent $\mathcal{K}$-constrained dense realization, and $\Sigma^s_{\mathcal{K}} = (Y, A^s_k)$ a dynamically equivalent $\mathcal{K}$-constrained sparse realization of $\Sigma$. Then for any dynamically equivalent $\mathcal{K}$-constrained realization of $\Sigma$ of the form $\Sigma_{\mathcal{K}} = (Y, A'_k)$, the following hold:

**P1** The unweighted reaction graph of $\Sigma_{\mathcal{K}}$ is the subgraph of the unweighted reaction graph of $\Sigma^d_{\mathcal{K}}$.

**P2** The unweighted reaction graph (i.e. the CRN structure) of $\Sigma^d_{\mathcal{K}}$ is unique.

**P3** The unweighted reaction graphs of all $\Sigma_{\mathcal{K}}$-s are identical (i.e. the graph structure of the CRN with given constraint set $\mathcal{K}$ and complex set $Y$ is unique) if and only if the unweighted directed graphs of $\Sigma^d_{\mathcal{K}}$ and $\Sigma^s_{\mathcal{K}}$ are identical.

*Proof.* The theorem is clearly a special case of Theorem 5.5.1, when certain elements of $A_k$ are constrained to be zero. However, we can also give an alternative proof based on elementary linear algebra.
**P1, P2**. The matrix equation $Y \cdot A_k = M$ (see eqs. (2.29) and (5.3)) obviously defines $m$ sets of linear equations of the form

$$Y \cdot [A_k]_{\cdot,i} = [M]_{\cdot,i}, \quad i = 1, \ldots, m. \tag{6.66}$$

Let us choose any $i$ indexing the sets of equations in (6.66). For simplicity, let $p = [A_k]_{\cdot,i}$, $b = [M]_{\cdot,i}$. Let us assume that there are $z$ elements of the constraint set (6.65) where $j_k = i$ for $k = 1, \ldots, s$. These constraints can be expressed by further linear equations of the form:

$$[A_k]_{h,i} = 0, \quad h = 1, \ldots, z. \tag{6.67}$$

The equation sets (6.66) and (6.67) can be written into a single set of equations as

$$\bar{Y} \cdot p = \bar{b}, \tag{6.68}$$

where $\bar{Y} \in \mathbb{R}^{(n+z)\times m}$ and $\bar{b} \in \mathbb{R}^{n+z}$.

The first case is when $\bar{b} = 0$ (i.e. we have a homogeneous set of equations). Assume that $p$ is a dense solution of (6.68). If $p$ has no zero elements then we are done. So assume that $p'$ is a solution of (6.68), too, such that $\exists\ j$ for which $p'_j \neq 0$ but $p_j = 0$. Then $p'' = p + \lambda p'$ for $\lambda \in \mathbb{R}$ is also a solution for (6.68) with $\bar{b} = 0$, and $\lambda$ can always be chosen such that there are more nonzero elements in $p''$ than in $p$, which is a contradiction.

If $\bar{b} \neq 0$ then the proof can be based on the following well known fact of linear algebra. Consider an inhomogenous set of linear equations:

$$Ax = b, \tag{6.69}$$

where $A \in \mathbb{R}^{m\times m}$, and $x, b \in \mathbb{R}^m$. If $x = x^p$ is any particular solution of (6.69) then the entire solution set for (6.69) can be characterized as

$$\{x^p + v \mid v \text{ is any solution of } Ax = 0\}. \tag{6.70}$$

Let us assume now that $p$ is a dense solution for (6.68), i.e. it contains the maximal possible number of nonzero elements. If $p$ has no zero elements, then the result to be proven is trivially satisfied. Therefore, without the loss of generality we can assume that the first $l < m$ elements of p are nonzero, while the rest are zero, i.e. $p_j \neq 0$ for $j = 1, \ldots, l$, and $p_j = 0$ for $j = l+1, \ldots, m$. This can always be achieved by the appropriate reordering of the elements of $p$. Assume now that $p' \in \mathbb{R}^m$ is also a solution for (6.68), but $p'_c \neq 0$ for some $c \in \mathbb{Z}$, $l+1 \leq c \leq m$. Then $p' = p + v$ for some $v$, where $\bar{Y} \cdot v = 0$, and $v_c \neq 0$. In this case, $p'' = p + \lambda \cdot v$ is also a solution for (6.68) for any $\lambda \in \mathbb{R}$ and $\lambda$ can always be chosen so that $p''_j \neq 0$ for $j = 1, \ldots, l$, and there is at least one index $l+1 \leq c \leq m$ for which $p''_c \neq 0$. However, this contradicts to the assumption that $p$ is a dense solution for (6.68).

**P3**. If the graph structure of the constrained realization is unique, then it trivially imples that the structures of the constrained dense and sparse realizations are identical, since there exists only one possible constrained reaction structure. If the structures of the constrained dense and sparse realizations are identical, then the number of nonzero reaction rates is the same in any constrained realizations including the constrained dense ones. Then it follows from **P1** that the constrained reaction structure is unique. □

### 6.3.2 Basic principle of the algorithm

Very shortly, the underlying principle of the presented algorithm is that it only removes (if possible) from the dense realization

(i) edges that cannot be parts of any weakly reversible realization,

(ii) edges the removal of which is necessarily implied by the deletion of edges belonging to set (i),

while maintaining dynamical equivalence. Besides Theorem 6.3.1, the correct operation of the algorithm is based on the following well-known result from graph theory: If each strongly connected component of a directed graph $G$ is contracted to a single vertex, the resulting directed graph is a directed acyclic graph [9]. (A directed graph is called *acyclic* if it has no nontrivial strongly connected subgraphs.) This implies that for obtaining a CRN superstructure including all possible structures, a dense realization must be computed. Directed edges between different strong components must be removed because they cannot lie on a directed cycle in any dynamically equivalent realization. If this is not possible, then there is no weakly reversible realization of the CRN. However, if the deletion is possible, it may imply the removal of additional reactions because of the linear kinetic constraints (see eqs. (6.1)-(6.4)). In general, this may impair the weak reversibility of the obtained network. In such a case, a new dense realization must be computed excluding the unnecessary edges identified in the previous step, and the procedure must be repeated until either a weakly reversible realization is found, or the deletion of undesired edges is no longer possible. In the latter case, no weakly reversible realization of the initial CRN exists with the given stoichiometric matrix $Y$.

### 6.3.3 Definition of input data structure and the necessary additional procedures

We will assume that an initial CRN realization is given with the matrices $(Y^{(0)}, A_k^{(0)})$, and $M = Y^{(0)} \cdot A_k^{(0)}$. The constraint set containing directed edges to be eliminated from the current realization is denoted as

$$\mathcal{K} = \{(p_1, q_1), \ldots, (p_s, q_s)\}, \quad s < r. \tag{6.71}$$

where $p_i$ and $q_i$ denote the indices of the initial and terminal vertices of the $i$th edge, respectively, and $r$ is the number of reactions in the CRN.

Now, the following simple procedure will be defined for later use.

$$L = \texttt{FindCrossComponentEdges}(A_k^{in}) \tag{6.72}$$

The input of the procedure is the Kirchhoff matrix $A_k^{in}$ of a CRN, and the output is a set $L$ containing the directed edges linking different strong components of the reaction graph. The strongly connected components of a directed graph can be determined in linear time using e.g. Kosaraju's, Tarjan's or Gabow's algorithm [9, 123]. Moreover, the examined CRN is weakly reversible if and only if it contains at least 2 reactions, and the output $L$ of `FindCrossComponentEdges` is empty.

In the following part of this subsection, appropriate modifications of the algorithm described in chapter 5 are given, adapted to the current problem.

#### Constraints corresponding to mass action dynamics

We will use the simple form of linear constraints given by (6.1)-(6.4) in section 6.1.

#### Checking whether a set of reactions is removable from a CRN realization

We call a set of reactions $\mathcal{K}$ *removable* from a CRN realization, if there exists a dynamically equivalent CRN realization that does not contain the directed edges in $\mathcal{K}$. To check this, it is worth separately defining the following LP-based and thus polynomial-time procedure to avoid unnecessary MILP computations that are known to be NP-hard.

The constraints (6.1)-(6.4) are completed with the following ones

$$[A_k]_{q_i,p_i} = 0 \quad \text{for} \quad i = 1, \ldots, s \tag{6.73}$$

where $(p_i, q_i) \in \mathcal{K}$ as it is written in eq. (6.71). The feasibility of the linear constraints (6.1)-(6.4) and (6.73) can be checked by adding e.g. the following linear objective function to be minimized:

$$G_{LP}(A_k) = \sum_{\substack{i,j=1 \\ i \neq j,\ (j,i) \notin \mathcal{K}}}^{m} [A_k]_{ij}. \tag{6.74}$$

Clearly, eqs. (6.1)-(6.4), (6.73)-(6.74) form a standard linear programming problem.

Based on the above, we will define the procedure to check whether a set $\mathcal{K}$ of directed edges is removable from a CRN realization or not in the following way:

$$F_{out} = \texttt{IsRemovable}(Y^{(i)}, A_k^{(i)}, \mathcal{K}), \tag{6.75}$$

where the input data are as follows: $(Y^{(i)}, A_k^{(i)})$ is a CRN realization, and $\mathcal{K}$ is a constraint set of the form (6.71) containing the tail and head index pairs of the directed edges to be removed from $(Y^{(i)}, A_k^{(i)})$. The output $F_{out}$ is a boolean variable: its value is `true` if there exists a dynamically equivalent realization to $(Y^{(i)}, A_k^{(i)})$ not containing the edges listed in $K$, and it is `false` if there does not exist such realization.

**Computing the dense realization excluding given directed edges**

If the procedure `IsRemovable` returns a `true` value, the dense realization of the CRN can be computed subject to the constraint that the edges listed in $\mathcal{K}$ are excluded from it. To define the corresponding MILP problem, first we add exactly the same linear constraints contained in eqs. (6.1)-(6.4), (6.73) as in the previous case. To make the forthcoming problem computationally tractable, we also introduce the following bounds for the decision variables

$$[A_k]_{ij} \leq u_{ij}, \quad u_{ij} > 0, \quad i,j = 1, \ldots, m, \quad i \neq j, \quad (j,i) \notin \mathcal{K} \tag{6.76}$$

$$[A_k]_{ii} \geq l_i, \quad l_i < 0, \quad i = 1, \ldots, m \tag{6.77}$$

Here we are searching for such $A_k$ that contains the maximal number of nonzero off-diagonal elements. For this, logical variables denoted by $\delta$ are introduced and the following compound statements are constructed

$$\delta_{ij} = 1 \leftrightarrow [A_k]_{ij} > \epsilon, \quad i,j = 1, \ldots, m, \quad i \neq j, \quad (j,i) \notin \mathcal{K}, \tag{6.78}$$

where the symbol "$\leftrightarrow$" denotes "if and only if", and $\epsilon$ is a sufficiently small positive value (i.e. elements of $A_k$ below $\epsilon$ are treated as zero). Considering also (6.76), statement (6.78) can be translated to the following linear inequalities

$$0 \leq [A_k]_{ij} - \epsilon\delta_{ij}, \quad i,j = 1, \ldots, m, \quad i \neq j, \quad (j,i) \notin \mathcal{K} \tag{6.79}$$

$$0 \leq -[A_k]_{ij} + u_{ij}\delta_{ij}, \quad i,j = 1, \ldots, m, \quad i \neq j \quad (j,i) \notin \mathcal{K}. \tag{6.80}$$

Now it is possible to compute the realization containing the maximal number of reactions by maximizing the objective function

$$G_{MILP}(\delta) = \sum_{\substack{i,j=1 \\ i \neq j,\ (j,i) \notin \mathcal{K}}}^{m} \delta_{ij}. \tag{6.81}$$

Finally, the following procedure is defined based on the MILP problem given by eqs. (6.1)-(6.4), (6.73), (6.76)-(6.77), and (6.79)-(6.81).

$$A_k^d = \texttt{FindConstrDenseRealization}(Y^{(i)}, A_k^{(i)}, \mathcal{K}), \tag{6.82}$$

where the input data set is the same as in the case of the procedure `IsRemovable` (see eq. (6.75) and the corresponding description). The output $A_k^d$ is a dense realization that does not contain the directed edges listed in the set $\mathcal{K}$. If the set $\mathcal{K}$ is empty, then the procedure is the same that computes dense realizations and that was described in chapter 5.

### 6.3.4 Formal description of the algorithm

Now we can give the formal description of the procedure for determining weakly reversible CRN realizations. The input data of the procedure is an initial CRN realization ($Y^{(0)}$,$A_k^{(0)}$). The output is an $m \times m$ matrix that is the Kirchhoff matrix of the weakly reversible realization if there exists such, or a zero matrix if the procedure found no weakly reversible realizations. In the algorithm pseudocode, the auxiliary variable *ExitCondition* is a boolean storing the exit condition from the main loop. The complete pseudocode of the procedure called `FindWeaklyReversibleRealization` with common notations and keywords can be found in Table 6.1.

### 6.3.5 Main properties of the algorithm

The above described algorithm always finds a dynamically equivalent weakly reversible realization, if it exists. This clearly follows from Theorem 6.3.1 and the basic principles of the algorithm described in subsection 6.3.2. From these facts it also follows that the algorithm finds the dense weakly reversible realization that structurally contains any other weakly reversible realizations (for illustration, see the results in subsection 6.3.1). We remark that the immediate deletion of the columns/rows corresponding to the isolated complexes from matrices $Y$ and $A_k$ after calling the procedure `FindConstrDenseRealization` is also possible, but this requires the renumbering of complexes. This is a technical detail of implementation and does not affect the principle or final output of the algorithm. (However, decreasing the number of optimization variables and constraints in each step in such a way might be required especially in the case of larger networks.)

### 6.3.6 Examples

The following examples were implemented in the MATLAB R13 computation environment using the YALMIP and the Multi-Parametric Toolboxes [110, 102]. The examples were run on a desktop PC with dual Intel Xeon 1.8GHz CPU and 2 Gigabytes of RAM. The implementation of dense realization computation was not parallel, therefore all the decision variables and constraints were put into a single optimization problem in procedure `FindConstrDenseRealization`. The strong components of the reaction graphs were identified using Kosaraju's algorithm [139].

```
A_k^out=FindWeaklyReversibleRealization(Y^(0),A_k^(0))
1   A_k^out:=0 ∈ R^{m×m}; ExitCondition:=false;
2   Y := Y^(0); A_k := A_k^(0); F_out:=true; K := {}; L := {};
3   while (ExitCondition=false) do
4   begin
5      if (K ≠ {}) then F_out:=IsRemovable(Y,A_k,K);
6      if (F_out =true) then
7      begin
8         A_k:=FindConstrDenseRealization(Y,A_k,K);
9         L:=FindCrossComponentEdges(A_k);
10        if (L = {}) then ExitCondition:=true; A_k^out:=A_k;
11        else K := K ∪ L;
12     end
13     else ExitCondition:=true;
14  end
15  return A_k^out;
```

Table 6.1: Pseudocode of the algorithm for finding weakly reversible realizations

**Example 6.3.1. Weakly reversible realizations of a simple irreversible network**. The simple network that can be seen in Fig. 6.8 a) was taken from [91]

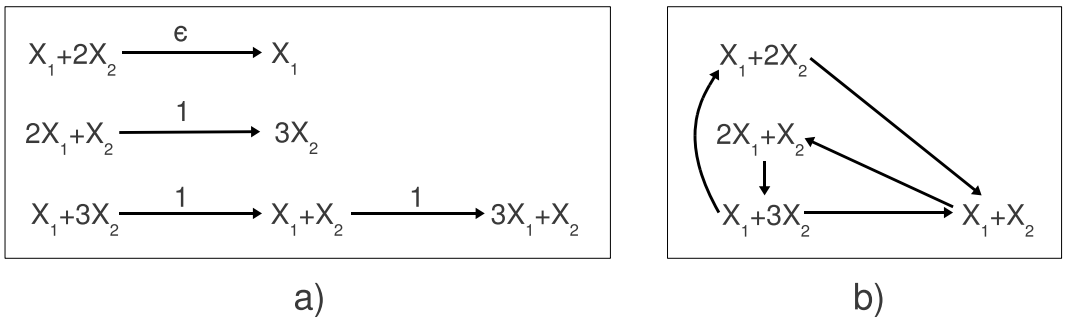


Figure 6.8: a) Simple irreversible network from [91], b) Structure of one of its possible weakly reversible realizations determined in [91]

(Example 3). In [91], it is shown that for any positive $\epsilon$, the network has a possible weakly reversible realization with the structure shown in Fig. 6.8 b). (The computation and analysis of the parameters of the CRN in Fig. 6.8 b) can be found in [91].) The complex composition matrix of the network is

$$Y = \begin{bmatrix} 1 & 1 & 2 & 0 & 1 & 1 & 3 \\ 2 & 0 & 1 & 3 & 3 & 1 & 1 \end{bmatrix}. \tag{6.83}$$

The nonzero elements of the Kirchhoff matrix $A_k \in \mathbb{R}^{7\times 7}$ with $\epsilon = 1.5$ are

$$[A_k]_{2,1} = 1.5,\ [A_k]_{4,3} = 1,\ [A_k]_{6,5} = 1,\ [A_k]_{7,6} = 1. \tag{6.84}$$

For this network, the algorithm described in section 6.3.4 and Table 6.1 works as follows. After the initialization steps, the dense realization containing all possible reactions with an empty constraint set $\mathcal{K}$ is computed (line 8 of the pseudocode). The Kirchhoff matrix of the dense realization is given by

$$A_k^{(1)} = \begin{bmatrix} -1.25 & 0 & 0.1 & 0 & 0.1 & 0.1 & 0 \\ 0.55 & 0 & 0.1 & 0 & 0.4333 & 0.5 & 0 \\ 0.1 & 0 & -1.4 & 0 & 0.1 & 0.1 & 0 \\ 0.3 & 0 & 0.8 & 0 & 0.3 & 0.1 & 0 \\ 0.1 & 0 & 0.2 & 0 & -1.1333 & 0.1 & 0 \\ 0.1 & 0 & 0.1 & 0 & 0.1 & -1.9 & 0 \\ 0.1 & 0 & 0.1 & 0 & 0.1 & 1 & 0 \end{bmatrix} \tag{6.85}$$

The structure of the dense realization is shown in Fig. 6.9. The following steps can

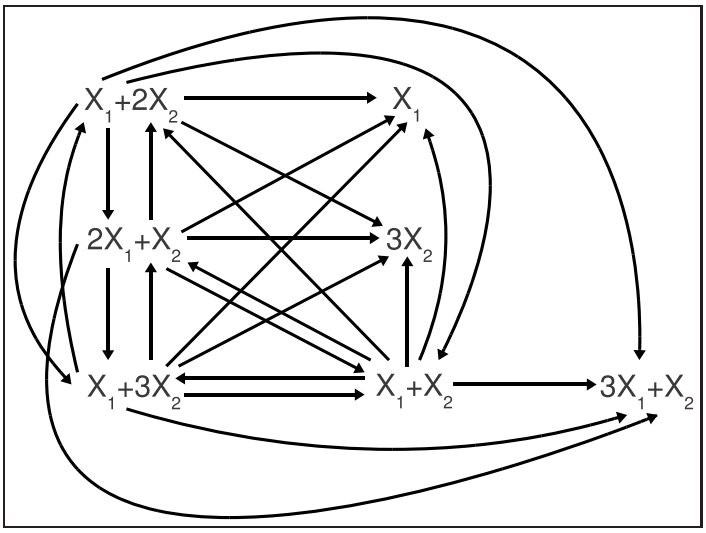


Figure 6.9: Structure of the dense realization of the reaction network shown in Fig. 6.8 a)

be followed using Fig. 6.10. The dense realization is not weakly reversible because there are edges between different strong components (line 9). The complexes of the single nontrivial strong component are indicated by boldface labels in Fig. 6.10. It is clear from the figure that the edges adjacent to the complexes $X_1$, $3X_2$, $3X_1 + X_2$ are to be removed. These edges are drawn with dotted arrows in the figure. Thus, the constraint list is

$$\mathcal{K} = \{(1,2),(1,4),(1,7),(3,2),(3,4),(3,7),(5,2),(5,4),(5,7),(6,2),(6,4),(6,7)\}.$$

The next iteration of the algorithm (line 5) gives that these edges can be removed from the realization. Now a new dense realization is computed excluding edges in $\mathcal{K}$ (line 8). The reactions of this dense realization are indicated by thick arrows in Fig. 6.10. Note that the constraint of excluding the reactions in $\mathcal{K}$ from the network resulted in the removal of directed edges $X_1 + X_2 \to X_1 + 2X_2$, $X_1 + 2X_2 \to 2X_1 + X_2$, $X_1 + 3X_2 \to 2X_1 + X_2$, and $X_1 + X_2 \to X_1 + 3X_2$, too, that were within the nontrivial strong component of the previous step. In this case, the resulting network remained weakly reversible (lines 9-10), so the algorithm can stop with success and

return the determined dynamically equivalent weakly reversible CRN. The structure of the resulting network is shown in Fig. 6.11(a). The Kirchhoff matrix of the obtained realization is the following

$$A_k^{(2)} = \begin{bmatrix} -3.2 & 0 & 1.8 & 0 & 0.1 & 0 & 0 \\ 0 & 0 & 0 & 0 & 0 & 0 & 0 \\ 0 & 0 & -2 & 0 & 0 & 2 & 0 \\ 0 & 0 & 0 & 0 & 0 & 0 & 0 \\ 0.1 & 0 & 0.1 & 0 & -1.05 & 0 & 0 \\ 3.1 & 0 & 0.1 & 0 & 0.95 & -2 & 0 \\ 0 & 0 & 0 & 0 & 0 & 0 & 0 \end{bmatrix} \tag{6.86}$$

The running time of the algorithm was 11s using the software environment described in the beginning of section 5.6.

It is interesting to note that the obtained weakly reversible realization is not complex balanced. However, using the polynomial-time algorithm described in section 6.2, we can compute a complex balanced realization with 6 reactions in just 0.1s, that is shown in Fig. 6.11(b). It is easy to see that the unweighted directed graphs of Figs. 6.8 b) and Fig. 6.11(b) are indeed the proper subgraphs of the structure visible in Fig. 6.11(a).

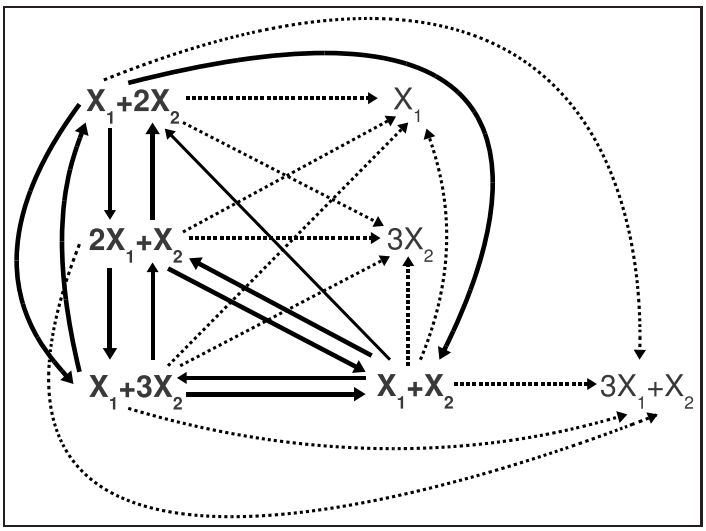


Figure 6.10: Illustration of the operation of the algorithm on the example given in section 6.3.1

**Example 6.3.2. Weakly reversible realization of a kinetic polynomial system**. Let us consider the kinetic polynomial system of Example 6.2.2 with equations (6.62). We again start from the canonic scheme given by **Algorithm 1** but with the following complex numbering that is different from (6.63):

$$\begin{aligned} &C_1 = 2X_3,\ C_2 = X_1 + 2X_3,\ C_3 = X_1 + X_2,\ C_4 = X_2,\ C_5 = X_3 + X_4,\ C_6 = X_1 + X_3 + X_4, \\ &C_7 = X_1 + 2X_2 + X_3,\ C_8 = 2X_2 + X_3,\ C_9 = X_2 + 2X_3,\ C_{10} = X_1,\ C_{11} = X_2 + X_3 + X_4, \\ &C_{12} = X_1 + X_2 + X_3,\ C_{13} = X_3,\ C_{14} = X_1 + 2X_2,\ C_{15} = 3X_4, \\ &C_{16} = X_3 + 3X_4,\ C_{17} = X_1 + X_2 + X_4,\ C_{18} = X_1 + 2X_2 + X_3 + X_4,\ C_{19} = 2X_4. \end{aligned} \tag{6.87}$$

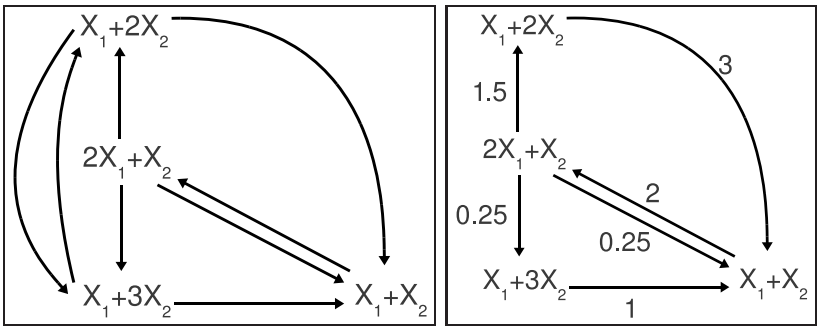


Figure 6.11: (a) The structure of the obtained dynamically equivalent weakly reversible CRN, (b) Complex balanced realization of the CRN described in section 6.3.1

The dense realization of the network contains 80 reactions, therefore it is not shown in a figure. Let us number the vertices of the reaction graph according to the complex numbering, i.e. vertex $i$ corresponds to complex $C_i$ for $i = 1, \ldots, 19$. For the sake of completeness, the list of the reactions (i.e. weighted directed edges) of the dense realization in the form (*source vertex number, destination vertex number, weight (i.e. rate coefficient)*) is given below:
(5, 1, 0.5), (7, 1, 0.1), (11, 1, 0.1), (15, 1, 0.8), (1, 2, 0.1), (3, 2, 0.1), (5, 2, 0.1), (7, 2, 0.1), (12, 2, 0.3), (1, 3, 0.1), (5, 3, 0.1), (7, 3, 0.1), (12, 3, 0.1), (1, 4, 0.1), (3, 4, 0.4), (5, 4, 0.1), (7, 4, 0.1), (11, 4, 0.1), (3, 5, 0.1), (7, 5, 0.1), (11, 5, 0.1), (15, 5, 0.1), (3, 6, 0.1), (5, 6, 0.1), (7, 6, 0.1), (1, 7, 0.1), (3, 7, 0.1), (5, 7, 0.2), (12, 7, 0.3), (1, 8, 0.1), (3, 8, 0.1), (5, 8, 0.3), (7, 8, 0.3), (11, 8, 1.2), (1, 9, 0.1), (5, 9, 0.1), (7, 9, 0.1), (11, 9, 0.2), (1, 10, 0.5), (3, 10, 0.8), (5, 10, 0.1), (7, 10, 0.1), (12, 10, 0.1), (3, 11, 0.1), (5, 11, 0.1), (7, 11, 0.1), (1, 12, 0.1), (3, 12, 0.1), (5, 12, 0.1), (7, 12, 0.1), (1, 13, 0.1), (3, 13, 0.1), (5, 13, 0.1), (7, 13, 0.1), (11, 13, 0.1), (15, 13, 0.1), (1, 14, 0.1), (3, 14, 0.1), (5, 14, 0.1), (7, 14, 0.1), (12, 14, 0.1), (3, 15, 0.1), (5, 15, 0.1), (7, 15, 0.7), (11, 15, 0.1), (5, 16, 0.25), (7, 16, 0.3), (11, 16, 0.7), (15, 16, 0.2), (3, 17, 0.1), (5, 17, 0.1), (7, 17, 0.1), (3, 18, 0.1), (5, 18, 0.1), (7, 18, 0.4), (3, 19, 0.1), (5, 19, 0.1), (7, 19, 0.1), (11, 19, 0.1), (15, 19, 0.1).

The dense realization has 13 strong components. Out of these, there is only one nontrivial strongly connected component containing the vertices 1, 3, 5, 7, 11, 12, and 15. After identifying all directed edges linking different strong components, we obtain that the following 53 edges given in the form (*source vertex number, destination vertex number*) should be deleted from the dense realization in the next step of the algorithm:
(1,2), (3,2), (5,2), (7,2), (12,2), (1,4), (3,4), (5,4), (7,4), (11,4), (3,6), (5,6), (7,6), (1,8), (3,8), (5,8), (7,8), (11,8), (1,9), (5,9), (7,9), (11,9), (1,10), (3,10), (5,10), (7,10), (12,10), (1,13), (3,13), (5,13), (7,13), (11,13), (15,13), (1,14), (3,14), (5,14), (7,14), (12,14), (5,16), (7,16), (11,16), (15,16), (3,17), (5,17), (7,17), (3,18), (5,18), (7,18), (3,19), (5,19), (7,19), (11,19), (15,19).

All the above listed edges were possible to remove from the dense realization (their removal implied the deletion of 12 additonal reactions), and the resulting constrained dense realization is shown in Fig.6.12(a). It is clear from the figure that edges adjacent to vertices no. 11 and 12 have to be removed in the following step. This final step is illustrated in Fig. 6.12(b), where the meaning of the line types is the same as in the case of Fig. 6.10. With the removal of edges (5,11), (5,12), (7,11), (7,12), the directed

edges (5,1), (7,1), (7,3), (5,3), (7,5) and (5,15) were also deleted, and the resulting weakly reversible realization (of deficiency 0) is shown in Fig. 6.13. The total running time of the algorithm was 80.5s. It can be checked that the obtained network is exactly the same as in Fig. 6.7. However, in this case the complex balanced property is not a condition for the correct operation of the algorithm.

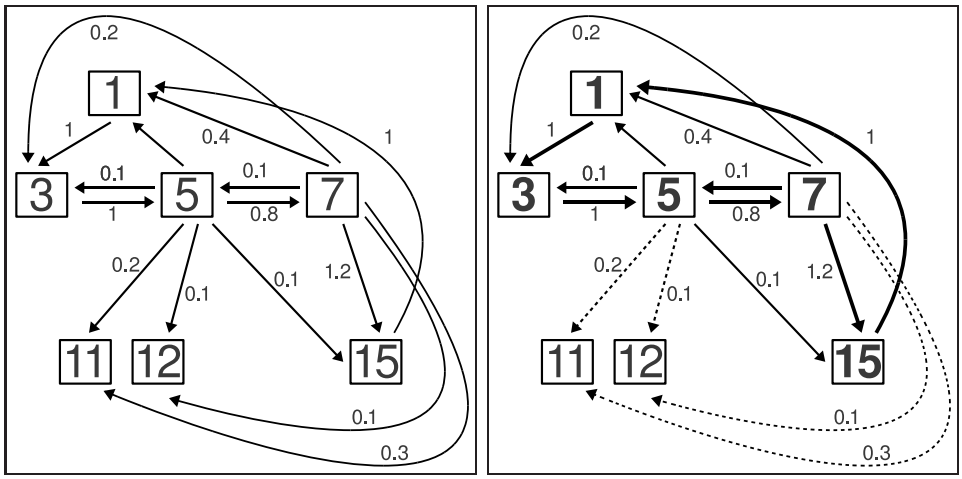


Figure 6.12: (a) Constrained dense CRN realization of Example 6.3.2 containing the vertices of the only nontrivial strong component of the dense realization, after removing 65 reactions, (b) Illustration of the final step of the algorithm on the CRN corresponding to Example 6.3.2

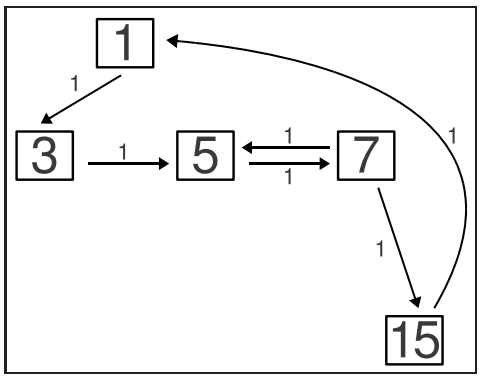


Figure 6.13: The obtained weakly reversible realization in Example 6.3.2

## 6.4 Including the the linear conjugacy concept into the optimization framework

According to Theorem 2.5.1, we can guarantee weak reversibility by imposing the condition

$$A_k \cdot b = \mathbf{0} \tag{6.88}$$

for some $b \in \mathbb{R}^m_{>0}$. This is clearly a nonlinear constraint in the reaction rate coefficients and the elements of $b$. In order to make it linear, we consider the matrix $\tilde{A}_k$ with entries

$$[\tilde{A}_k]_{ij} = [A_k]_{ij} \cdot b_j. \tag{6.89}$$

It is clear from (6.89) that $\tilde{A}_k$ is also a Kirchhoff matrix and that $\mathbf{1} \in \mathbb{R}^m$ (the $m$-dimensional vector containing only ones) lies in $\ker(\tilde{A}_k)$. Moreover, it is easy to see that $\tilde{A}_k$ encodes a weakly reversible network if and only if $A_k$ corresponds to a weakly reversible network. We can therefore check weak reversibility of the chemical reaction network corresponding to $A_k$ with the linear conditions

$$\textbf{(WR')} \quad \begin{cases} \sum_{i=1}^{m} [\tilde{A}_k]_{ij} = 0, \quad j = 1, \dots, m \\ \sum_{i=1}^{m} [\tilde{A}_k]_{ji} = 0, \quad j = 1, \dots, m \\ [\tilde{A}_k]_{ij} \geq 0, \quad i, j = 1, \dots, m, \ i \neq j \\ [\tilde{A}_k]_{ii} \leq 0, \quad i = 1, \dots, m. \end{cases} \tag{6.90}$$

By solving for the diagonal elements of $\tilde{A}_k$, the set of constraints (6.90) can be simplified to

$$\textbf{(WR)} \quad \begin{cases} \sum_{i=1, i\neq j}^{m} [\tilde{A}_k]_{ij} = \sum_{i=1, i\neq j}^{m} [\tilde{A}_k]_{ji}, \quad j = 1, \dots, m \\ [\tilde{A}_k]_{ij} \geq 0, \quad i, j = 1, \dots, m, \ i \neq j. \end{cases} \tag{6.91}$$

Naturally, the above constraints are used together with (6.1)-(6.4) and (6.5)-(6.6) that ensure dynamical equivalence.

No condition comparable to $Y \cdot A_k = M$ exists for the matrix $\tilde{A}_k$ so that we are left to optimization with respect to the internal entries of both $A_k$ and $\tilde{A}_k$. Given appropriate choices of $0 < \epsilon \ll 1$ and $u_{ij} > 0$, $i, j = 1, \dots, m$, $i \neq j$, we can impose

$$\textbf{(WR-S)} \quad \begin{cases} 0 \leq [\tilde{A}_k]_{ij} - \epsilon\delta_{ij}, \quad i, j = 1, \dots, m, \ \ i \neq j \\ 0 \leq -[\tilde{A}_k]_{ij} + u_{ij}\delta_{ij}, \quad i, j = 1, \dots, m, \ \ i \neq j \end{cases} \tag{6.92}$$

as well as (6.79)-(6.80) to ensure that both $A_k$ and $\tilde{A}_k$ contain zero and non-zero entries in the same places so that they correspond to reaction graphs with the same structure.

### 6.4.1 Computing weakly reversible linearly conjugate networks

While the results of [91] give conditions for two networks to be linearly conjugate, and therefore exhibit the same qualitative dynamics, no general methodology is provided for determining linearly conjugate networks when only a single network is provided.

In cases where the dynamics of a network is suspected to behave like a weakly reversible network, it is beneficial to extend the optimization algorithm outlined in

section 2.5.1 to linearly conjugate networks. This can be accomplished by modifying the set of constraints (6.1-6.4) to

$$\textbf{(LC)} \quad \begin{cases} Y \cdot A_b = T^{-1} \cdot M \\ \sum_{i=1}^{m} [A_b]_{ij} = 0, \quad j = 1, \ldots, m \\ [A_b]_{ij} \geq 0, \quad i, j = 1, \ldots, m, \ i \neq j \\ [A_b]_{ii} \leq 0, \quad i = 1, \ldots, m \\ \epsilon \leq c_j \leq 1/\epsilon, \quad j = 1, \ldots, n \end{cases} \tag{6.93}$$

where $M = Y \cdot A_k$, $T = \text{diag}\{c_1, \ldots, c_n\}$, $0 < \epsilon \ll 1$, and replacing the set of translated constraints (6.8)-(6.9) by

$$\textbf{(LC-S)} \quad \begin{cases} 0 \leq [A_b]_{ij} - \epsilon\delta_{ij}, \quad i, j = 1, \ldots, m, \ \ i \neq j \\ 0 \leq -[A_b]_{ij} + u_{ij}\delta_{ij}, \quad i, j = 1, \ldots, m, \ \ i \neq j \\ \delta_{ij} \in \{0, 1\}, \quad i, j = 1, \ldots, m, i \neq j, \end{cases} \tag{6.94}$$

where $u_{ij} > 0$ for $i, j = 1, \ldots, m, i \neq j$.

$A_b$ has the same structure as the kinetics matrix $A'_k$ corresponding to the conjugate network, and this matrix has the same structure as the matrix $\tilde{A}_k$ given by (6.89) (replacing $A_k$ by $A'_k$). Consequently, the problem of determining a sparse or dense weakly reversible network which is linearly conjugate to a given kinetics can be given by minimizing or maximizing the sum of the integer variables $\delta_{ij}$ over the constraint sets (6.93), (6.94), (6.91), and (6.92). The kinetics matrix $A'_k$ for the linearly conjugate network is then given by (2.52).

### 6.4.2 Examples

In this subsection we will consider two examples from the literature which demonstrate how the MILP optimization algorithm outlined in this section is capable of efficiently finding sparse and dense weakly reversible networks which are linearly conjugate to a given network. We also consider one new example which illustrates how the algorithm is capable of finding networks with linearly conjugate dynamics for which no trivial linear conjugacy exists.

**Example 6.4.1.** Consider the initial CRN of Example 6.3.1 that is shown in Fig. 6.8(a). We recall that this network was first considered in [91] where the authors showed that it was linearly conjugate to a specified weakly reversible network for all values of $\epsilon > 0$. It was further analysed with the value $\epsilon = 1.5$ in Example 6.3.1 where a dense weakly reversible realization was found through successive MILP optmizations. This result will be reproduced here using the one-step MILP algorithm described in this section.

We have

$$Y = \begin{bmatrix} 1 & 1 & 2 & 0 & 1 & 1 & 3 \\ 2 & 0 & 1 & 3 & 3 & 1 & 1 \end{bmatrix}$$

and

$$M = \begin{bmatrix} 0 & 0 & -2 & 0 & 0 & 2 & 0 \\ -3 & 0 & 2 & 0 & -2 & 0 & 0 \end{bmatrix}.$$

and set $\epsilon = 1/\alpha = 2/3$ and $u_{ij} = 20$, $i, j = 1, \ldots, 7, i \neq j$. The MILP problem for a dense weakly reversible linearly conjugate network, possibly accounting for a

non-trivial linear conjugacy mapping, is

$$\text{minimize} \quad \sum_{i,j=1}^{7} -\delta_{ij}$$

over the constraint set

$$\begin{aligned}
Y \cdot A_b &= T^{-1} \cdot M \\
\sum_{i=1}^{m} [A_b]_{ij} &= 0, \quad j = 1, \ldots, m \\
\sum_{i=1, i\neq j}^{m} [\tilde{A}_k]_{ij} &= \sum_{i=1, i\neq j}^{m} [\tilde{A}_k]_{ji}, \quad j = 1, \ldots, m \\
0 &\leq [A_b]_{ij} - \epsilon \cdot \delta_{ij}, i, j = 1, \ldots, 7, i \neq j \\
0 &\leq -[A_b]_{ij} + u_{ij} \cdot \delta_{ij}, i, j = 1, \ldots, 7, i \neq j \\
0 &\leq [\tilde{A}_k]_{ij} - \epsilon \cdot \delta_{ij}, i, j = 1, \ldots, 7, i \neq j \\
0 &\leq -[\tilde{A}_k]_{ij} + u_{ij} \cdot \delta_{ij}, i, j = 1, \ldots, 7, i \neq j,
\end{aligned}$$

where $T = \text{diag}\{c_1, \ldots, c_n\}$, and the decision variables

$$\begin{aligned}
[A_b]_{ij} \geq 0, [\tilde{A}_k]_{ij} \geq 0, \text{ for } i, j = 1, \ldots, 7, i \neq j \\
[A_b]_{ii} \leq 0, \text{ for } i = 1, \ldots, 7 \\
\epsilon \leq c_i \leq 1/\epsilon, \text{ for } i = 1, 2 \\
\delta_{ij} \in \{0, 1\}, \text{ for } i, j = 1, \ldots, 7, i \neq j.
\end{aligned}$$

Solving for $A_b$ with GLPK and applying (2.52) gives the kinetics matrix

$$A_k = \begin{bmatrix}
-\frac{13}{3} & 0 & \frac{2}{3} & 0 & \frac{2}{3} & 0 & 0 \\
0 & 0 & 0 & 0 & 0 & 0 & 0 \\
0 & 0 & -2 & 0 & 0 & 2 & 0 \\
0 & 0 & 0 & 0 & 0 & 0 & 0 \\
\frac{2}{3} & 0 & \frac{2}{3} & 0 & -\frac{4}{3} & 0 & 0 \\
\frac{11}{3} & 0 & \frac{2}{3} & 0 & \frac{2}{3} & -2 & 0 \\
0 & 0 & 0 & 0 & 0 & 0 & 0
\end{bmatrix}$$

and values $c_1 = 1, c_2 = 1$ (i.e. the linear transformation is the identity). The network structure is given graphically in Fig. 6.14(a). Although the rate constants differ due to differing bounds, this has the same network structure as the dense weakly reversible network obtained in Example 6.3.1.

A sparse weakly reversible network is generated by optimizing

$$\text{minimize} \quad \sum_{i,j=1}^{7} \delta_{ij}$$

over the same constraint set. Solving for $A_b$ with GLPK with the bound $\epsilon = 0.1$ and

applying (2.52) gives the kinetic matrix

$$A_k = \begin{bmatrix} -150 & 0 & 0 & 0 & 500 & 0 & 0 \\ 0 & 0 & 0 & 0 & 0 & 0 & 0 \\ 0 & 0 & -100 & 0 & 0 & 10 & 0 \\ 0 & 0 & 0 & 0 & 0 & 0 & 0 \\ 0 & 0 & 100 & 0 & -500 & 0 & 0 \\ 150 & 0 & 0 & 0 & 0 & -10 & 0 \\ 0 & 0 & 0 & 0 & 0 & 0 & 0 \end{bmatrix}$$

and values $c_1 = 10$ and $c_2 = 5$. This is therefore an example of a network with a non-trivial linear conjugacy and corresponds to the weakly reversible network given in Fig. 6.14(b).

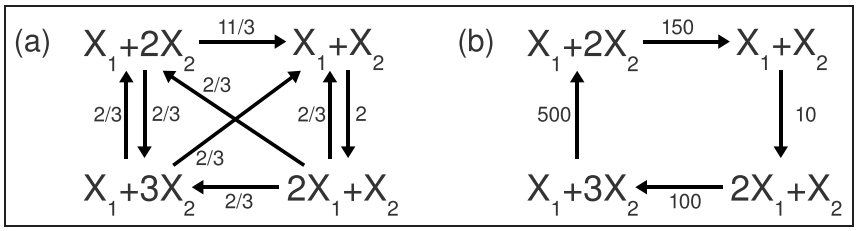


Figure 6.14: Dense (a) and sparse (b) weakly reversible networks which are linearly conjugate to the initial CRN

**Example 6.4.2.** Let us consider again the kinetics scheme of Examples 6.2.2 and 6.3.2 with equations (6.62) and complex numbering given by (6.63).

In Example 6.3.2 the determination of a dense weakly reversible realization for the same system required three MILP optimizations, three searches for strongly connected components, and took 80.5s to complete. Carrying out the MILP optimization algorithm described in this section for a dense and then for a sparse weakly reversible network, with bounds $\epsilon = 0.1$ and $u_{ij} = 10$, $i, j = 1, \ldots, 19$, we arrive at the same solution

$$\tilde{k}_{18} = \tilde{k}_{29} = \tilde{k}_{82} = 0.1, \;\; \tilde{k}_{92} = \tilde{k}_{9(17)} = 0.001, \;\; \tilde{k}_{(17)1} = 0.01,$$
$$c_1 = c_2 = c_3 = c_4 = 0.1,$$

and the rest of the entries zero (the transformation is a scaling of the identity). This corresponds to the network given in Figure 6.15 which has the same network structure as the network obtained in Example 6.3.2. The presented one-step algorithm was able to obtain the answer in a single MILP optimization step and took less than a tenth of a second to compute. (The difference of rate constants from the results of Example 6.3.2 occurs as a result of the scaling of concentration variables permitted by linear conjugacy.)

**Example 6.4.3.** Consider the kinetics scheme

$$\begin{aligned} \dot{x}_1 &= x_1 x_2^2 - 2x_1^2 + x_1 x_3^2 \\ \dot{x}_2 &= -x_1^2 x_2^2 + x_1 x_3^2 \\ \dot{x}_3 &= x_1^2 - 3x_1 x_3^2. \end{aligned} \tag{6.95}$$

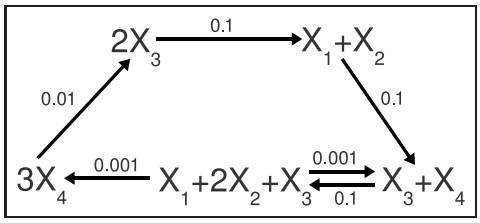


Figure 6.15: Weakly reversible realization of the kinetic system of Example 6.4.2. This realization is both dense and sparse.

The complexes corresponding to the canonic realization are

$$\begin{aligned} &C_1 = X_1 + 2X_2, C_2 = 2X_1 + 2X_2, C_3 = 2X_1 + X_2, \\ &C_4 = 2X_1, C_5 = X_1, C_6 = 2X_1 + X_3, C_7 = X_1 + 2X_3 \\ &C_8 = 2X_1 + 2X_3, C_9 = X_1 + X_2 + 2X_3, C_{10} = X_1 + X_3. \end{aligned} \tag{6.96}$$

With this fixed complex set, we can carry out the MILP optimization procedure to find sparse and dense weakly reversible networks which are linearly conjugate to a network with kinetics (6.95). We have

$$Y = \begin{bmatrix} 1 & 2 & 2 & 2 & 1 & 2 & 1 & 2 & 1 & 1 \\ 2 & 2 & 1 & 0 & 0 & 0 & 0 & 0 & 1 & 0 \\ 0 & 0 & 0 & 0 & 0 & 1 & 2 & 2 & 2 & 1 \end{bmatrix}$$

and

$$M = \begin{bmatrix} 1 & 0 & 0 & -2 & 0 & 0 & 1 & 0 & 0 & 0 \\ 0 & -1 & 0 & 0 & 0 & 0 & 1 & 0 & 0 & 0 \\ 0 & 0 & 0 & 1 & 0 & 0 & -3 & 0 & 0 & 0 \end{bmatrix}.$$

With the bounds $\epsilon = 1/20$ and $u_{ij} = 20$ for $i, j = 1, \ldots, 10$, $i \neq j$, the algorithm gives us the sparse network given in Figure 6.16(a) (conjugacy constants $c_1 = 20$, $c_2 = 2$, and $c_3 = 5$) and the dense network given in Figure 6.16(b) (conjugacy constants $c_1 = 20/3$, $c_2 = 20/33$, and $c_3 = 5/3$). It is interesting to note that the sparse and dense networks utilize different complexes and that the conjugacy constants differ between the sparse and dense networks. It is also important to emphasize finally, that it can be shown that there are no weakly reversible dynamically equivalent realizations of the dynamics (6.95) with the complex set (6.96), but the computation results show that the dynamics is linearly conjugate to several weakly reversible deficiency 0 structures.

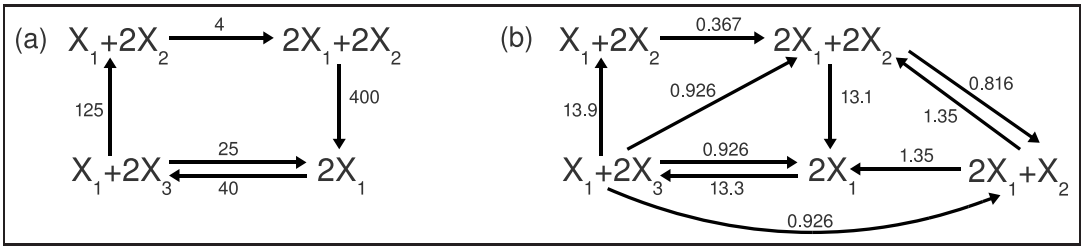


Figure 6.16: Weakly reversible networks which are linearly conjugate to a network with the kinetics (6.95). The network in (a) is sparse while the network in (b) is dense.

## 6.5 Further related results and extensions

In this section, some further additions to the previously presented results will be described shortly.

### 6.5.1 Realizations of deficiency zero CRNs with one terminal strong linkage class are unique

The result shown in this subsection has been published in [J18]. The main result here is that deficiency zero CRNs with one terminal strong linkage class cannot have multiple different realizations, if the set of complexes is fixed. For this, we will use the following standard notations. The dimension of a vector space $V$ is denoted by $\dim(V)$. For an arbitrary matrix $M$, its rank, image and kernel is denoted by $\mathrm{rank}(M)$, Im $M$, and Ker $M$, respectively. Furthermore, let us denote the $i$th column of a matrix $M$ with $[M]_{.,i}$.

Additionally, the following relations known from linear algebra and CRN theory will be used. (For **R1**-**R4**, the reader is referred to e.g. [129], while **R5**, **R6** can be found in [49] and [72], respectively)

**R1** For any two matrices $A$, $B$ for which $AB$ exists $\mathrm{rank}(AB) \leq \min(\mathrm{rank}(A), \mathrm{rank}(B))$.

**R2** (Rank-nullity theorem) For any $k \times l$ matrix $M$, $\dim(\text{Im } M) + \dim(\text{Ker } M) = l$.

**R3** For any matrices $A$, $B$ such that the product $BA$ exists

$$\dim(\text{Im } A \cap \text{Ker } B) = \dim(\text{Im } A) - \dim(\text{Im}(BA)) = \dim(\text{Ker}(BA)) - \dim(\text{Ker } A)$$

**R4** The maximal rank of a set $V = \{v^{(1)}, \ldots, v^{(k)}\}$ of $n$-dimensional vectors for which $\sum_{i=1}^{n} v_i^{(j)} = 0$, for $j = 1, \ldots, k$ and $k >= n$, is $n-1$. To see this, let us form the following matrix from the vectors $v^{(1)}, \ldots, v^{(k)}$

$$M = [v^{(1)}\ v^{(2)}\ \ldots\ v^{(k)}] \tag{6.97}$$

The maximal row rank of $M$ is clearly $n-1$, since the zero vector can be constructed as a nontrivial linear combination (i.e. a simple addition) of the rows of $V$. The row and column ranks of any matrix are always equal, therefore the maximal number of linearly independent vectors in $V$ is $n-1$.

**R5** If a CRN with the Kirchhoff matrix $A_k \in \mathbb{R}^{m \times m}$ has one terminal strong linkage class, then $\dim(\text{Im } A_k) = m - 1$.

**R6** If each linkage class of a CRN given by $(Y, A_k)$ contains precisely one terminal strong linkage class, then the deficiency $d$ of the network is $d = \dim(\text{Im } A_k \cap \text{Ker } Y)$.

Taking into consideration the preliminary facts **R1**-**R6**, we can now state the following result.

**Theorem 6.5.1.** Any deficiency zero CRN given by $(Y, A_k)$ with one terminal strong linkage class is parametrically and therefore structurally unique, if the set of complexes is fixed, i.e. there is no Kirchhoff matrix $A'_k$ different from $A_k$ such that $Y \cdot A_k = Y \cdot A'_k$.

*Proof.* (Indirect) Let us assume that there exists a Kirchhoff matrix $A'_k \neq A_k$ such that $YA_k = YA'_k$. Then $Y(A_k - A'_k) = 0$. Let $\hat{A}_k = A_k - A'_k$. It is clear that $\hat{A}_k$ is also a column conservation matrix (not necessarily Kirchhoff), and that the columns of $\hat{A}_k$ belong to the kernel of $Y$, i.e. $[\hat{A}_k]_{\cdot,i} \in \text{Ker } Y$ for $i = 1, \ldots, m$. From this it follows that $\dim(\text{Ker } Y) \geq 1$ since $\hat{A}_k$ is nonzero.

From **R5** we know that $\dim(\text{Im } A_k) = m - 1$. From **R3** and **R6** it follows that $\dim(\text{Im } A_k) = \dim(\text{Im}(YA_k))$, i.e. $\dim(\text{Im}(YA_k)) = m - 1$. Using **R1** we get that $\dim(\text{Im } Y) \geq m - 1$ that implies $\dim(\text{Ker } Y) \leq 1$. From the two estimations on the dimension of Ker $Y$ we obtain that $\dim(\text{Ker } Y) = 1$, and (by using **R2**) that $\dim(\text{Im } Y) = m - 1$.

Since $\hat{A}_k$ is a column conservation matrix, for any $v \in \text{Ker } Y$ it is true that $\sum_{i=1}^{m} v_i = 0$. Then, according to **R4**, Ker $Y \subset$ Im $A_k$, and therefore $\dim(\text{Im } A_k \cap \text{Ker } Y)$ cannot be zero, which is a contradiction. □

Deficiency zero weakly reversible networks with one linkage class form an important subset of the CRNs for which Theorem 6.5.1 is valid. Theorem 6.5.1 is naturally valid for CRNs composed of multiple linkage classes each of which has precisely one terminal linkage class, if the sets of species belonging to the individual linkage classes are mutually disjoint. In this case, the linkage classes can be treated as separate independent CRNs. However, if there are common species between the linkage classes, then zero deficiency and even (weak) reversibility of the linkage classes are not sufficient for the uniqueness of the realization, as the following example will show.

**Example 6.5.1.** Consider the reaction network the graph of which is shown in Fig. 6.17(a). Let us number the complexes as

$$C_1 = X_1,\ C_2 = 2X_1 + X_2,\ C_3 = 2X_2,\ C_4 = 3X_1 + X_2.$$

Then the matrices of the description (2.29) are the following:

$$Y = \begin{bmatrix} 1 & 2 & 0 & 3 \\ 0 & 1 & 2 & 1 \end{bmatrix},\ A_k = \begin{bmatrix} -1 & 2 & 0 & 0 \\ 1 & -2 & 0 & 0 \\ 0 & 0 & -3 & 2 \\ 0 & 0 & 3 & -2 \end{bmatrix}, \tag{6.98}$$

$$M = YA_k = \begin{bmatrix} 1 & -2 & 9 & -6 \\ 1 & -2 & -3 & 2 \end{bmatrix}. \tag{6.99}$$

Let us consider the following Kirchhoff matrix:

$$A'_k = \begin{bmatrix} -1 & 3 & 0 & 0 \\ 1 & -7 & 0 & 0 \\ 0 & 1 & -3 & 2 \\ 0 & 3 & 3 & -2 \end{bmatrix}. \tag{6.100}$$

It can be checked that $M = YA_k = YA'_k$. It is noticable from Fig. 6.17(b) that the deficiency of the second realization with $A'_k$ is 1, because it contains only one linkage class.

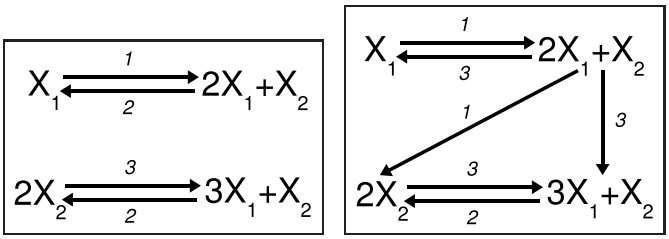


(a) (b)

Figure 6.17: (a) Simple reaction network of Example 6.5.1, (b) Dynamically equivalent one linkage class realization of the CRN

### 6.5.2 Dense realizations can be found in polynomial time

Computing dense realizations is treated originally in a MILP-framework in chapter 5. However, using the structural uniqueness of such realizations it is easy to give a polynomial-time algorithm based on a finite series of linear programming (LP) optimization steps. The idea of the improved algorithm is simple: the reaction $C_p \to C_q$ belongs to the dense realization if and only if there exists any dynamically equivalent realization where $[A_k]_{qp} > 0$. This result directly follows from the fact that the unweighted reaction graphs of constrained dense realizations give a unique super-structure. The corresponding condition can be effectively checked for each non-diagonal element of $A_k$ with the solution of the following standard linear programming (LP) problem:

$$\begin{aligned}
&\text{for} \quad p, q = 1, \ldots, m, \quad q \neq p \\
&\quad \text{maximize } f_{qp} = [A_k]_{qp} \\
&\quad \text{subject to :} \\
&\quad\quad Y \cdot A_k = M \\
&\quad\quad \sum_{i=1}^{m} [A_k]_{ij} = 0, \quad j = 1, \ldots, m \\
&\quad\quad [A_k]_{ij} \geq 0, \quad i, j = 1, \ldots, m, \quad i \neq j, \\
&\quad\quad [A_k]_{ii} \leq 0, \quad i = 1, \ldots, m
\end{aligned} \tag{6.101}$$

Let us denote the obtained objective function value corresponding to $(p, q)$ by $\gamma_{pq}$. (If the objective function value happens to be unbounded in (6.101) then an appropriate positive value for $\gamma_{pq}$ should be selected which is an acceptable positive upper bound for the corresponding rate coefficient.) Then, in the final step, a sufficiently small lower bound (denoted by $\epsilon_{ij}$) for the identified reactions with nonzero objective function value should be given to determine a possible dense realization by the solution of the following LP feasibility problem:

$$\begin{aligned}
&Y \cdot A_k = M \\
&\sum_{i=1}^{m} [A_k]_{ij} = 0, \quad j = 1, \ldots, m \\
&[A_k]_{ij} = 0, \quad \text{if } \gamma_{ij} = 0 \\
&[A_k]_{ij} \geq \epsilon_{ij}, \quad \text{if } \gamma_{ij} > 0 \\
&[A_k]_{ii} \leq 0, \quad i = 1, \ldots, m
\end{aligned} \tag{6.102}$$

A feasible solution of the above constraint set is a possible dense realization. Thus, the solution of the problem requires $m(m-1)+1$ LP steps, where $m$ is the number of complexes in the network. This method naturally works for constrained dense realizations, too, if the corresponding further constraints are added to the optimization. A significant analogous result worth to be mentioned here is that although many problems in process network synthesis are computationally hard because of structural complexity, using the notion of P-graphs the generation of a so-called maximal superstructure containing all feasible process networks performing a given task can be solved in polynomial time [62].

With this modification, the algorithm given in section 6.3 for computing weakly reversible realizations will be polynomial-time, too. Only the procedure for finding constrained dense realizations (called `FindConstrDenseRealization`) has to be changed in the method.

For comparison, the polynomial-time variant of the method finds the weakly reversible realization of the kinetic system in Example 6.3.2 in 10.3s instead of the 80.5s measured with the MILP-based solution.

### 6.5.3 Definition and computation of core reactions

We will call a reaction a *core reaction*, if it is present in any dynamically equivalent realization of a CRN with a given complex set (and possibly an additional constraint set). Other reactions, the rate coefficient of which can be zero in certain realizations, are called *non-core reactions*. It clearly follows from the definition, but is remarked separately that the set of core reactions is generally not identical to the set of reactions of a sparse realization.

The outline of the computation method for determining core reactions is the following. Firstly, a dense realization of the network has to be computed to get all the mathematically possible reactions. Then, for each reaction $C_p \to C_q$ in the dense realization, the feasibility of the following constraint set has to be checked:

$$\begin{aligned}
&Y \cdot A_k = M \\
&\sum_{i=1}^{m} [A_k]_{ij} = 0, \quad j = 1, \ldots, m \\
&[A_k]_{ij} \geq 0, \quad i, j = 1, \ldots, m, \quad i \neq j, \quad (i,j) \neq (q,p) \\
&[A_k]_{ii} \leq 0, \quad i = 1, \ldots, m \\
&[A_k]_{qp} = 0
\end{aligned} \tag{6.103}$$

where the off-diagonal elements of matrix $A_k$ are the decision variables, and the known matrices are $Y$ and $M$. It is clearly visible that this task is an LP feasibility problem. Then, reaction $C_p \to C_q$ is a core-reaction if and only if the set defined by (6.103) is empty (i.e. the corresponding LP problem is infeasible), because in this case there is no such dynamically equivalent CRN realization where $C_p \to C_q$ is not present.

The previous computation of core reactions can effectively speed up the algorithm for finding weakly reversible realizations (section 6.3), since core reactions are not removable from any dynamically equivalent realization. This means that if two different strong components in the reaction graph are linked by a core reaction, then there is no dynamically equivalent weakly reversible realization of the network. The notion of core reactions is illustrated on a biological model in Example A.2.3 in the Appendix.

Finally, we briefly remark the following related results. Firstly, the notion of "core" and "non-core complexes" can be defined analogously to the reactions and they can be determined through the solution of LP problems, too, using the results of subsection 6.1.1. Secondly, the parametric uniqueness of a given CRN with a given complex set can be numerically checked by first solving (6.101) and then by solving the same constraint set with the modified objective function $f'_{qp} = -[A_k]_{qp}$.

### 6.5.4 The unweighted reaction graph of dense linearly conjugate networks also defines a super-structure

Luckily, the main result of section 5.5 can be extended to linearly conjugate networks as follows.

**Theorem 6.5.2.** Consider a CRN given by the pair $(Y, A_k)$ and assume that $A'_k$ is such a Kirchhoff matrix that contains the maximal number of nonzero off-diagonal elements for which there exists a positive definite diagonal $T$ matrix such that

$$Y \cdot A_k = T \cdot Y \cdot A'_k. \tag{6.104}$$

Then the directed unweighted reaction graph corresponding to any Kirchhoff matrix $A''_k$ for which there exists a positive definite diagonal $T''$ such that $Y \cdot A_k = T'' \cdot Y \cdot A''_k$ is the subgraph of the reaction graph defined by $A'_k$.

*Proof.* Using indirect reasoning, we will construct a linearly conjugate network that leads to contradiction. For this, assume that $A''_k$ is such that

$$Y \cdot A_k = T'' \cdot Y \cdot A''_k, \tag{6.105}$$

where $T''$ is a positive definite diagonal matrix, $A''_k$ is Kirchhoff matrix, and $\exists(i, j)$, $i \neq j$ for which $[A''_k]_{ij} > 0$, but $[A'_k]_{ij} = 0$. Then $T'' = Q \cdot T$ for a positive diagonal $Q$ matrix with $Q = T'' \cdot T^{-1}$, and using (6.104) we can write:

$$T'' \cdot Y \cdot A'_k = Q \cdot T \cdot Y \cdot A'_k = Q \cdot Y \cdot A_k. \tag{6.106}$$

Now we proceed with the calculations as:

$$T'' \cdot Y \cdot A'_k + T'' \cdot Y \cdot A''_k = T'' \cdot Y \cdot (A'_k + A''_k) = T'' \cdot Y \cdot \bar{A}_k, \tag{6.107}$$

where $\bar{A}_k = A'_k + A''_k$ is clearly a valid Kirchhoff matrix. On the other hand, from (6.105) and (6.106) we have:

$$T'' \cdot Y \cdot A'_k + T'' \cdot Y \cdot A''_k = Q \cdot Y \cdot A_k + Y \cdot A_k = (Q + I) \cdot Y \cdot A_k, \tag{6.108}$$

where $I$ denotes the identity matrix of appropriate dimension. From (6.107) and (6.108) it follows that

$$T'' \cdot Y \cdot \bar{A}_k = (Q + I) \cdot Y \cdot A_k, \tag{6.109}$$

and thus

$$Y \cdot A_k = (Q + I)^{-1} \cdot T'' \cdot Y \cdot \bar{A}_k. \tag{6.110}$$

It is visible from (6.110) that we constructed a linearly conjugate network to $(Y, A_k)$ with a kinetics matrix that contains more nonzero off-diagonal elements than $A'_k$ has, which is a contradiction. □

## 6.6 Summary

Additional problems of determining certain dynamical equivalent or linearly conjugate CRN structures were solved in this chapter. MILP-based numerical procedures were given for the determination of dynamically equivalent CRN realizations that contain the minimal/maximal number of complexes or which are fully reversible. It was shown that the computation of dynamically equivalent detailed balanced and complex balanced CRN realizations can be traced back to simple LP problems where the values of any possible equilibrium point of the system are also used as parameters. A numerical method was given for the computation of dynamically equivalent weakly reversible CRN realizations that is based on a finite series of MILP optimization steps. Then the optimization framework for determining dynamically equivalent CRN realizations was extended to include the linear conjugacy of reaction networks. The parameters of the linear conjugacy transformation are additional unknowns in the optimization. Using this extension, a one-step MILP procedure was developed for the computation of linearly conjugate weakly reversible reaction networks that is numerically much more efficient than the previous approach in section 6.3. However, it was shown later that the MILP step can be avoided from the graph-theoretical approach of section 6.3 making the algorithm polynomial time, while it is not possible (at least in a straightforward way) to eliminate the MILP step from the method described in subsection 6.4.1. It was also shown that deficiency zero CRNs with one strong terminal linkage class are parametrically unique and that dense realizations of CRNs can be determined in polynomial time. Moreover, the so-called core reactions of CRNs were defined that are obligatory components of any equivalent realizations with a given complex set. Finally, it was shown that the unweighted reaction graph of dense linearly conjugate networks defines a super-structure, similarly to the case of dynamical equivalence.

# Chapter 7

# Conclusions

## 7.1 New scientific results

The new scientific contributions of the thesis are summarized in the following thesis points.[1] Thesis points 1, 2, 3 and 4 are related to chapters 3, 4, 5 and 6 of the dissertation, respectively. The corresponding publications are listed at the end of each thesis point.

1. **Analysis of quasi-polynomial systems**
   New results and computational methods were developed for the dynamical analysis of quasi-polynomial systems.

   (a) It was shown that a given positive equilibrium point of a Lotka-Volterra model is globally stable in the positive orthant with a certain logarithmic (or entropy-like) Lyapunov function if and only if there exists a local dissipative-Hamiltonian description in the neighborhood of its equilibrium point, where the Hamiltonian function is a diagonal quadratic form.

   (b) It was shown that the computation of a state-dependent time-rescaling transformation that is frequently applied for proving global stability of quasi-polynomial systems, can be traced back to the solution of a bilinear matrix inequality where the unknowns are the coefficients of the Lyapunov function and the parameters of the time-rescaling transformation.

   *Related publications:* [C1], [C2], [J2], [C3], [J3], [C4].

2. **Hamiltonian description of reversible chemical reaction networks with mass-action kinetics**
   It was shown that mass-action type chemical reaction networks with linearly independent reversible reaction-pairs possess a global pseudo-Hamiltonian and around the equilibrium point a local dissipative-Hamiltonian description in an appropriately transformed state-space.

   *Related publications:* [C5], [C6], [BC1], [C7], [J4], [J5].

[1] I strived to include only those results in the thesis points where my contribution was essential.

3. **Computation and properties of dense and sparse realizations of kinetic systems**
   Assuming a given complex set, dense and sparse dynamically equivalent realizations of kinetic systems were defined and analysed that contain the maximal and minimal number of nonzero reaction rate coefficients, respectively. Important properties of dense CRN realizations were determined and proved.

   (a) A numerical procedure was given for the determination of dynamically equivalent dense and sparse realizations of reaction networks. The problem was solved as a mixed integer linear programming (MILP) problem where the continuous decision variables are the nonnegative reaction rate coefficients while objective function to be minimized/maximized is the sum of the associated binary variables. The characteristics of mass action kinetics were taken into consideration as constraints in the optimization problem.

   (b) The following properties of dense and sparse realizations of a given chemical reaction network were proved. (i) The graph structure of the dense realizations is unique. (ii) The unweighted reaction graph (i.e. the structure) of any dynamically equivalent realization of a kinetic system is the subgraph of the unweighted reaction graph of the dense realization. (iii) The reaction graph structure of a kinetic system is unique if and only if the structures of its dense and sparse realizations are identical.

   The above results were extended to the case of dynamically equivalent constrained realizations where a subset of possible reactions is excluded from the network.

   *Related publications:* [C8], [J6], [J7], [BC2], [C9], [J8].

4. **Computation of dynamically equivalent and linearly conjugate reaction network structures with preferred properties**
   New optimization-based numerical methods were developed for the computation of chemical reaction network structures that are dynamically equivalent or linearly conjugate to a given reaction network or kinetic dynamical system, and possess certain prescribed properties. The possible set of chemical complexes was assumed to be a'priori given.

   (a) A MILP-based numerical procedure was given for the determination of dynamically equivalent CRN realizations containing the minimal and maximal number of complexes.

   (b) A MILP-based numerical algorithm was proposed for the computation of fully reversible dynamically equivalent CRN realizations.

   (c) It was shown that the computation of dynamically equivalent detailed balanced and complex balanced CRN realizations can be traced back to linear programming where the values of any possible equilibrium point of the system are also used as parameters.

   (d) A numerical method was given for the computation of dynamically equivalent weakly reversible CRN realizations. The method is based on a finite series of MILP optimization steps. It was shown that the algorithm can be improved to have polynomial time-complexity.

(e) The optimization framework for determining dynamically equivalent CRN realizations was extended to include the linear conjugacy of reaction networks. The parameters of the linear conjugacy transformation are additional unknowns in the optimization. Using the extension, a one-step MILP procedure was developed for the computation of linearly conjugate weakly reversible reaction networks.

*Related publications:* [BC2], [J20], [J9], [J10], [J8], [C10], [J11].

## 7.2 Utilization of the results and possible future work

As it was shortly summarized in section 3.3, starting from the stability analysis of QP and LV models, a method was given for the construction of a globally stabilizing feedback that was applied to process models [C3, J15]. Moreover, we gave a computation algorithm for determining invariants of QP systems that are explicit in at least one variable. With this method, we computed new, previously not published invariants for some systems that are frequently studied in literature. The same algorithm was also suitable for showing the lack of reachability of certain fermentation process models for which previously it was necessary to totally integrate the nonlinear reachability distribution [J12]. We successfully studied the stability of the zero dynamics of a nonlinear gas-turbine model identified previously from real measurement data by embedding the model into QP form [C2, J16]. Similarly, transforming the dynamics to polynomial form allowed us to study the identifiability of GnRH neuron models and to work out effective new parameter estimation methods for them [J17, J19, C11, C12, C13].

Using the Hamiltonian description presented in chapter 4, we proposed passivity-based controllers for kinetic systems [C4, C5, J4]. The group of methods for computing different dynamically equivalent realizations of reaction networks gave a computational solution to important problems raised long ago. They certainly form an important improvement in the realization practice of kinetic systems, since we can decide the existence of possible structures with important properties. With this, the scope of classical CRNT results has been clearly extended as it was originally intended. This is hopefully a useful step towards a thermodynamical view on nonnegative systems, even on such models that are not coming from (bio)chemistry. Moreover, the optimization approach for the analysis of different CRN structures can give the basic building blocks of a possible solution of the synthesis problem, i.e. when we want to realize a given polynomial dynamics with a (realistic) reaction network. This emphasizes again the significance of **Algorithm 1** for producing the canonic mechanism. It is also important to mention that the methods presented in (sub)sections 5.4, 6.3, 6.5.2 and 6.5.3 are parallel in their original forms and therefore they can be effectively implemented in a grid or multi-core hardware environment.

Of course, numerous important and interesting problems remained open. From the analysis of GnRH neuron models mentioned above, and from other related literature results it is expected that the QP system class can be successfully used in the solution of parameter estimation problems for dynamical systems. The methods in chapters 5 and 6 assumed that the set of complexes is a'priori given and fixed. Therefore the possibility of the targeted selection of new complexes in order to obtain additional information about the studied kinetic system is also of interest. Two important problems are also open in this topic, namely the computation of a realization with minimal

deficiency and the existence/computation of a deficiency zero weakly reversible realization. Starting from the dense realization might also be of some help in these cases, too, similarly to the algorithm shown in section 6.3. Based on the preliminary results of initial discussions and computations, it seems that some of the methods computing dynamically equivalent CRN realizations can be extended to handle a range of parameters using interval techniques (see, e.g. [109, 30]). Similarly, it is expected that more interesting computation problems can be formulated using the concept of linear conjugacy. As it is suggested by Example 6.1.2 where it was possible to manually find a general solution based on the numerical results, the symbolic extension of some of the methods in chapters 5 and 6 may be possible. The solution of any of the following control theoretic problems would be a significant improvement, too: feedback equivalence to a kinetic, complex balanced or weakly reversible deficiency zero system, or the design of static/dynamic kinetic controllers using the stability results of CRNT.

# Appendix A

# Further examples

This appendix contains additional examples that could not be fit into the main text because of space limitations.

## A.1 Time-rescaling of QP models

**Example A.1.1. Example with a rank deficient $M$ matrix.** Consider the following open generalized mass-action law system

$$\begin{aligned} \dot{y}_1 &= 0.5y_1 - y_1^{2.25} - 0.5y_1^{1.5}y_2^{0.25} + u_1 \\ \dot{y}_2 &= y_2 - 0.5y_2^{1.75} + u_2 \end{aligned} \tag{A.1}$$

where $y_1$ and $y_2$ are the concentrations of chemical species $\mathcal{A}_1$ and $\mathcal{A}_2$ ($[\frac{moles}{m^3}]$), while $u_1$ and $u_2$ (the manipulable inputs) are their volume-specific component mass inflow rates ($[\frac{moles}{m^3 sec}]$). The above two differential equations originate from the component mass conservation equations constructed for a perfectly stirred balance volume [75] under the following modelling assumptions:

1. constant temperature and overall mass,
2. constant physico-chemical properties (e.g. density),
3. presence of an inert solvent in a great excess,
4. presence of the following reaction network:
   - autocatalytic generation of the species $\mathcal{A}_1$ and $\mathcal{A}_2$ (e.g. by polymer degradation when they are the monomers and the polymers are present in a great excess) giving rise to the reaction rates $0.5y_1$ and $y_2$ (the first terms in the right-hand sides) respectively,
   - a self-degradation of these species described by the reaction rates $-y_1^{2.25}$ and $-0.5y_2^{1.75}$ (the second terms on the right-hand sides) respectively,
   - a catalytic degradation of the specie $\mathcal{A}_1$ catalyzed by specie $\mathcal{A}_2$ that corresponds to $-0.5y_1^{1.5}y_2^{0.25}$ in the first equation only (the third term).

The control aim is to drive the system to a positive equilibrium

$$y_1^* = 2.4082\ \frac{moles}{m^3}, \quad y_2^* = 16.3181\ \frac{moles}{m^3}.$$

This goal can be achieved e.g. by the following nonlinear feedback:

$$\begin{aligned} u_1 &= 0.5 y_1 y_2^{0.75} \\ u_2 &= 0.5 y_1^{1.25} y_2 + 0.5 y_1^{0.5} y_2^{1.25}. \end{aligned} \tag{A.2}$$

The above inputs being the component mass flow rates fed to the system (they are both positive) are needed for compensating for the degradation of the specie $\mathcal{A}_1$ and $\mathcal{A}_2$.

By substituting eq. (A.2) into eq. (A.1), we obtain the controlled system that is a QP system with the following matrices

$$A = \begin{bmatrix} -1 & 0.5 & -0.5 \\ 0.5 & -0.5 & 0.5 \end{bmatrix} \tag{A.3}$$

$$B = \begin{bmatrix} 1.25 & 0 \\ 0 & 0.75 \\ 0.5 & 0.25 \end{bmatrix}, \quad L = \begin{bmatrix} 0.5 \\ 1 \end{bmatrix} \tag{A.4}$$

The eigenvalues of the Jacobian matrix of the system at the equilibrium point are $-6.4076$ and $-0.7768$.

Since the rank of $M = B \cdot A$ in this case is only 2, we can use the algorithm described in [66] to prove that the LMI (2.20) is not feasible in this case.

However, by solving (3.47) applying the algorithm described in [97] we find that we can use the following time-reparametrization:

$$\Omega = \begin{bmatrix} -0.25 & -0.5 \end{bmatrix}^T, \tag{A.5}$$

and the diagonal matrix containing the coefficients of the Lyapunov function is:

$$C = \mathrm{diag}([1 \;\; 2 \;\; 2 \;\; 2]). \tag{A.6}$$

The eigenvalues of $\tilde{M}^T \cdot C + C \cdot \tilde{M}$ in this case are

$$\lambda_1 = 0, \;\; \lambda_2 = 0, \;\; \lambda_3 = -4.5, \;\; \lambda_4 = -2.5, \tag{A.7}$$

which again proves the global stability of the studied equilibrium point.

The above example shows that time-reparametrization can be used (through adding more degrees of freedom to the problem) in the design of feedbacks for nonlinear systems. We mention that a similar principle is utilized in [145].

## A.2 Computation of CRN structures

**Example A.2.1.** This example illustrates the structural non-uniqueness of sparse realizations. The starting point is the reaction network described in [28] as Fig. 6 in section 6. The network is replotted in Fig. A.1(a). For the sake of simplicity, let us choose all the reaction rate coefficients to be 1 in the network. The $Y$ and $A_k$ matrices of the original reaction system are

$$Y = \begin{bmatrix} 0 & 0 & 0 & 0 & 1 & 0 & 0 & 0 & 0 & 0 & 0 \\ 0 & 1 & 0 & 0 & 0 & 0 & 0 & 0 & 1 & 2 & 1 \\ 0 & 0 & 1 & 0 & 0 & 0 & 1 & 2 & 1 & 0 & 0 \\ 0 & 0 & 0 & 1 & 0 & 2 & 1 & 0 & 0 & 0 & 1 \end{bmatrix}, \tag{A.8}$$

$$A_k = \begin{bmatrix} -4 & 1 & 1 & 1 & 1 & 0 & 0 & 0 & 0 & 0 & 0 \\ 1 & -1 & 0 & 0 & 0 & 0 & 0 & 0 & 0 & 0 & 0 \\ 1 & 0 & -1 & 0 & 0 & 0 & 0 & 0 & 0 & 0 & 0 \\ 1 & 0 & 0 & -1 & 0 & 0 & 0 & 0 & 0 & 0 & 0 \\ 1 & 0 & 0 & 0 & -7 & 1 & 0 & 1 & 0 & 1 & 0 \\ 0 & 0 & 0 & 0 & 1 & -1 & 0 & 0 & 0 & 0 & 0 \\ 0 & 0 & 0 & 0 & 1 & 0 & 0 & 0 & 0 & 0 & 0 \\ 0 & 0 & 0 & 0 & 1 & 0 & 0 & -1 & 0 & 0 & 0 \\ 0 & 0 & 0 & 0 & 1 & 0 & 0 & 0 & 0 & 0 & 0 \\ 0 & 0 & 0 & 0 & 1 & 0 & 0 & 0 & 0 & -1 & 0 \\ 0 & 0 & 0 & 0 & 1 & 0 & 0 & 0 & 0 & 0 & 0 \end{bmatrix} \tag{A.9}$$

The first column of zeros in $Y$ denotes the zero complex. Four different dynamically equivalent sparse realizations are shown in Fig. A.1(b)-(e). The Kirchhoff matrix of the network in Fig. A.1(b) is

$$A_k^s = \begin{bmatrix} -3 & 1 & 1 & 1 & 1 & 0 & 0 & 0 & 0 & 0 & 0 \\ 1 & -1 & 0 & 0 & 0 & 0 & 0 & 0 & 0 & 0 & 0 \\ 0 & 0 & -1 & 0 & 0 & 0 & 0 & 0 & 0 & 0 & 0 \\ 0 & 0 & 0 & -1 & 0 & 0 & 0 & 0 & 0 & 0 & 0 \\ 1 & 0 & 0 & 0 & -7 & 1 & 0 & 1 & 0 & 1 & 0 \\ 0 & 0 & 0 & 0 & 0 & -1 & 0 & 0 & 0 & 0 & 0 \\ 1 & 0 & 0 & 0 & 4 & 0 & 0 & 0 & 0 & 0 & 0 \\ 0 & 0 & 0 & 0 & 0 & 0 & 0 & -1 & 0 & 0 & 0 \\ 0 & 0 & 0 & 0 & 0 & 0 & 0 & 0 & 0 & 0 & 0 \\ 0 & 0 & 0 & 0 & 2 & 0 & 0 & 0 & 0 & -1 & 0 \\ 0 & 0 & 0 & 0 & 0 & 0 & 0 & 0 & 0 & 0 & 0 \end{bmatrix} \tag{A.10}$$

The coefficient matrix of the differential equations is given by

$$M = YA_k = YA_k^s = \begin{bmatrix} 1 & 0 & 0 & 0 & -7 & 1 & 0 & 1 & 0 & 1 & 0 \\ 1 & -1 & 0 & 0 & 4 & 0 & 0 & 0 & 0 & -2 & 0 \\ 1 & 0 & -1 & 0 & 4 & 0 & 0 & -2 & 0 & 0 & 0 \\ 1 & 0 & 0 & -1 & 4 & -2 & 0 & 0 & 0 & 0 & 0 \end{bmatrix} \tag{A.11}$$

It is visible that the computed sparse realizations contain 12 reactions. The number of non-isolated complexes in the sparse structures is 9 or 10, while the original network contains 11 reacting complexes. It is easy to compute that the deficiencies of the original structure in Fig. A.1(a) and that of the sparsest realization in Fig. A.1(b) are $d_1 = 6$ ($m_1 = 11$, $l_1 = 1$, $s_1 = 4$) and $d_2 = 4$ ($m_2 = 9$, $l_2 = 1$, $s_2 = 4$), respectively. The deficiency of each network shown in Figs. A.1(c)-(e) is 5. These results show that additional constraints in the optimization procedure may be used to select the required sparse realization from the set of possible alternatives. It is interesting to compare that the equivalent simplified realization on the right hand side of Fig. 6. in the original publication [28] contains 8 complexes but 14 reactions, and has a deficiency of 3. This shows the not surprising fact that the minimization of the number of reactions (although it reduces the number of reacting complexes in many cases) does not necessarily lead to lower deficiency.

**Example A.2.2. Equivalent reversible realization of an irreversible reaction network.** Let us start from the reaction network that is depicted in Fig. A.2. This network contains 9 complexes, 2 linkage classes and 8 irreversible reaction steps. The

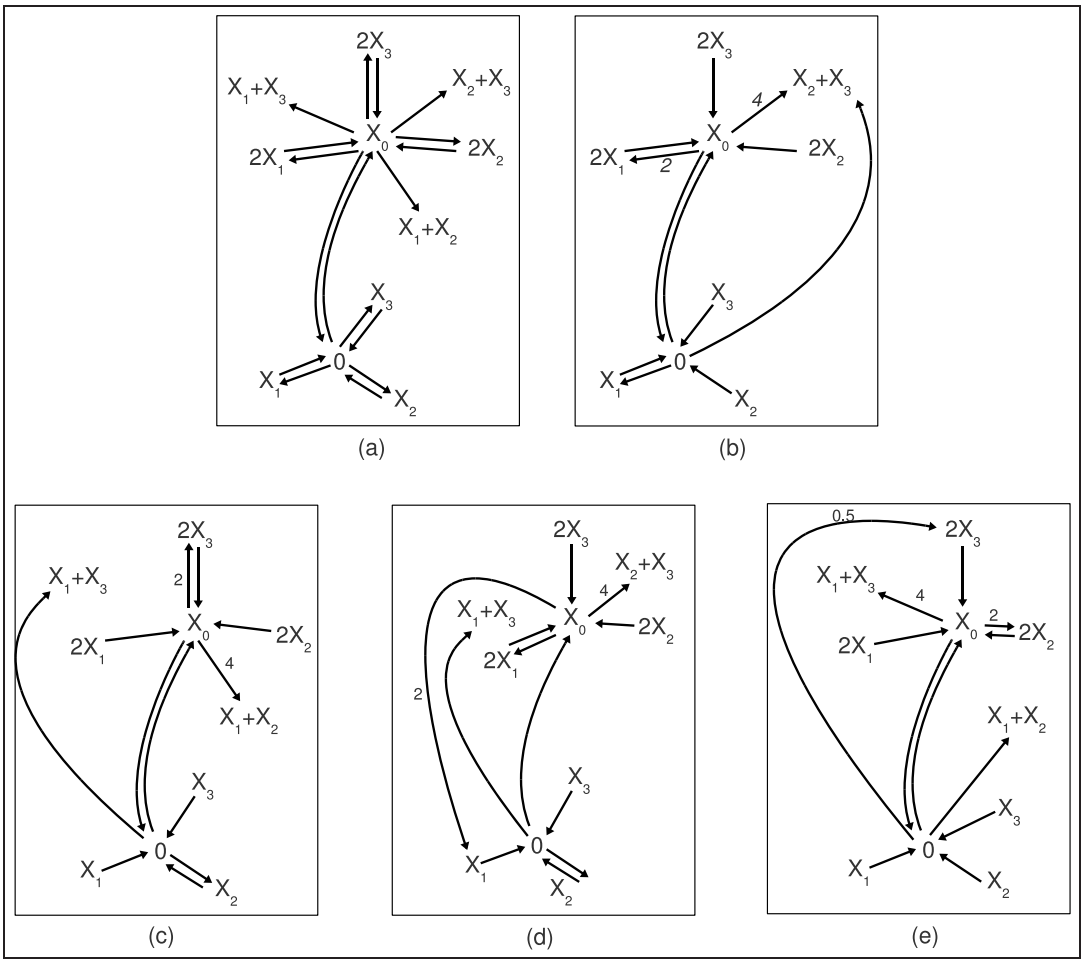


Figure A.1: (a) Initial reaction network of Example A.2.1. (b)-(e) Different sparse realizations of the initial network. (Only reaction rates different from 1 are indicated separately.)

rank of the stoichiometric subspace is 3, therefore the deficiency of the network is 4. The matrices characterizing the network are given by

$$Y = \begin{bmatrix} 2 & 1 & 1 & 2 & 0 & 1 & 0 & 1 & 0 \\ 0 & 0 & 1 & 1 & 0 & 0 & 1 & 1 & 0 \\ 0 & 0 & 0 & 0 & 1 & 1 & 1 & 1 & 0 \end{bmatrix}, \tag{A.12}$$

$$A_k = \begin{bmatrix} -2 & 0 & 0 & 0 & 0 & 0 & 0 & 0 & 0 \\ 1 & 0 & 3.5 & 0 & 0 & 0 & 0 & 0 & 0 \\ 0 & 0 & -5.5 & 0 & 0 & 0 & 0 & 0 & 0 \\ 1 & 0 & 0.5 & 0 & 0 & 0 & 0 & 0 & 0 \\ 0 & 0 & 0 & 0 & -1.5 & 0 & 0 & 0 & 0 \\ 0 & 0 & 0 & 0 & 0.5 & 0 & 0 & 0 & 0 \\ 0 & 0 & 0 & 0 & 0.5 & 0 & 0 & 0 & 0 \\ 0 & 01.5 & 0 & 0 & 0 & 0 & 0 & 0 & \\ 0 & 0 & 0 & 0 & 0.5 & 0 & 0 & 0 & 0 \end{bmatrix}. \tag{A.13}$$

Running the algorithm described in section 6.1.2 with parameters $\epsilon = 10^{-8}$, $\epsilon_2 = 0.05$, $\gamma = 0.01$, where the objective function to be minimized was the number of nonzero

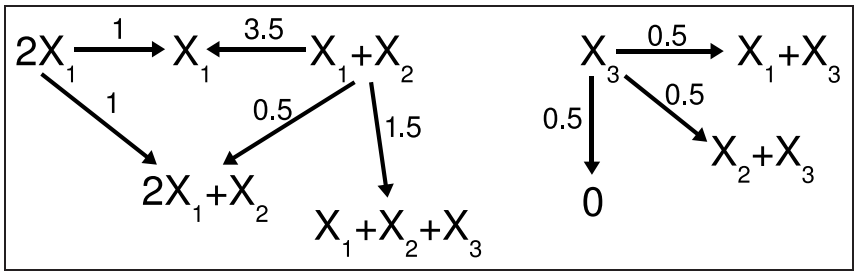


Figure A.2: Irreversible reaction network with a deficiency of 4

reaction rate coefficients, gave the following Kirchhoff matrix:

$$A'_k = \begin{bmatrix} -1 & 0 & 2 & 0 & 0 & 0 & 0 & 0 & 0 \\ 0 & 0 & 0 & 0 & 0 & 0 & 0 & 0 & 0 \\ 1 & 0 & -3.5 & 0 & 0.5 & 0 & 0 & 0 & 0 \\ 0 & 0 & 0 & 0 & 0 & 0 & 0 & 0 & 0 \\ 0 & 0 & 1.5 & 0 & -0.5 & 0 & 0 & 0 & 0 \\ 0 & 0 & 0 & 0 & 0 & 0 & 0 & 0 & 0 \\ 0 & 0 & 0 & 0 & 0 & 0 & 0 & 0 & 0 \\ 0 & 0 & 0 & 0 & 0 & 0 & 0 & 0 & 0 \\ 0 & 0 & 0 & 0 & 0 & 0 & 0 & 0 & 0 \end{bmatrix}. \tag{A.14}$$

It is again easy to verify that

$$Y \cdot A_k = Y \cdot A'_k = \begin{bmatrix} -1 & 0 & 0.5 & 0 & 0.5 & 0 & 0 & 0 & 0 \\ 1 & 0 & -3.5 & 0 & 0.5 & 0 & 0 & 0 & 0 \\ 0 & 0 & 1.5 & 0 & -0.5 & 0 & 0 & 0 & 0 \end{bmatrix}. \tag{A.15}$$

The above result implies that the Deficiency Zero Theorem can be applied to the dynamics of the original irreversible reaction network shown in Fig. A.2. Moreover, due to the existence of a deficiency 0 reversible realization with linearly independent reaction-pairs, the dynamics of the reaction networks exhibit a dissipative Hamiltonian structure as it was shown in chapter 4.

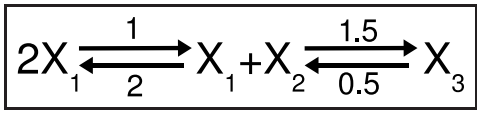


Figure A.3: Zero deficiency reversible reaction network dynamically equivalent to the one shown in Fig. A.2

**Example A.2.3. A positive feedback motif**. In this example we will show that there exists multiple dynamically equivalent realizations for a well-known basic building block in systems biology. The examined system is a positive feedback motif shown in Fig. A.4(a) and taken from [116] containing 5 species, 11 complexes and 9 reactions. This basic motif is also discussed in [2]. The network contains a gene that promotes its own transcription and translation after dimerization. In the model, $X_1$ and $X_2$ denote the concentrations of protein monomers and dimers, respectively. $X_3$ and $X_4$ are the concentrations of unoccupied and occupied promoters, respectively, and $X_5$ corresponds to the mRNA. The degradation of dimers is ignored. The roles of the reaction rate coefficients are the following: $k_1$ and $k_2$ are the dimerization and

re-dimerization rates, respectively. $k_3$ and $k_4$ are the binding and dissociation rates of the dimer to the promoter, while $k_5$ and $k_6$ denote the activated and basal transcription rates, respectively. $k_7$ is the degradation rate of the mRNA, $k_8$ is the degradation rate of the monomer, and $k_9$ denotes the translation rate. The time-evolution of the species-concentrations is described by the following ODEs:

$$\dot{x}_1 = -2k_1x_1^2 + 2k_2x_2 + k_9x_5 - k_8x_1 \tag{A.16}$$
$$\dot{x}_2 = k_1x_1^2 - k_2x_2 - k_3x_2x_3 + k_4x_4 \tag{A.17}$$
$$\dot{x}_3 = -k_3x_2x_3 + k_4x_4 \tag{A.18}$$
$$\dot{x}_4 = k_3x_2x_3 - k_4x_4 \tag{A.19}$$
$$\dot{x}_5 = k_5x_4 + k_6x_3 - k_7x_5 \tag{A.20}$$

Our starting point is that we have a dynamic model of the process in the standard polynomial form of (A.16)-(A.20), the parameters of which are known from the results of identification and/or from literature. As we will see below, without well-defined constraints on the possible set of complexes and reactions, exactly the same dynamics can be realized in principle by a wide range of mechanisms.

The matrices characterizing the stoichiometry and graph structure of the system are the following (indicating only the nonzero non-diagonal elements of $A_k$):

$$Y = \begin{bmatrix} 2 & 1 & 1 & 0 & 0 & 0 & 0 & 0 & 0 & 0 & 0 \\ 0 & 0 & 0 & 1 & 1 & 0 & 0 & 0 & 0 & 0 & 0 \\ 0 & 0 & 0 & 1 & 0 & 1 & 1 & 0 & 0 & 0 & 0 \\ 0 & 0 & 0 & 0 & 0 & 0 & 0 & 1 & 1 & 0 & 0 \\ 0 & 1 & 0 & 0 & 0 & 1 & 0 & 1 & 0 & 1 & 0 \end{bmatrix}, \tag{A.21}$$

$$A_k(2,1) = k_1,\ A_k(1,2) = k_2,\ A_k(4,3) = k_3,\ A_k(3,4) = k_4,\ A_k(5,4) = k_5,$$
$$A_k(7,6) = k_6,\ A_k(9,8) = k_7,\ A_k(9,10) = k_8,\ A_k(11,8) = k_9. \tag{A.22}$$

We used the following parameter values that were taken from the Appendix of [116].

$$k_1 = k_2 = k_3 = k_4 = 10^7,\ k_5 = 1.7,\ k_6 = 0.025,\ k_7 = 0.1,\ k_8 = 0.05,\ k_9 = 0.5, \tag{A.23}$$

where the units of measure are $[\mathrm{M}^{-1}]$ for $k_1, \ldots, k_4$, and $[\mathrm{min}^{-1}]$ for $k_5, \ldots, k_9$. The dynamically equivalent dense realization of the network is shown in Fig. A.4(b), where the 8 core and 4 non-core reactions are indicated separately. The three different sparse structures are shown in the subplots of Fig. A.5 The first subplot is identical to the original structure shown in Fig. A.4(a). This means that the mechanism cannot be described exactly with less than 9 reactions. It turns out from the second and third subplots that (at least mathematically), the degradation of mRNA is dynamically not a necessary element of the model. However, the biological plausibility of the mathematically possible structures and reactions always has to be carefully examined.

As it is expected, the possible structures of sparse/dense realizations and the corresponding core and non-core reactions can change with the modification of parameter values. This is illustrated in Fig. A.6(a), where the following randomly generated parameter values were used:

$$k_1 = 18.9,\ k_2 = 7.1,\ k_3 = 15.4,\ k_4 = 12.7,\ k_5 = 10.6,\ k_6 = 3.5,$$
$$k_7 = 11.3,\ k_8 = 9.1,\ k_9 = 4.0. \tag{A.24}$$

It is visible that the structure of the dense realization is the same as in Fig. A.4(b) but the core reactions are different from the ones shown there. Here the degradation of mRNA is described by a core reaction but interestingly, the reaction corresponding to translation is not a core one. Naturally, this implies that the possible sparse realization structures with the second parametrization are different from the ones shown in Fig. A.5. Note that here the only goal was to illustrate the possible change of core and non-core reactions, and therefore the biological relevance of the parameter values in eq. (A.24) is not assumed in this case.

In the next step, let us assume that another complex, namely $X_2 + X_4$ is allowed in the model (again not necessarily assuming biological meaningfullness in this particular case). With the addition of this new complex, the stoichiometric matrix of the system can be written as

$$Y' = \begin{bmatrix} 2 & 1 & 1 & 0 & 0 & 0 & 0 & 0 & 0 & 0 & 0 & 0 \\ 0 & 0 & 0 & 1 & 1 & 0 & 0 & 0 & 0 & 0 & 0 & 1 \\ 0 & 0 & 0 & 1 & 0 & 1 & 1 & 0 & 0 & 0 & 0 & 0 \\ 0 & 0 & 0 & 0 & 0 & 0 & 0 & 1 & 1 & 0 & 0 & 1 \\ 0 & 1 & 0 & 0 & 0 & 1 & 0 & 1 & 0 & 1 & 0 & 0 \end{bmatrix}. \tag{A.25}$$

The dense CRN realization of the dynamics (A.16)-(A.20) with the updated $Y'$ matrix given in eq. (A.25) using the original parameters described in (A.23) is shown in Fig. A.6(b), where the core and non-core reactions are again indicated. It is apparent that now there are only 5 core reactions, and none of the remaining 12 reactions are essential to realize the dynamics (A.16)-(A.20). This means that the introduction of a new complex increased the flexibility of the network (i.e. mathematically, the majority of the reactions can be substituted by other ones and the network still maintains its original dynamics). Of course, not any combination of the non-core reactions can be omitted from the network, because the sparse realizations show that at least 9 reactions are needed to keep dynamical equivalence. It can be computed easily that the theoretical maximum number of sparse realizations with different structures is $\binom{12}{17-9} = 495$. However, as the numerical experiments show, majority of these structures do not give a practically feasible dynamically equivalent realization.

The above results clearly show that certain mechanisms may remain undetectable (or they are falsely detected) even if we have complete species concentration measurements and full information about possible complex formation, that are not very realistic assumptions. Moreover, the sparsest dynamically equivalent structure of mass-action models is not unique, therefore sparsity enforcing approaches for determining "true" reaction structures are not enough in themselves without the necessary amount of prior information given in the form of additional constraints.

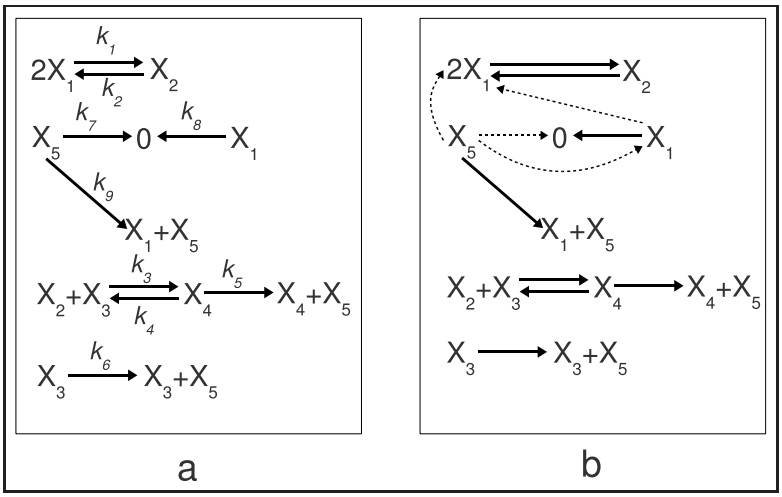


Figure A.4: Positive feedback motif: original reaction graph and dense realization structure. (a) This subfigure shows the reaction graph of a gene regulation network model with positive feedback used in Example A.2.3. (b) This subfigure shows all the mathematically possible reactions that can result in the same dynamical behaviour as the original biologically meaningful network shown in subfigure (a). The core-reactions in the dense realization are shown with solid arrows, while the non-core reactions are indicated with dashed arrows.

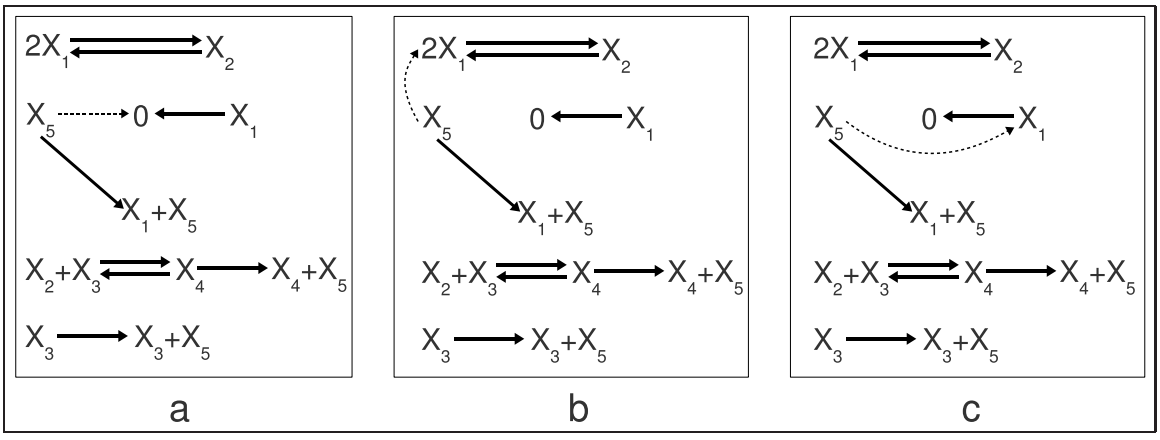


Figure A.5: Sparse realization structures for the positive feedback motif. Three different dynamically equivalent structures can be given for the positive feedback motif with the minimal number of reactions. The core and non-core reactions are indicated in the same way as in Fig. A.4(b).

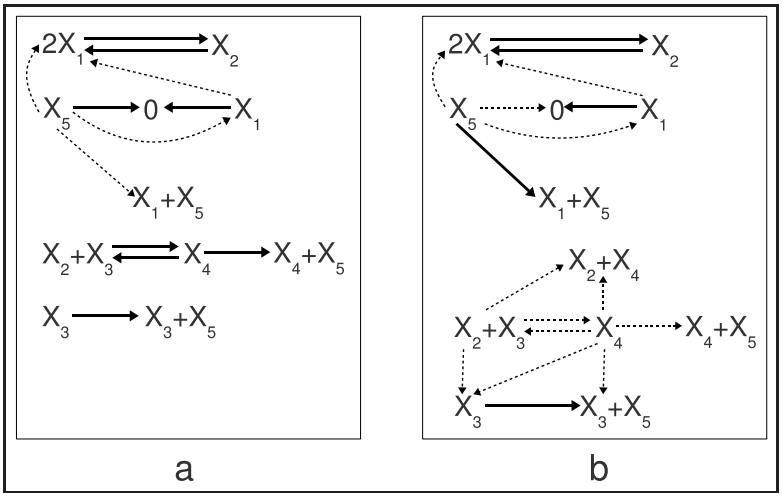


Figure A.6: The effect of modifying the complex set and the parameters. (a) The core and non-core reactions of the dense realization of the positive feedback motif are shown in this subfigure with a randomly selected parametrization that is different from the initial one. (b) The core and non-core reactions of the dense realization of the positive feedback motif can be seen in this subfigure when an additional complex $X_2 + X_4$ is involved into the model.

# References


[1] M.J. Ablowitz, A. Ramani, and H. Segur. A connection between nonlinear evolution equations and ordinary differential equations of P-type I. *Journal of Mathematical Physics*, 21:715–721, 1980.

[2] U. Alon. *An Introduction to Systems Biology: Design Principles of Biological Circuits*. Chapman & Hall, CRC, 2007.

[3] D. F. Anderson. Boundedness of trajectories for weakly reversible, single linkage class reaction systems. *Journal of Mathematical Chemistry*, accepted:to appear, 2011. DOI: 10.1007/s10910-011-9886-4.

[4] D. F. Anderson. A proof of the Global Attractor Conjecture in the single linkage class case. *SIAM Journal on Applied Mathematics*, accepted:to appear, 2011. http://arxiv.org/abs/1101.0761.

[5] D. Angeli. A tutorial on chemical network dynamics. *European Journal of Control*, 15:398–406, 2009.

[6] V. I. Arnold, K. Vogtmann (Translator), and A. Weinstein (Translator). *Mathematical Methods of Classical Mechanics (Graduate Texts in Mathematics)*. Springer, 1989.

[7] C. Aykanat and A. Pinar. Permuting sparse rectangular matrices into block-diagonal form. *SIAM Journal on Scientific Computing*, 25:1860–1879, 2004.

[8] V. Balakrishnan and E. F. (Eds.). Linear matrix inequalities in control theory and applications. special issue of the International Journal of Robust and Nonlinear Control, 1996. vol. 6, no. 9/10, pp. 896-1099.

[9] J. Bang-Jensen and G. Gutin. *Digraphs: Theory, Algorithms and Applications*. Springer, 2001.

[10] J. R. Banga. Optimization in computational systems biology. *BMC Systems Biology*, 2:47–54, 2008.

[11] G. Belov. On linear programming approach for the calculation of chemical equilibrium in complex thermodynamic systems. *Journal of Mathematical Chemistry*, 47:446–456, 2010.

[12] A. Bemporad and M. Morari. Control of systems integrating logic, dynamics, and constraints. *Automatica*, 35:407–427, 1999.

[13] R. Bhatia. *Matrix Analysis*. Springer Verlag, New York, Berlin, 1996.

[14] S. Boyd, L. El-Ghaoui, E. Feron, and V. Balakrishnan. *Linear Matrix Inequalities in Systems and Control Theory*. SIAM Books, Philadelphia, PA, 1994.

[15] S. Boyd and L Vandenberghe. *Convex Optimization*. Cambridge University Press, 2004.

[16] L. Brenig. Complete factorisation and analytic solutions of generalized Lotka-Volterra equations. *Physics Letters A*, 133:378–382, 1988.

[17] L. Brenig and A. Goriely. Universal canonical forms for the time-continuous dynamical systems. *Phys. Rev. A*, 40:4119–4122, 1989.

[18] H. B. Callen. *Thermodynamics and an introduction to thermostatistics*. John Wiley and Sons, New York, 1980.

[19] Y.-Y. Cao, J. Lam, and Y.-X. Sun. Static output feedback stabilization: An ILMI approach. *Automatica*, 12:1641–1645, 1998.

[20] M. Chaves. Input-to-state stability of rate-controlled biochemical networks. *SIAM Journal on Control and Optimization*, 44:704–727, 2005.

[21] M. Chaves and E. D. Sontag. State-estimators for chemical reaction networks

of Feinberg-Horn-Jackson zero deficiency type. *European Journal of Control*, 8:343–359, 2002.

[22] V. Chellaboina, S. P. Bhat, W. M. Haddad, and D. S. Bernstein. Modeling and analysis of mass-action kinetics – nonnegativity, realizability, reducibility, and semistability. *IEEE Control Systems Magazine*, 29:60–78, 2009.

[23] D. Cheng, T. Shen, and T.J. Tarn. Pseudo-Hamiltonian realization and its application. *Communications in Information and Systems*, 2:91–120, 2002.

[24] L. O. Chua. Stationary principles and potential functions for nonlinear networks. *Journal of the Franklin Institute*, 296:91–114, 1973.

[25] G. Craciun, A. Dickenstein, A. Shiu, and B. Sturmfels. Toric dynamical systems. *Journal of Symbolic Computation*, 44:1551–1565, 2009.

[26] G. Craciun and M. Feinberg. Multiple equilibria in complex chemical reaction networks: I. The injectivity property. *SIAM Journal on Applied Mathematics*, 65 (5):1526–1546, 2005.

[27] G. Craciun and M. Feinberg. Multiple equilibria in complex chemical reaction networks: II. The species-reaction graph. *SIAM Journal on Applied Mathematics*, 66 (4):1321–1338, 2006.

[28] G. Craciun and C. Pantea. Identifiability of chemical reaction networks. *Journal of Mathematical Chemistry*, 44:244–259, 2008.

[29] G. Craciun, Y. Tang, and M. Feinberg. Understanding bistability in complex enzyme-driven reaction networks. *Proc. of the National Academy of Sciences of the USA*, 103 (23):8697–8702, 2006.

[30] T. Csendes. Interval analysis and verification of mathematical models. In P. Baveye, J. Mysiak, and M. Laba, editors, *Uncertainties in Environmental Modelling and Consequences for Policy Making*, pages 79–100. Springer, 2009.

[31] A. Császár, L. Jicsinszky, and T. Turányi. Generation of model reactions leading to limit cycle behaviour. *Reaction Kinetics and Catalysis Letters*, 18:65–71, 1981.

[32] A. Császár, P. Érdi, L. Jicsinszky, J. Tóth, and T. Turányi. Several exact results on deterministic exotic kinetics. *Zeitschrift für Physikalische Chemie - Leipzig*, 264:449–463, 1983.

[33] G. B. Dantzig. Maximization of a linear function of variables subject to linear inequalities. In *Activity Analysis of Production and Allocation*, pages 339–347. Wiley & Chapman-Hall, 1947.

[34] G. B. Dantzig and M. N. Thapa. *Linear programming 1: Introduction*. Springer-Verlag, 1997.

[35] G. B. Dantzig and M. N. Thapa. *Linear Programming 2: Theory and Extensions*. Springer-Verlag, 2003.

[36] A. Dickenstein and M. P. Millan. How far is complex balancing from detailed balancing? Technical report, arXiv:1001.0947v1 [math.DS], 2010. http://arxiv.org/pdf/1001.0947v1.

[37] T. De Donder. *Thermodynamic Theory of Affinity: A Book of Principles*. Oxford University Press, 1936.

[38] D. L. Donoho. For most large undetermined systems of linear equations the minimal l1-norm solution is also the sparsest solution. *Communications on Pure and Applied Mathematics*, 59(7):903–934, 2006.

[39] D. L. Donoho and J. Tanner. Sparse nonnegative solution of underdetermined linear equations by linear programming. *Proc. of the National Academy of Sciences of the USA (PNAS)*, 102(27):9446–9451, 2005.

[40] R. Díaz-Sierra, B. Hernández-Bermejo, and V. Fairén. Graph-theoretic description of the interplay between non-linearity and connectivity in biological systems. *Mathematical Biosciences*, 156:229–253, 1999.

[41] D. Eberard, B. M. Maschke, and A. J. van der Schaft. Energy-conserving formulation of RLC-circuits with linear resistors. In *17th International Symposium on Mathematical Theory of Networks and Systems*, pages 71–76, 2006.

[42] I. R. Epstein and J. A. Pojman. *An Introduction to Nonlinear Chemical Dynamics: Oscillations, Waves,Patterns and Chaos (Topics in Physical Chemistry)*. Oxford University Press, 1998.

[43] L. T. Fan, B. Bertók, and F. Friedler. A graph-theoretic method to identify candidate mechanisms for deriving the rate law of a catalytic reaction. *Computers and Chemistry*, 26:265–292, 2002.

[44] L. Farina and S. Rinaldi. *Positive Linear Systems: Theory and Applications*. Wiley, 2000.

[45] Gy. Farkas. Local controllability of reactions. *Journal of Mathematical Chemistry*, 24:1–14, 1998.

[46] Gy. Farkas. On local observability of chemical systems. *Journal of Mathematical Chemistry*, 24:15–22, 1998.

[47] Gy. Farkas. Kinetic lumping schemes. *Chemical Engineering Science*, 54:3909–3915, 1999.

[48] M. Feinberg. Complex balancing in general kinetic systems. *Archive for Rational Mechanics and Analysis*, 49:187–194, 1972.

[49] M. Feinberg. *Lectures on chemical reaction networks*. Notes of lectures given at the Mathematics Research Center, University of Wisconsin, 1979.

[50] M. Feinberg. Chemical reaction network structure and the stability of complex isothermal reactors - I. The deficiency zero and deficiency one theorems. *Chemical Engineering Science*, 42 (10):2229–2268, 1987.

[51] M. Feinberg. Necessary and sufficient conditions for detailed balancing in mass action systems of arbitrary complexity. *Chemical Engineering Science*, 44:1819–1827, 1989.

[52] A. Figueiredo, T.M. Rocha Filho, and L. Brenig. Algebraic structures and invariant manifolds of differential systems. *Journal of Mathematical Physics*, 39:2929–2946, 1998.

[53] A. Figueiredo, T.M. Rocha Filho, and L. Brenig. Necessary conditions for the existence of quasi-polynomial invariants: the quasi-polynomial and Lotka-Volterra systems. *Physica A*, 262:158–180, 1999.

[54] A. Figueiredo, I. M. Gleria, and T. M. Rocha Filho. Boundedness of solutions and Lyapunov functions in quasi-polynomial systems. *Physics Letters A*, 268:335–341, 2000.

[55] T.M. Rocha Filho, A. Figueiredo, and L. Brenig. QPSI: A Maple package for the determination of quasi-polynomial symmetries and invariants. *Computer Physics Communications*, 117:263–272, 1999.

[56] T. M. Rocha Fliho, I. M. Gléria, A. Figueiredo, and L. Brenig. The Lotka-Volterra canonical format. *Ecological Modelling*, 183:95–106, 2005.

[57] C. A. Floudas. *Deterministic Global Optimization: Theory, Methods and Applications*. Kluwer, 2010.

[58] C. A. Floudas, I. G. Akrotirianakis, S. Caratzoulas, C. A. Meyer, and J. Kallrath. Global optimization in the 21st century: Advances and challenges. *Computers*

*and Chemical Engineering*, 29:1185–1202, 2005.

[59] C.A. Floudas. *Nonlinear and mixed-integer optimization.* Oxford University Press, 1995.

[60] F. Friedler, L. T. Fan, and B. Imreh. Process network synthesis: problem definition. *Networks*, 31:119–124, 1998.

[61] F. Friedler, K. Tarján, Y. W. Huang, and L. T. Fan. Graph-theoretic approach to process synthesis: axioms and theorems. *Chemical Engineering Science*, 47:1973–1988, 1992.

[62] F. Friedler, K. Tarján, Y. W. Huang, and L. T. Fan. Graph-theoretic approach to process synthesis: polynomial algorithm for maximal structure generation. *Computer and Chemical Engineering*, 17:929–942, 1993.

[63] K. Gatermann and B. Huber. A family of sparse polynomial systems arising in chemical reaction systems. *Journal of Symbolic Computation*, 33:275–305, 2002.

[64] J. C. Geromel. On the determination of a diagonal solution of the Lyapunov equation. *IEEE Transactions on Automatic Control*, AC-30:404–406, 1985.

[65] I. M. Gléria, A. Figueiredo, and T. M. Rocha Filho. Stability properties of a general class of nonlinear dynamical systems. *Journal of Physics A - Mathematical and General*, 34:3561–3575, 2001.

[66] I.M. Gléria, A. Figueiredo, and T.M. Rocha Filho. A numerical method for the stability analysis of quasi-polynomial vector fields. *Nonlinear Analysis*, 52:329–342, 2003.

[67] V. Gopal and L. T. Biegler. Nonsmooth dynamic simulation with linear programming based methods. *Computers and Chemical Engineeering*, 21:675–689, 1997.

[68] A.N. Gorban and I.V. Karlin. Method of invariant manifold for chemical kinetics. *Chemical Engineering Science*, 58:4751–4768, 2003.

[69] A.N. Gorban, I.V. Karlin, and A.Y. Zinovyev. Invariant grids for reaction kinetics. *Physica A*, 33:106–154, 2004.

[70] I. E. Grossmann, editor. *Global Optimization in Engineering Design.* Kluwer, 2010.

[71] I. E. Grossmann and J. Santibanez. Applications of mixed integer linear programming in process synthesis. *Computers and Chemical Engineering*, 4:205, 1980.

[72] J. Gunawardena. Chemical reaction network theory for in-silico biologists. Technical report, Bauer Center for Genomics Research, Harvard University, 2003. http://vcp.med.harvard.edu/papers/crnt.pdf.

[73] J. Haag, A. Wouver, and P. Bogaerts. Dynamic modeling of complex biological systems: a link between metabolic and macroscopic description. *Mathematical Biosciences*, 193:25–49, 2005.

[74] W. M. Haddad, VS. Chellaboina, and Q. Hui. *Nonnegative and Compartmental Dynamical Systems.* Princeton University Press, 2010.

[75] K.M. Hangos and I.T. Cameron. *Process Modelling and Model Analysis.* Academic Press, London, 2001.

[76] B. Hernández-Bermejo and V. Fairén. Nonpolynomial vector fields under the Lotka-Volterra normal form. *Physics Letters A*, 206:31–37, 1995.

[77] B. Hernández-Bermejo and V. Fairén. Lotka-Volterra representation of general nonlinear systems. *Math. Biosci.*, 140:1–32, 1997.

[78] B. Hernández-Bermejo and V. Fairén. Hamiltonian structure and Darboux theo-

rem for families of generalized Lotka-Volterra systems. *Journal of Mathematical Physics*, 39:6162–6174, 1998.

[79] B. Hernandez-Bermejo, V. Fairén, and L. Brenig. Algebraic recasting of nonlinear systems of ODEs into universal formats. *Journal of Physics A - Mathematical and General*, 31:2415–2430, 1998.

[80] B. Hernández-Bermejo and L. Brenig. Quasipolynomial generalization of Lotka-Volterra mappings. *Journal of Physics A - Mathematical and General*, 35:5453–5469, 2002.

[81] K. Homlström, M.M. Edvall, and A.O. Göran. TOMLAB for large-scale robust optimization. In *Nordic MATLAB Conference*, 2003.

[82] F. Horn. Necessary and sufficient conditions for complex balancing in chemical kinetics. *Archive for Rational Mechanics and Analysis*, 49:172–186, 1972.

[83] F. Horn and R. Jackson. General mass action kinetics. *Archive for Rational Mechanics and Analysis*, 47:81–116, 1972.

[84] N. Hudon and M. Guay. Local dissipative Hamiltonian realization by feedback regulation. In *49th IEEE Conference on Decision and Control, CDC 2010*, pages 5930–5935, 2010.

[85] N. Hudon, K. Hoeffner, and M. Guay. Equivalence to dissipative Hamiltonian realization. In *Proc. of the 47th IEEE Conference on Decision and Control,*, pages 3163–3168, 2008.

[86] V. Hárs and J. Tóth. On the inverse problem of reaction kinetics. In M. Farkas and L. Hatvani, editors, *Qualitative Theory of Differential Equations*, volume 30 of *Coll. Math. Soc. J. Bolyai*, pages 363–379. North-Holland, Amsterdam, 1981.

[87] A. Isidori. *Nonlinear Control Systems*. Springer, Berlin, 1999.

[88] D. Jeltsema and J. M. A. Scherpen. A dual relation between port-controlled Hamiltonian systems and the Brayton-Moser equations for nonlinear switched RLC networks. *Automatica*, 39:969–979, 2003.

[89] D. Jeltsema and J. M. A. Scherpen. Multidomain modeling of nonlinear networks and systems. *IEEE Control Systems Magazine*, 29:28–59, 2009.

[90] R.D. Braatz J.G. VanAntwerp. A tutorial on linear and bilinear matrix inequalities. *Journal of Process Control*, 10:363–385, 2000.

[91] M. D. Johnston and D. Siegel. Linear conjugacy of chemical reaction networks. *Journal of Mathematical Chemistry*, 49:1263–1282, 2011.

[92] M. Kargar, H. Poormohammadi, L. Pirhaji, M. Sadeghi, H. Pezeshk, and C. Eslahchi. Enhanced evolutionary and heuristic algorithms for haplotype reconstruction problem using minimum error correction model. *MATCH Communications in Mathematical and in Computer Chemistry*, 62(2):261–274, 2009.

[93] E. Kaszkurewicz and A. Bhaya. *Matrix Diagonal Stability in Systems and Computation*. Birkhauser, Boston, 2000.

[94] S. Kauchali, W. C. Rooney, L. T. Biegler, D. Glasser, and D. Hildebrandt. Linear programming formulations for attainable region analysis. *Chemical Engineering Science*, 57:2015–2028, 2002.

[95] H. K. Khalil. On the existence of positive diagonal $P$ such that $PA + A^T P < 0$. *IEEE Transactions on Automatic Control*, AC-27:181–184, 1982.

[96] J.A. Klein, D.T. Wu, and R. Gani. Computer aided mixture design with specified property constraints. *Computers and Chemical Engineering*, 16:S229–S236, 1992.

[97] M. Kocvara and M. Stingl. A code for convex nonlinear and semidefinite programming. *Optimization Methods and Software*, 8:317–333, 2003.

[98] M. Kocvara and M. Stingl. TOMLAB/PENBMI solver (Matlab Toolbox), 2005. PENOPT Gbr.

[99] K. Kovács, B. Vizvári, M. Riedel, and J. Tóth. Decomposition of the permanganate/oxalic acid overall reaction to elementary steps based on integer programming theory. *Physical Chemistry, Chemical Physics*, 6:1236–1242, 2004.

[100] Z. Kovács, Z. Ercsey, F. Friedler, and L. T. Fan. Separation-network synthesis: global optimum through rigorous super-structure. *Computers and Chemical Engineering*, 24:1881–1900, 2000.

[101] F. J. Krambeck. The mathematical structure of chemical kinetics in homogeneous single-phase systems. *Archive for Rational Mechanics and Analysis*, 38:317–347, 1970.

[102] M. Kvasnica, P. Grieder, and M. Baotić. Multi-Parametric Toolbox (MPT), 2004.

[103] S. Labruine and R. Conte. A geometrical method towards first integrals for dynamical systems. *Journal of Mathematical Physics*, 37:6198–6206, 1996.

[104] P. De Leenheer and D. Aeyels. Stabilization of positive systems with first integrals. *Automatica*, 38:1583–1589, 2002.

[105] G. Li, H. Rabitz, and J. Tóth. A general analysis of nonlinear lumping in chemical kinetics. *Chemical Engineering Science*, 49:343–361, 1994.

[106] G. Li, A. S. Tomlin, H. Rabitz, and J. Tóth. Determination of approximate lumping schemes by a singular perturbation method. *Journal of Chemical Physics*, 99:3562–3574, 1993.

[107] H. Liang, H. Tong, and FS. Bai. Computing the permanental polynomial of C-60 in parallel. *MATCH Communications in Mathematical and in Computer Chemistry*, 60(2):349–358, 2008.

[108] Y-C. Lin, L. T. Fan, S. Shafie, B. Bertók, and F. Friedler. Graph-theoretic approach to the catalytic-pathway identification of methanol decomposition. *Computers and Chemical Engineering*, 34:821–824, 2010.

[109] F. Llaneras and J. Picó. An interval approach for dealing with flux distributions and elementary modes activity patterns. *Journal of Theoretical Biology*, 246:290–308, 2007.

[110] J. Löfberg. Yalmip : A toolbox for modeling and optimization in MATLAB. In *Proceedings of the CACSD Conference*, Taipei, Taiwan, 2004.

[111] A. Makhorin. GLPK 4.9, 2006. http://www.gnu.org/software/glpk/glpk.html.

[112] G. Marlovits, M. Wittmann, Z. Noszticzius, and V. Gáspár. A new chemical oscillator in a novel open reactor - the CLO2-I-2-Acetone system in a membrane fed stirred tank reactors. *Journal of Physical Chemistry*, 99:5359–5364, 1995.

[113] I. Maros. *Computational Techniques of the Simplex Method*. Kluwer, 2003.

[114] B.M. Maschke, A.J. Van der Schaft, and P.C. Breedveld. An intrinsic Hamiltonian formulation of the dynamics of LC-circuits. *IEEE Transactions on Circuits and Systems*, CAS-42:73–82, 1995.

[115] R.I. McLachlan, G.R.W. Quispel, and N. Robidoux. Unified approach to Hamiltonian systems, Poisson systems, gradient systems and systems with Lyapunov functions or first integrals. *Physical Review Letters*, 81:2399–2403, 1998.

[116] Y. Mileyko, R. I. Joh, and J. S. Weitz. Small-scale copy number variation and large-scale changes in gene expression. *Proceedings of the National Academy of Sciences of the United States of America*, 105:16659–16664, 2008.

[117] Y. Moreau, S. Louies, J. Vandewalle, and L. Brenig. Embedding recurrent neural

networks into predator-prey models. *Neural Networks*, 12:237–245, 1999.

[118] I. Nagy, B. Kovács, and J. Tóth. Detailed balance in ion channels: application of Feinberg's theorem. *React. Kinet. Catal. Lett.*, 96:263–267, 2009.

[119] G. L. Nemhauser and L. A. Wolsey. *Integer and Combinatorial Optimization*. John Wiley & Sons, 1999.

[120] G. Nicolis and C. Nicolis. Thermodynamic dissipation versus dynamical complexity. *Journal of Chemical Physics*, 18:8889–8898, 1999.

[121] G. Nicolis and I. Prigogine. *Self-organization in Nonequilibrium Systems: From Dissipative Structures to Order through Fluctuations*. John Wiley & sons, New York, 1977.

[122] Z. Noszticzius and J. Bódiss. Contribution to the chemistry of the Belousov-Zhabotinskii (BZ) type reactions. *Berichte der Bunsen-Gesellschaft - Physical Chemistry Chemical Physics*, 84:366–369, 1980.

[123] E. Nuutila and E. Soisalon-Soininen. On finding the strongly connected components in a directed graph. *Information Processing Letters*, 49:9–14, 1994.

[124] R. Ortega, A. Loría, P. J. Nicklasson, and H. Síra-Ramírez. *Passivity-Based Control of Euler-Lagrange Systems: Mechanical, Electrical and Electromechanical Applications*. Springer-Verlag, 1998.

[125] S. A. Papoulias and I. E. Grossmann. A structural optimization approach in process synthesis-I. Utility systems. *Computers and Chemical Engineering*, 7:695–706, 1983.

[126] S. A. Papoulias and I. E. Grossmann. A structural optimization approach in process synthesis-II. Heat recovery networks. *Computers and Chemical Engineering*, 7:707–721, 1983.

[127] S. A. Papoulias and I. E. Grossmann. A structural optimization approach in process synthesis-III. Total processing systems. *Computers and Chemical Engineering*, 7:723–734, 1983.

[128] S. Prajna, A. J. van der Schaft, and G. Meinsma. An LMI approach to stabilization of linear port-controlled Hamiltonian systems. *Systems and Control Letters*, 45:371–385, 2002.

[129] V. V. Prasolov. *Problems and Theorems in Linear Algebraic*. American Mathematical Society, 1996.

[130] R. Raman and I. E. Grossmann. Integration of logic and heuristic knowledge in MINLP optimization for process synthesis. *Computers and Chemical Engineering*, 16(3):155–171, 1992.

[131] R. Raman and I.E. Grossmann. Relation between MILP modelling and logical inference for chemical process synthesis. *Computers and Chemical Engineering*, 15:73–84, 1991.

[132] R. Raman and I.E. Grossmann. Modelling and computational techniques for logic based integer programming. *Computers and Chemical Engineering*, 18:563–578, 1994.

[133] S. S. Rao. *Engineering Optimization - Theory and Practice*. Wiley-Interscience, 1996.

[134] C. Roos, T. Terlaky, and J. Vial. *Interior Point Methods for Linear Optimization*. Springer Science, 2006.

[135] N. Samardzija, L. D. Greller, and E. Wassermann. Nonlinear chemical kinetic schemes derived from mechanical and electrical dynamical systems. *Journal of Chemical Physics*, 90 (4):2296–2304, 1989.

[136] C. Scherer and S. Weiland. *Linear Matrix Inequalities in Control*. DISC, http://www.er.ele.tue.nl/sweiland/lmi.pdf, 2000.

[137] E. Schrödinger. *What is Life? (with Mind and Matter and Autobiographical Sketches)*. Cambridge University Press, 1967.

[138] F. Schwartz. Symmetries of differential equations: from Sophus Lie to computer algebra. *SIAM Review*, 30:450–481, 1988.

[139] M. Sharir. A strong-connectivity algorithm and its application in data flow analysis. *Computers and Mathematics with Applications*, 7:67–72, 1981.

[140] A. Shiu. The smallest mass-preserving chemical reaction network. In *MBI: Mathematical and Computational Models in Biological Networks*, University of California, Berkeley, October 2008.

[141] D. Siegel and D. MacLean. Global stability of complex balanced mechanisms. *Journal of Mathematical Chemistry*, 27:89–110, 2000.

[142] S. Smale. On the mathematical foundations of electrical circuit theory. *Journal of Differential Geometry*, 7:193–210, 1972.

[143] E. Sontag. Structure and stability of certain chemical networks and applications to the kinetic proofreading model of T-cell receptor signal transduction. *IEEE Transactions on Automatic Control*, 46:1028–1047, 2001.

[144] E. D. Sontag. *Mathematical Control Theory: Deterministic and Finite Dimensional Systems*. Springer, 1998.

[145] E. Szádeczky-Kardoss and B. Kiss. On-line trajectory time-scaling to reduce tracking error. In *Intelligent Engineering Systems and Computational Cybernetics*, pages 3–14. Springer, 2009.

[146] Y. Takeuchi. *Global Dynamical Properties of Lotka-Volterra Systems*. World Scientific, Singapore, 1996.

[147] H.D. Tuan, P. Apkarian, and Y. Nakashima. A new Lagrangian dual global optimization algorithm for solving bilinear matrix inequalities. *International Journal of Robust and Nonlinear Control*, 10:561–578, 2000.

[148] J. Tóth, G. Li, H. Rabitz, and A. S. Tomlin. The effect of lumping and expanding on kinetic differential equations. *SIAM Journal on Applied Mathematics*, 57:1531–1556, 1997.

[149] Arjan van der Schaft. *L2-Gain and Passivity Techniques in Nonlinear Control*. Springer, Berlin, 2000.

[150] Y. Wang, C. Li, and D. Cheng. Generalized Hamiltonian realization of time-invariant nonlinear systems. *Automatica*, 39:1437–1443, 2003.

[151] A. Weinstein. The local structure of Poisson manifolds. *Journal of Differential Geometry*, 18:523–557, 1983.

[152] P. Wellstead. Systems biology and the spirit of Tustin. *IEEE Control Systems Magazine*, Feb.:57–71, 102, 2010.

[153] H. P. Williams. *Model building in mathematical programming*. Wiley, 1993.

[154] J. Yang, W. J. Bruno, W. S. Hlavacek, and J. E. Pearson. On imposing detailed balance in complex reaction mechanisms. *Biophysical Journal*, 91:1136–1141, 2006.

[155] P. Érdi and J. Tóth. *Mathematical Models of Chemical Reactions. Theory and Applications of Deterministic and Stochastic Models*. Manchester University Press, Princeton University Press, Manchester, Princeton, 1989.

[156] H.C. Öttinger. *Beyond Equilibrium Thermodynamics*. John Wiley & Sons, 2005.

# Publications of the author related to the thesis

[B1] K. M. Hangos, J. Bokor, and G. Szederkényi. *Analysis and Control of Nonlinear Process Systems*. Springer-Verlag, 2004.

[BC1] K. M. Hangos and G. Szederkényi. *In J. Bao and P. Lee. Process Control: The Passive Systems Approach*, chapter title "Process Control Based on Physically Inherent Passivity", pages 193–224. Advances in Industrial Control. Springer, 2007.

[BC2] G. Szederkényi, K. M. Hangos, and D. Csercsik. *In Coping with Complexity: Model Reduction and Data Analysis. A. N. Gorban and D. Roose (eds.)*, chapter title "Computing realizations of reaction kinetic systems with given properties", pages 253–268. Number 75 in Lecture Notes in Computational Science and Engineering. Springer, 2010.

[J1] K.M. Hangos, J. Bokor, and G. Szederkényi. Hamiltonian view of process systems. *AIChE Journal*, 47:1819–1831, 2001. IF: 1.793.

[J2] G. Szederkényi and K.M. Hangos. Global stability and quadratic Hamiltonian structure in Lotka-Volterra and quasi-polynomial systems. *Physics Letters A*, 324:437–445, 2004. IF: 1.454.

[J3] G. Szederkényi, K.M. Hangos, and A. Magyar. On the time-reparametrization of quasi-polynomial systems. *Physics Letters A*, 334:288–294, 2005. IF: 1.55.

[J4] I. Otero-Muras, G. Szederkényi, K.M. Hangos, and A.A. Alonso. Dynamic analysis and control of biochemical reaction networks. *Mathematics and Computers in Simulation*, 79:999–1009, 2007. IF: 0.93.

[J5] I. Otero-Muras, G. Szederkényi, A.A. Alonso, and K.M. Hangos. Local dissipative Hamiltonian description of reversible reaction networks. *Systems and Control Letters*, 57:554–560, 2008. IF: 2.073.

[J6] G. Szederkényi. Comment on "Identifiability of chemical reaction networks" by G. Craciun and C. Pantea. *Journal of Mathematical Chemistry*, 45:1172–1174, 2009. IF: 1.381.

[J7] G. Szederkényi. Computing sparse and dense realizations of reaction kinetic systems. *Journal of Mathematical Chemistry*, 47:551–568, 2010. IF: 1.259.

[J8] G. Szederkényi, K. M. Hangos, and T. Péni. Maximal and minimal realizations of reaction kinetic systems: Computation and properties. *MATCH Communications in Mathematical and in Computer Chemistry*, 65(2):309–332, 2011. IF: 3.29 (2010).

[J9] M. D. Johnston, D. Siegel, and G. Szederkényi. A linear programming approach to weak reversibility and linear conjugacy of chemical reaction networks. *Journal of Mathematical Chemistry*, accepted:to appear, 2011. IF: 1.259 (2010).

[J10] G. Szederkényi and K. M. Hangos. Finding complex balanced and detailed balanced realizations of chemical reaction networks. *Journal of Mathematical Chemistry*, 49:1163–1179, 2011. IF: 1.259 (2010).

[J11] G. Szederkényi, K. M. Hangos, and Zs. Tuza. Finding weakly reversible realizations of chemical reaction networks using optimization. *MATCH Communications in Mathematical and in Computer Chemistry*, 67:193–212, 2012. IF: 3.29 (2010).

[J12] G. Szederkényi, M. Kovács, and K. M. Hangos. Reachability of nonlinear fedbatch fermentation processes. *International Journal of Robust and Nonlinear Control*, 12:1109–1124, 2002. IF: 1.02.

[J13] G. Szederkényi, N. R. Kristensen, K. M. Hangos, and S. B. Jorgensen. Nonlinear analysis and control of a continuous fermentation process. *Computers and Chemical Engineering*, 26:659–670, 2002. IF: 0.784.

[J14] B. Pongrácz, G. Szederkényi, and K.M. Hangos. An algorithm for determining a class of invariants in quasi-polynomial systems. *Computer Physics Communications*, 175:204–211, 2006. IF: 1.595.

[J15] A. Magyar, G. Szederkényi, and K.M. Hangos. Globally stabilizing feedback control of process systems in generalized Lotka-Volterra form. *Journal of Process Control*, 18:80–91, 2008. IF: 1.606.

[J16] B. Pongrácz, P. Ailer, K. M. Hangos, and G. Szederkényi. Nonlinear reference tracking control of a gas turbine with load torque estimation. *International Journal of Adaptive Control and Signal Processing*, 22:757–773, 2008. IF: 1.4.

[J17] D. Csercsik, I. Farkas, G. Szederkényi, E. Hrabovszky, Z. Liposits, and K. M. Hangos. Hodgkin-Huxley type modelling and parameter estimation of GnRH neurons. *Biosystems*, 100:198–207, 2010. IF: 1.478.

[J18] D. Csercsik, G. Szederkényi, and K. M. Hangos. Parametric uniqueness of deficiency zero reaction networks. *Journal of Mathematical Chemistry*, accepted:to appear, 2011. DOI: 10.1007/s10910-011-9902-8, IF: 1.259 (2010).

[J19] D. Csercsik, K. M. Hangos, and G. Szederkényi. Identifiability analysis and parameter estimation of a single Hodgkin-Huxley type voltage dependent ion channel under voltage step measurement conditions. *Neurocomputing*, accepted:to appear, 2011. IF: 1.429 (2010).

[J20] K. M. Hangos and G. Szederkényi. Mass action realizations of reaction kinetic system models on various time scales. *Journal of Physics – Conference Series*, 268:012009/1–16, 2011.

[J21] D. Csercsik, G. Szederkényi, and K. M. Hangos. Modelling of rapid and slow transmission using the theory of reaction kinetic networks. *ERCIM News*, 82:22–23, 2010.

[C1] A. Magyar, G. Szederkényi, and K.M. Hangos. Quadratic stability of process systems in generalized Lotka-Volterra form. In *6th IFAC Symposium on Nonlinear Control Systems, NOLCOS 2004*, pages 357–362, Stuttgart, Germany, 2004.

[C2] B. Pongrácz, P. Ailer, G. Szederkényi, and K.M. Hangos. Stability of zero dynamics of a low power gas turbine. In *12th Mediterranean Control Conference on Control and Automation – MED'04*, pages 1–6 (on CD), Kusadasi, Turkey, 2004.

[C3] A. Magyar, G. Szederkényi, and K.M. Hangos. Quasi-polynomial system representation for the analysis and control of nonlinear systems. In P. Horacek, M. Simandl, and P. Zitek, editors, *Proc. of the 16th IFAC World Congress*, pages 1–6, paper ID: Tu–A22–TO/5, Prague, Czech Republic, 2005.

[C4] K.M. Hangos, G. Szederkényi, and I. Otero-Muras. Process control based on physical insight: passivity and hamiltonian system models. In J. Bokor and K.M. Hangos, editors, *Proceedings of the Workshop on System Identification and Control Systems*, pages 129–146. BME AVVC, Budapest, Hungary, 2006.

[C5] I. Otero-Muras, G. Szederkényi, A.A. Alonso, and K.M. Hangos. Dynamic analysis and control of chemical and biochemical reaction networks. In *International Symposium on Advanced Control of Chemical Processes - ADCHEM 2006*, pages 165–170, Gramado, Brazil, 2006.

[C6] I. Otero-Muras, G. Szederkényi, K.M. Hangos, and A.A. Alonso. Dynamic anal-

ysis and control of biochemical reaction networks. In *5th Vienna International Conference on Mathematical Modelling - MATHMOD 2006*, pages 4.1–4.10, Vienna, Austria, 2006.

[C7] A. Magyar, G. Szederkényi, and K. M. Hangos. Control of mass action law based reaction networks. In *Proceedings of the 16th International Conference on Process Control*, pages 1–6 (on CD), Strbske Pleso, Slovakia, 2007.

[C8] K. M. Hangos and G. Szederkényi. Special positive systems: the QP and the reaction kinetic system class. In K. M. Hangos and L. Nádai, editors, *Proceedings of the Workshop on Systems and Control Theory in honor of József Bokor on his 60th birthday*, pages 121–139, Budapest, Hungary, 2009. BME AVVC, MTA-SZTAKI.

[C9] G. Szederkényi. Computing reaction kinetic realizations of positive nonlinear systems using mixed integer programming. In *8th IFAC Symposium on Nonlinear Control Systems - NOLCOS 2010*, pages 1–6 (on CD), Bologna, Italy, 2010.

[C10] G. Szederkényi. Dynamically equivalent reaction networks: a computational point of view. In *8th European Conference on Mathematical and Theoretical Biology, and Annual Meeting of The Society for Mathematical Biology, Kraków, Poland*, Kraków, Poland, 2011. (invited lecture with abstract).

[C11] D. Csercsik, G. Szederkényi, K. M. Hangos, and I. Farkas. Model synthesis and identification of a Hodgkin-Huxley-type GnRH neuron model. In *Proceedings of the 10th European Control Conference*, pages 3058–3063, Budapest, Hungary, 2009. ISBN: 978-963-311-369-1.

[C12] D. Csercsik, G. Szederkényi, K. M. Hangos, and I. Farkas. Dynamical modeling and identification of a GnRH neuron. In *7th IFAC Symposium on Modelling and Control in Biomedical Systems*, pages 437–442, Aalborg, Denmark, 12-14 August 2009. IFAC.

[C13] D. Csercsik, G. Szederkényi, and K. M. Hangos. Identifiability of a Hodgkin-Huxley type ion channel under voltage step measurement conditions. In M. Kothare, M. Tade, A. Vande Wouwer, and I. Smets, editors, *9th International Symposium on Dynamics and Control of Process Systems - DYCOPS 2010*, pages 318–323, Leuven, Belgium, 2010. IFAC. no. MoAT3.4.

# The author's additional main publications

[J22] Cs. Fazekas, G. Szederkényi, and K.M. Hangos. Parameter estimation of a simple primary circuit model of a VVER plant. *IEEE Transactions on Nuclear Science*, 55(5):2643–2653, 2008. IF: 1.518.

[J23] Cs. Fazekas, G. Szederkényi, and K.M. Hangos. A simple dynamic model of the primary circuit in VVER plants for controller design purposes. *Nuclear Engineering and Design*, 237:1071–1087, 2007. IF: 0.446.

[J24] A. Gábor, C. Fazekas, G. Szederkényi, and K. M. Hangos. Modeling and identification of a nuclear reactor with temperature effects and Xenon posioning. *European Journal of Control*, 17:104–115, 2011. IF: 0.67 (2010).

[J25] P. Gáspár, Z. Szabó, G. Szederkényi, and J. Bokor. Design of a two-level controller for an active suspension system. *Asian Journal of Control*, accepted:available online, 2011. IF: 0.578 (2010).

[J26] K.M. Hangos, G. Szederkényi, and Zs. Tuza. The effect of model simplification assumptions on the differential index of lumped process models. *Computers and Chemical Engineering*, 28:129–137, 2004. IF: 1.678.

[J27] Z. Szabó, G. Szederkényi, P. Gáspár, I. Varga, K. M. Hangos, and J. Bokor. Identification and dynamic inversion-based control of a pressurizer at the Paks NPP. *Control Engineering Practice*, 18:554–565, 2010. IF: 1.4.

[J28] Sz. Rozgonyi, K. M. Hangos, and G. Szederkényi. Determining the domain of attraction of hybrid non-linear systems using maximal Lyapunov functions. *Kybernetika*, 46:19–37, 2010. IF: 0.445.

[J29] K.M. Hangos and G. Szederkényi. Process systems: theory and applications from different aspects. *ERCIM News*, no. 56.:35–36, 2004.

[J30] T. Péni and G. Szederkényi. Model predictive control for the hybrid primary circuit dynamics of a pressurized water nuclear power plant. *Periodica Polytechnica Electrical Engineering*, 53:37–44, 2009.

[J31] T. Péni, I. Varga, G. Szederkényi, and J. Bokor. Robust model predictive control with state estimation for an industrial pressurizer system. *Hungarian Journal of Industrial Chemistry*, 33:89–96, 2005.

[J32] G. Stikkel and G. Szederkényi. Meddig teszteljünk? *Híradástechnika*, 58:36–41, 2003.

[C14] Cs. Fazekas, G. Szederkényi, and K.M. Hangos. Model identification of the primary circuit at the Paks Nuclear Power Plant. In *26th IASTED International Conference on Modeling, Identification, and Control - MIC 2007*, pages 464–469, Innsbruck, Austria, 2007. Acta Press.

[C15] Cs. Fazekas, G. Szederkényi, and K.M. Hangos. Identification of the primary circuit dynamics in a pressurized water nuclear power plant. In *17th IFAC World Congress*, pages 10640–10645, Seoul, Korea, 2008.

[C16] P. Gáspár, Z. Szabó, G. Szederkényi, and J. Bokor. Two-level controller design for an active suspension system. In *16th Mediterranean Conference on Control and Automation, MED'08*, pages 439–444, Ajaccio, Corsica, France, 2008.

[C17] P. Gáspár and G. Szederkényi. Combined LPV and nonlinear control of an active suspension system. In *Proc. of the 2007 IEEE International Symposium on Industrial Electronics (ISIE2007)*, pages 215–220, Vigo, Spain, 2007.

[C18] P. Gáspár, G. Szederkényi, Z. Szabó, and J. Bokor. The design of a two-level controller for suspension systems. In *17th IFAC World Congress*, pages 3386–3391, Seoul, Korea, 2008.

[C19] E. Németh, Cs. Fazekas, G. Szederkényi, and K.M. Hangos. Modeling and simulation of the primary circuit of the Paks nuclear power plant for control and diagnosis. In *6th EUROSIM Congress on Modelling and Simulation*, pages 1–6 (on CD), Ljubljana, Slovenia, 2007.

[C20] T. Péni, G. Szederkényi, and J. Bokor. Model predictive control of the hybrid primary circuit dynamics in a pressurized water nuclear power plant. In *Proc. of the European Control Conference (ECC 2007)*, pages 5361–5367, Kos, Greece, 2007.

[C21] T. Péni, G. Szederkényi, J. Bokor, and K.M. Hangos. Dynamic inversion based velocity tracking control of road vehicles. In *6th IFAC Symposium on Nonlinear Control Systems, NOLCOS 2004*, pages 1199–1204, Stuttgart, Germany, 2004.

[C22] T. Péni, I. Varga, G. Szederkényi, and J. Bokor. Robust model predictive control of a nuclear power plant pressurizer subsystem. In *25th IASTED International Conference, Modeling, Identification, and Control - MIC 2006*, pages 167–172, Lanzarote, Spain, 2006.

[C23] G. Szederkényi. Design and implementation of the primary loop pressure con-

troller in the Paks Nuclear Power Plant. In *NSF Workshop on Real Time Control of Hybrid Systems*, Budapest, Hungary, 2007. (invited lecture).

[C24] G. Szederkényi. Identifiability study of a pressurizer in a pressurized water nuclear power plant. In *10th European Control Conference - ECC'09*, pages 3503–3508, 2009.

[C25] G. Szederkényi, T. Péni, P. Gáspár, and J. Bokor. Networked control approaches for a nuclear power plant pressurizer subsystem. In *1st IFAC Workshop on Estimation and Control of Networked Systems*, pages 1–6 (on CD), paper no. FrGT1.4, Venice, Italy, 2009.

[C26] G. Szederkényi, Z. Szabó, J. Bokor, and K.M. Hangos. Analysis of the networked implementation of the primary circuit pressurizer controller at a nuclear power plant. In *16th Mediterranean Conference on Control and Automation, MED'08*, pages 1604–1609, Ajaccio, Corsica, France, 2008.

[C27] I. Varga, G. Szederkényi, P. Gáspár, and J. Bokor. Implementation of dynamic inversion-based control of a pressurizer at the Paks NPP. In *2008 IEEE Multi-conference on Systems and Control*, San Antonio, Texas, USA, 2008.

[C28] I. Varga, G. Szederkényi, K.M. Hangos, and J. Bokor. Modeling and model identification of a pressurizer at the Paks nuclear power plant. In *14th IFAC Symposium on System Identification – SYSID 2006*, pages 678–683, Newcastle, Australia, 2006.